Cyclic resistant geotechnical design and parameter selection for offshore engineering and other applications

Dimensionnement aux chargements cycliques et sélection des paramètres pour l'ingénierie des fondations offshore et autres applications

Knut H. Andersen, Alain A. Puech and Richard J. Jardine
Norwegian Geotechnical Institute, Oslo, Norway; Fugro GeoConsulting, Nanterre ,France, and Imperial College London

ABSTRACT: Cyclic loading due to wind, wave and wind-turbine loading is of crucial importance in offshore foundation engineering. Designers often have to consider cyclic bearing capacity and stiffness, as well as permanent displacements due to cycling and potentially changing patterns of soil reaction stresses. These features are illustrated by drawing on offshore engineering prototype observations, field, model and soil element testing studies before setting out cyclic design procedures for gravity base foundations, suction anchors, monopiles and deep driven piles. Similar approaches may be used to consider the geotechnical effects of cycling imposed by seasons, earthquakes, ice, machinery or other processes in applications ranging from sea barriers to large bridges and foundations to roads or high-speed trains. A main objective has been to offer guidance for obtaining the soil parameters for design of foundations under cyclic loading.

RÉSUMÉ : Les chargements cycliques induits par le vent, la houle et le fonctionnement des éoliennes sont d'une importance capitale pour l'ingénierie des fondations offshore. Le concepteur doit le plus souvent considérer la capacité portante et la raideur cycliques mais aussi les déplacements permanents engendrés par les cycles et de possibles évolutions des réactions du sol. Ces particularités sont illustrées par un panorama d'observations recueillies sur des prototypes de structures offshore et de résultats d'essais in situ, sur modèles et sur échantillons de sol. On décrit ensuite les procédures de dimensionnement sous chargement cyclique des fondations de plates-formes gravitaires, d'ancres à succion, de monopieux d'éoliennes et de pieux battus de grandes longueurs. Des approches similaires peuvent être utilisées pour prendre en compte les effets géotechniques des charges cycliques imposées par les variations saisonnières, les séismes, les glaces, les machineries et autres processus tels que rencontrés dans les ouvrages de défense à la mer, les grands ponts ou les fondations de routes et de trains à grande vitesse. L'objectif principal a été de proposer des recommandations pour l'obtention des paramètres de sol nécessaires pour le dimensionnement des fondations sous chargements cycliques.

KEYWORDS: cyclic loading, foundation design, laboratory testing, soil parameters

MOTS-CLES: chargement cyclique, dimensionnement de fondations, essais de laboratoire, paramètres de sol

1 INTRODUCTION

This document has been prepared under the auspices of ISSMGE TC-209, which is concerned with advancing offshore geotechnical engineering. Its main aim is to contribute to comprehensive cyclic design guidance for offshore and other civil engineering applications.

The offshore oil and gas industry has advanced cyclic design in recent decades, developing procedures for considering the effects of large cyclic loads caused principally by waves and wind. Well-established guidance is available for Gravity Base Structure (GBS) and other shallow foundation types, in API RP 2GEO, 2011; DNV Foundations, 1992. Jardine et al 2012 summarise equivalent developments in cyclic assessment methods for offshore piled foundations. The offshore wind-turbine industry is also adapting cyclic design methodologies: see DnV-OS-J101, 2010 or BSH, 2007.

Far less attention is given currently to cyclic loading in general civil engineering and building foundation guidelines. National codes and Eurocode 7 reflect a generally lower level of elaboration. Closer attention is paid to the topic in earthquake geotechnical engineering, pavement studies and in foundation design for heavy rotating machines. Andersen (2009) emphasized cases where cyclic loading is important for coastal structures (harbour facilities, breakwaters, storm surge barriers etc.) and also foundations, slopes, embankments and cuts subjected to variable seasonal, wind, operating or seismic loads. The present lack of guidance regarding piles under cyclic loading is being addressed in the ambitious SOLCYP Research and Development project (Puech et al., 2012) underway in France that considers a wide range of applications including high rise towers and chimneys, energy transport pylons, high-speed train infrastructure and crane foundations, as well as offshore energy facilities. Results from SOLCYP are incorporated into this paper.

The paper describes how foundation design can be approached when cyclic loading is important, summarises some relevant calculation procedures and focuses on reporting current best offshore practice for determining cyclic design parameters. The latter has developed through advanced laboratory testing, performed on high quality samples, combined with model and full-scale field studies. In-situ testing based approaches have yet to be developed comprehensively, although this avenue may prove more promising in the future.

Ten main sections are set out between this introduction and the final conclusions covering:

- The range of offshore foundation types considered
- Cyclic loading characteristics
- The key aspects to consider in cyclic design

- Calculation procedures for offshore shallow foundations and suction anchors
- Calculation procedures for offshore piles
- Cyclic soil parameters required for foundation design
- Derivation of cyclic soil parameters from laboratory tests
- Guidance on interpreting and presenting results
- Existing data bases of cyclic loading test results
- Application to other types of structures and cyclic regimes, describing how cyclic design methodologies can be applied to applications outside offshore engineering, noting the broader spread of cyclic loading regimes and the potential demands of the mainstream civil engineering industry.

2 OFFSHORE FOUNDATION TYPES

The choice of cyclic design procedure depends on the foundation type under consideration. This paper follows the historical development of offshore cyclic design development, starting with large North Sea Gravity Base Structures (GBS) (Andersen, 1976), before extending to suction anchor cases (Andersen and Jostad, 1999) and then offshore piles. The first two, relatively shallow (low depth L to Diameter D ratio), applications illustrate the NGI's 'cyclic contour diagram network' method for addressing soil behaviour and foundation response. Low L/D skirted foundations, offshore jacket mud-mats and sea-bed templates can be analysed in similar ways, as may suction anchors and even monopiles.

The piling sections that follow draw on an earlier paper (Jardine et al., 2012) that focused on deeper foundations and argued that closer attention should be given to cyclic resistance in routine practice. Most offshore jackets and floating structures rely on piles with $10 < L/D < 70$. The piles usually comprise open ended steel tubes, although bored piles are used in some special applications. Pile driving adds complexity, setting up new stress conditions at the soil/pile interface. The effective stresses generated redistribute with time in the soil mass and over the pile surface during loading. While different approaches are available for low 'L/D' foundations, wind-turbine monopiles and sometimes even suction caissons have also been analysed by extending conventional offshore pile methods. This practice is also discussed, referring to recent research.

3 CYCLIC LOADS

The term "cyclic" loading is used generically to characterise variable loads that have clearly repeated patterns and a degree of regularity in amplitude and return period. Cyclic loads can be essentially of environmental origin (seasons, waves, tide, current, wind, earthquakes, ice sheets) or anthropogenic (due to traffic, blasting operations, plant operations or rotating machinery).

Cyclic loading characteristics vary considerably between cases as illustrated by Figure 3.1. For example, seasons cycle over months, tidal forces usually follow 12 hour periods, while large sea-waves cycle over 10-20s and earthquake periods are far shorter. The durations of extreme cycling events also vary, ranging from 1 to 2 days for an offshore design storm to less than 1 minute for most earthquakes. Design critical cases range from a few extreme cycles to millions of low level fluctuations.

The most severe cyclic storm or earthquake load histories are often composed of a succession of irregular amplitude waves that are distributed relatively randomly with time. However, the cyclic field, laboratory-model and soil-element tests that are conducted to explore cyclic loading effects are usually restricted to tests that can be conducted within limited time-frames and at cyclic rates that allow suitable control, precision and data capture rates. The most common practice is to conduct uniform cycling with load or displacement series' that employ a fixed frequency and regular amplitude. Such regular-cycle tests can be defined by their number of cycles N, period (T), average load (Q_a), cyclic load amplitude (Q_{cy}) - or their displacement equivalents (Figure 3.2).

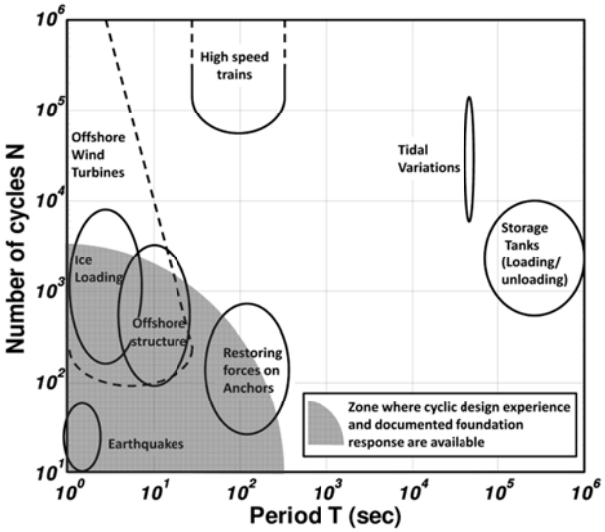

Figure 3.1: Periods and number of cycles characterising typical cyclic loading events.

Regular cyclic loading can be symmetrical ($Q_a = 0$) but is more normally non-symmetrical due to a non-zero average component. Even GBS cases have dead-weight vertical or steady current/wind components. One-way loading imposes $Q_{cy} < Q_a$ while two-way loading leads to $Q_{cy} > Q_a$. Cycle-counting methods (often derived from 'rainflow' analyses, see ASTM E1049-85 which may overestimate number of large waves) are often used to transform the expected field cyclic load histories into idealised series' of regular cycles that may be matched with the outcomes of the uniform cycling imposed in laboratory or field tests performed to aid practical cyclic design.

There are cases where two or more cyclic loading frequencies need to be considered simultaneously. This can occur with offshore wind power structures, for example, that are subject to cycling forced by wind and waves periods as well as secondary cycles related to their rotor rotation frequencies. Another cause of multi-mode cycling can be the combination of an external forcing frequency and cyclic motions set up by the structure resonating at a frequency determined by its own weight and stiffness. The foundation of the Great Belt bridge in Denmark provides one example where design had to address actions from floating and breaking ice sheets that imposed load cycles with periods of about 10s that generated significant bridge pier vibrations. The latter, secondary, foundation loading cycled at a higher frequency of about 1Hz; Andersen, 2009.

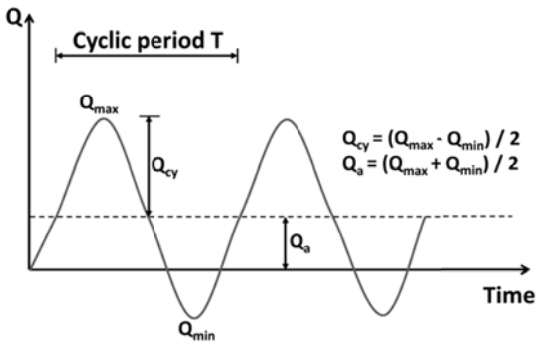

Figure 3.2: Cyclic loading definitions. Note Q_a is often referred in the literature to as $Q_{average}$, Q_{ave} , Q_{av} or Q_{mean}, and Q_{cy} as Q_{cyc}, Q_{cyclic} or Q_c

4 FOUNDATION DESIGN ASPECTS

The major requirements to be addressed in cyclic foundation design are: (1) ensuring sufficient bearing capacity; (2) making sure that cyclic displacements are tolerable; (3) providing equivalent soil spring stiffnesses for use in dynamic soil-structure analyses; (4) assessing whether long term settlements due to permanent straining during cyclic loading are tolerable, (5) considering also movements developed post-cycling through creep and pore pressure dissipation, and (6) assessing how the base and side soil reaction stresses developed at the soil-structure interface may change due to cycling. These aspects are outlined briefly below and discussed in more detail by Andersen (2004).

4.1 *Capacity*

Cyclic bearing capacities must be sufficient to (i) carry the structure and its external cyclic loads and keep deformations within acceptable limits, while (ii) maintaining a sufficient reserve against uncertainty in soil conditions and parameters, calculation method performance and loading. The ultimate capacity developed under cyclic loading can differ considerably from the monotonic (drained or potentially undrained) loading capacity. One example is shown in Figure 4.1, which compares the capacities developed under cyclic and monotonic loading in two model tests footing on clay. The capacity developed under some dozens of high-level cycles is smaller than the monotonic capacity in this case. However, the relative capacities depend on the number of cycles, the ratio between cyclic and average loads, the composition of the cyclic amplitudes and the load period. Rate effects can cause the capacity developed under a small number of fast cycles to exceed the monotonic capacity; the monotonic capacity can also be improved in some cases by pre-applying many low-level cycles and allowing creep and drainage.

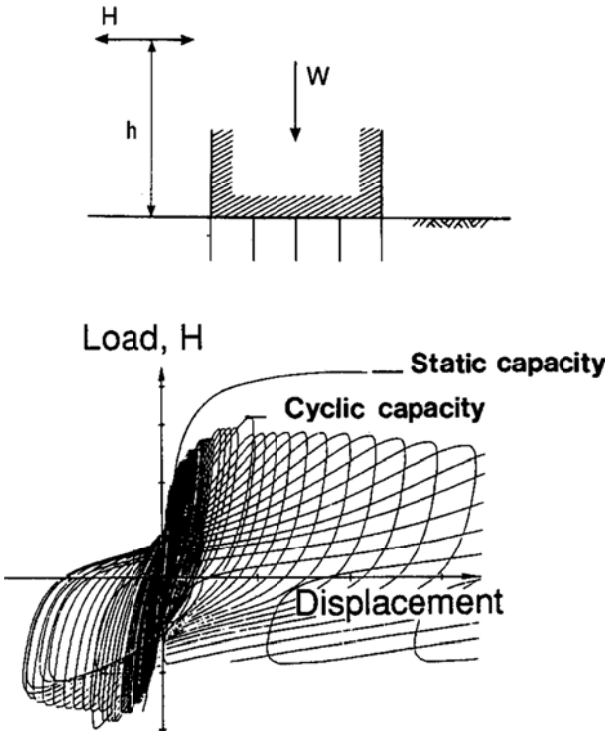

Figure 4.1: Results from model tests with monotonic and cyclic loading of a 0.4m diameter footing with 0.1m long skirts in a soft clay with Ip=28% and shear strength of about 10kPa (Dyvik et al. 1989)

Another example is shown in Figure 4.2a, which compares the cyclic and monotonic axial loading responses of a (D=420mm, L=13.5m) bored pile installed in the highly overconsolidated Flanders clay at Merville (Northern France). This system is relatively resistant to one-way cyclic loading. However, batches of cycles applied (at 0.5 Hz) to give load maxima amounting to 90% of the static capacity led to failure by steadily accumulating permanent displacements. The static capacities were defined by relatively rapid incremental loading tests typically achieving failure in 30 minutes.

Jardine et al. (2012) show that axial capacity degradation is more severe with sensitive clays and in soils (such as sands) that have higher interface shear friction angles, δ. Figure 4-2b compares the static and cyclic response of two identical piles (D=420mm, L=8m) bored in dense Flanders sand at Loon-Plage, near Dunkirk in Northern. France. The sand has far higher δ angles than the plastic Merville clay. One-way (first time) cyclic loading on pile F5 generated large permanent displacements at loads well below the static capacity (about 1100kN) developed in a conventional incremental static test on a control pile (F4) after a displacement of 0.1D.

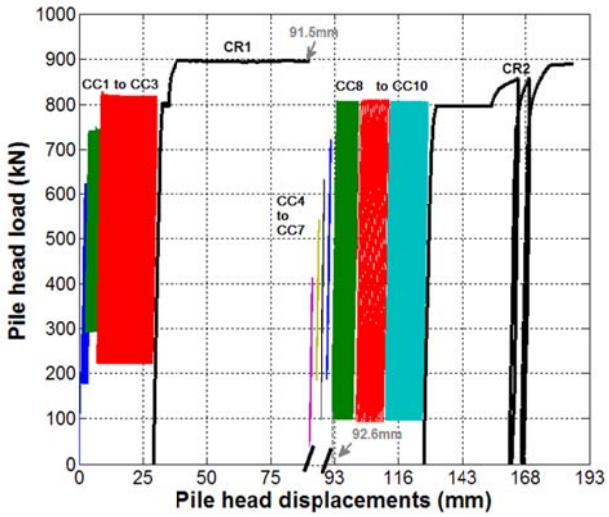

Figure 4.2a: Cyclic field tests on a bored pile in Flanders clay (Benzaria et al., 2013). CC: cyclic tests each with N = 1000, CR: monotonic rapid tests. Pile loaded in compression

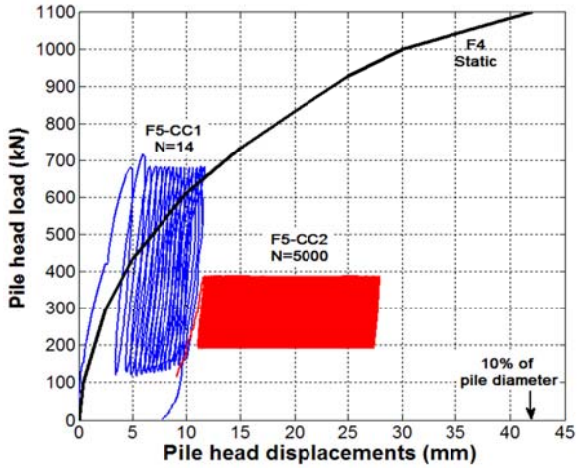

Figure 4.2b: Field tests on two identical piles bored in dense Flanders sands (Benzaria et al., 2013). Static (F4) and cyclic (F5) responses. Piles loaded in compression

It is also well established that high-level two-way loading leads to far more marked capacity losses than one-way loading: see the Haga clay or Dunkirk sand driven pile cases reviewed by Jardine et al. (2012).

4.2 *Cyclic displacements*

Structural serviceability and fatigue life may be sensitive to the displacements experienced under cycling. These issues are critical with wind-turbines, for example, while cyclic movements have to be contained. Limits have to be maintained with other offshore platform types to control stresses in structural elements or in connections with wells, risers or pipelines.

The North Sea Brent B Condeep platform provides an illustration. In this case, the oil wells positioned beneath the base were considered liable to distress if horizontal seafloor displacements exceeded 150mm. Design calculations indicated that the foundation scheme should be able to keep cyclic horizontal displacements and rotations within tolerable values (≈ 65mm and ≈ $7 \cdot 10^{-4}$ radians respectively) even if the design storm arrived during the first winter after platform installation. Analysis indicated that movements would be reduced by around 70% if the design storm developed after full dissipation of the pore pressures set up in the underlying stiff glacial clay and dense sand layers by the platform's weight: see Figure 4.3. Later field monitoring showed that the prototype foundation was approximately 30% softer for horizontal displacements and approximately 5% stiffer for rotations than anticipated in design.

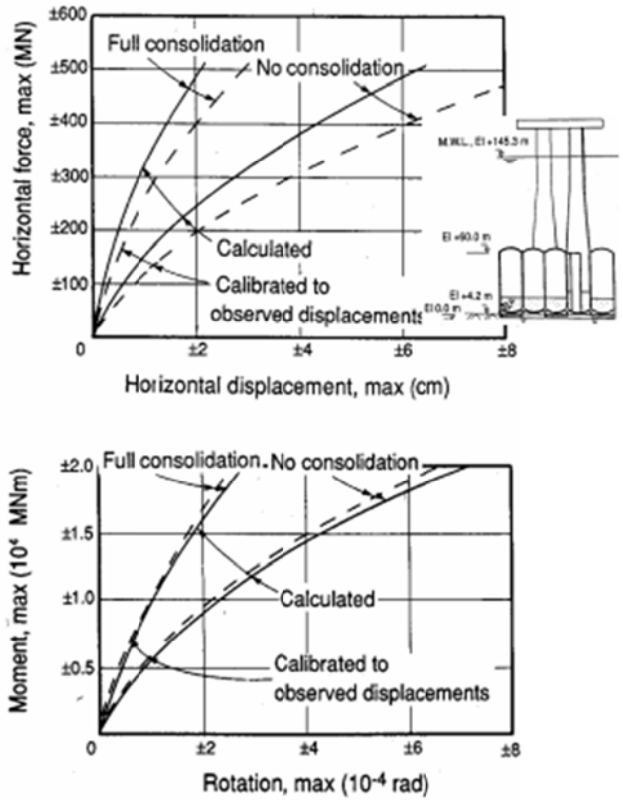

Figure 4.3: Cyclic displacements of the Brent B Condeep platform at seafloor elevation (Andersen & Aas 1980). Design loads comprise a horizontal load of 500MN and moment of $2 \cdot 10^4$ MNm

The SOLCYP group show that high level axial or lateral cyclic loading can generate large permanent displacements with bored piles. Figure 4.2 demonstrated the results of axial cyclic loading field tests on 420mm diameter piles in sand and overconsolidated clay, while lateral cyclic loading centrifuge tests performed on low OCR kaolin are presented in Figure 4.4 for a pile with 0.9m equivalent prototype diameter.

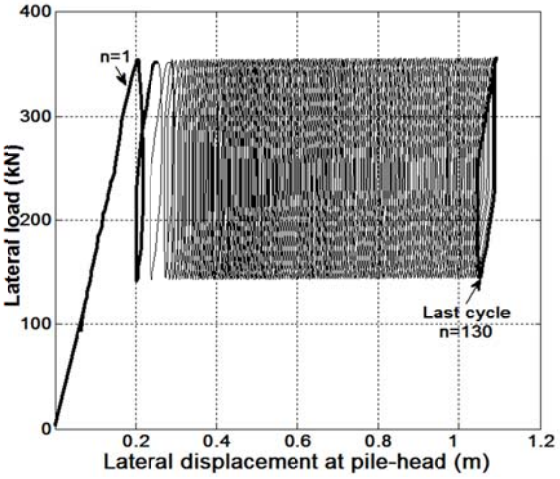

Figure 4.4: Centrifuge tests in low OCR kaolin; equivalent prototype pile diameter = 0.9m; one-way horizontal loading; cyclic displacements

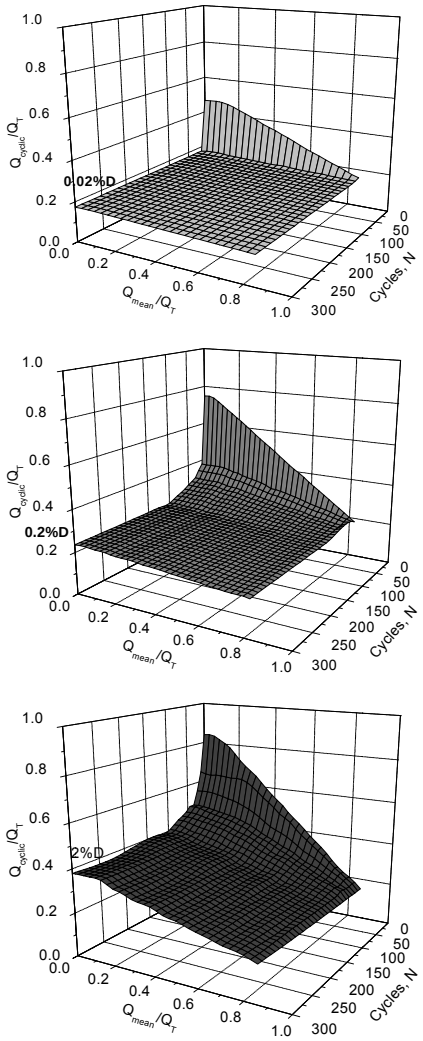

Fig. 4.5: Permanent displacements as functions of N and cyclic loading parameters from metastable and unstable axial cycling tests on 19m long, 456mm diameter, steel tubular piles driven in dense Dunkirk sand. Note Q_T = tension capacity; Rimoy et al., 2013

Jardine and Standing (2000 and 2012) and Jardine et al. (2006) report trends from multiple axial cyclic loading tests on 456mm diameter, 19m long steel tubular piles driven at the Dunkirk test site. Rimoy et al. (2013) show that permanent displacements depend systematically on the cyclic loading level, degree of cyclic stability and number of cycles. Figure 4.5 shows the conditions under which permanent pile head displacements accumulated in individual cyclic tests to reach 0.02% D (top), 0.2% D (middle) and 2% D (bottom) where D = pile diameter.

Rimoy et al. (2013) also showed that pile stiffness under cyclic loading was also highly non-linear at Dunkirk, although less affected by the numbers of cycles imposed until failure is approached. The upper part of Figure 4.6 highlights the stiffness non-linearity by showing how the overall pile head secant stiffness k = Q/δ (where Q = load and δ pile head displacement, both are sum of average and cyclic components) fell with load during the first-time monotonic testing of piles R2 to R6. The k values are normalized by a reference value (k_{ref}) defined from the first load step (that applied Q_{ref} = 200 kN) while loads Q are normalized by Q_{ref}. These patterns are typical for large pile and other foundation types; see Jardine et al. (1986 and 2005b).

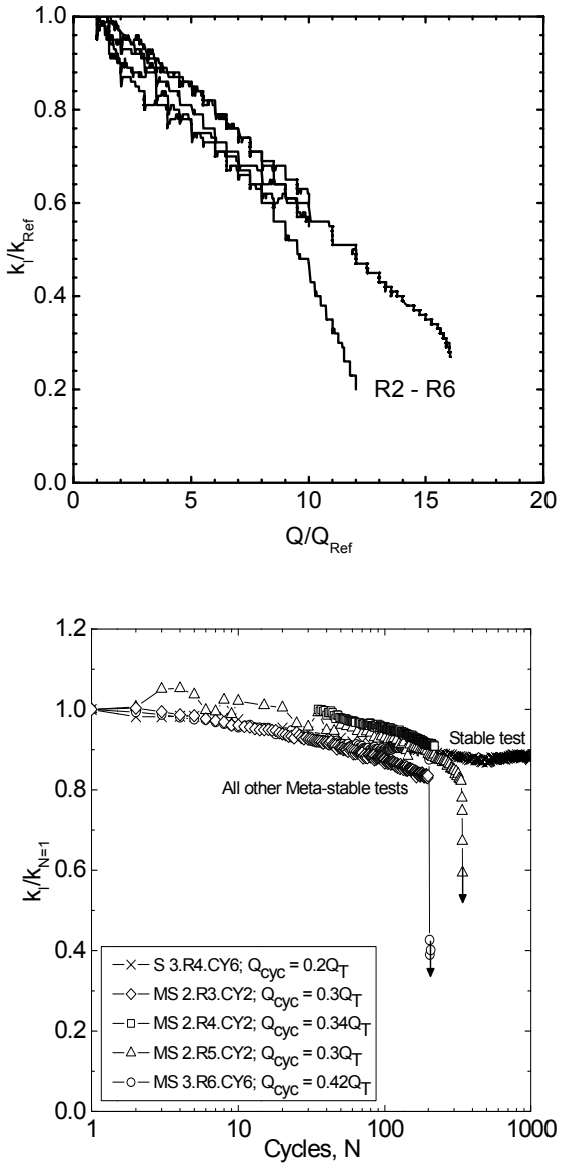

Fig. 4.6: Axial stiffness characteristics from static and metastable cyclic tests on steel piles driven in Dunkirk dense sand; Rimoy et al., 2013

The lower traces in Figure 4.6 show how axial stiffness varied with N in five typical stable and metastable tests, normalized by $k_{N=1}$, the (non-linear) stiffness developed over first cycle; after Rimoy et al 2013. The stiffness under cyclic loading showed only modest reductions (< 20%) over hundreds of cycles. However, sudden stiffness reductions were seen over the final few cycles of the two tests that developed full cyclic failure.

4.3 *Equivalent cyclic soil spring stiffnesses*

A key task in offshore design is to avoid damaging resonant motions developing under cyclic loading. The Brent B Condeep GBS platform monitoring data shown in Figure 4.7 indicate an example where the first resonance periods for the combined soil-structure system were found to be 1.78s, 1.71s and 1.19s respectively, all falling well below the predominant wave load period range (10s to 15s). The structural stiffness and weight changes associated with moving to progressively deeper water conditions lead to increasing resonant periods that eventually approach the wave load period, which encourages dynamic load amplification and structural problems. Such trends apply to all slender structures as their slenderness ratio (L/D) increases.

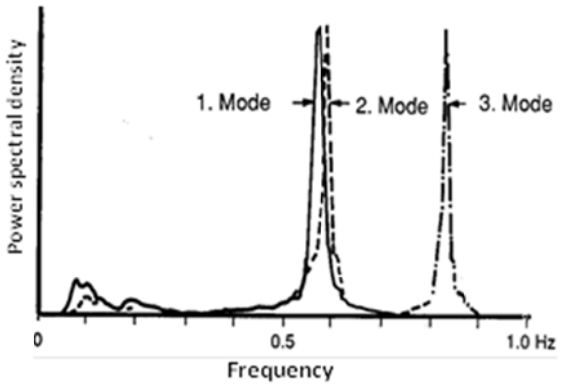

Figure 4.7: Measured acceleration spectra from the Brent B Condeep gravity base platform (Hansteen, 1980)

The resonant frequencies of wind-turbines, for example, are sensitive to their horizontal foundation stiffness characteristics. Monopiles based offshore often have embedded diameters in excess of 5 meters and slenderness ratios in the range of 5 to 10. They are designed to work as 'soft-stiff' structures, with first natural frequencies that fall between their two critical excitation frequency bands (1P and 3P) in order to avoid resonance. The 1P and 3P excitation frequencies are functions of the operational rotor rate, which for modern turbines is typically between 7 and 12 rpm (Andersen et al., 2012). As illustrated in Figure 4.8, the first natural frequency is constrained within a narrow band and needs to be known with a high level of confidence. Any initial stiffness estimation errors could have significant consequences, as can any long-term cyclic effects that change the foundation frequencies and move an initially optimally designed system towards resonance and fatigue problems. One possible remedial measure might be to alter the operational rotor frequency.

It is common when assessing structural dynamic characteristics to sub-divide the interacting soil and structural domains and consider each separately. Soils conditions are often represented in dynamic structural analyses by equivalent 'soil springs' whose stiffnesses have to be specified from independent simplified geotechnical analyses. As noted above, foundation stiffness behaviour may be highly non-linear and great care is needed to derive appropriate simplified 'spring' characteristics.

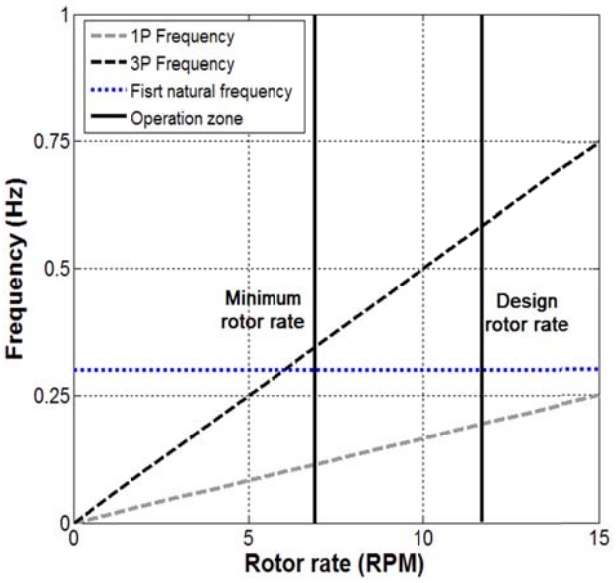

Figure 4.8: Simplified Campbell diagram for wind turbine soft-stiff design (after Andersen et al., 2012).

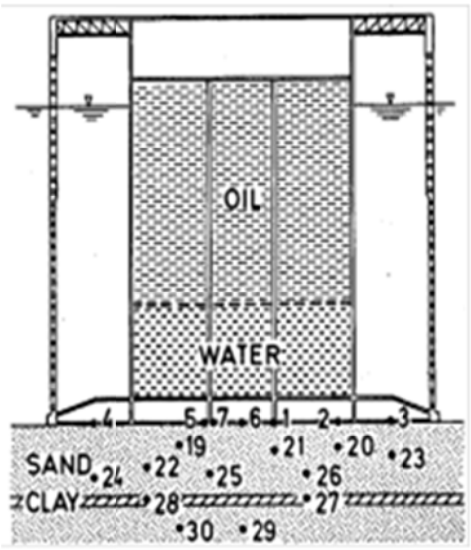

4.4 *Permanent displacements due to cyclic loading*

Cyclic loads add to permanent loads in causing permanent deformations that may distress structural elements or connections to offshore platforms. Significant settlements also reduce the free-board between the deck and the sea. Similarly, wind-power structures have to maintain strictly set verticality limits under markedly non-symmetrical cyclic loading conditions.

The deformations developed due to cyclic loading can be separated into two components; (1) those due to permanent strains developed during the cyclic loading and (2) strains due to dissipation of cyclically induced pore pressure and creep. Settlement due to cyclic loading is illustrated in Figure 4.9, reporting the response of the Ekofisk Oil Storage Tank during first its installation and ballasting, and then a severe storm in late 1973. The settlements increased sharply by ≈ 60mm during the November storms.

As discussed above, piles develop significant permanent displacements under high level cyclic axial loading. Similar trends apply under lateral loading, with displacement rates that depend on the loading style and loading severity. Centrifuge test data from lateral loading tests on normally consolidated soft kaolin are presented in Figure 4.10a as an example. Non-symmetrical horizontal loading generated large permanent lateral pile head displacements which trebled within 500 cycles. The additional displacements naturally lead to large increases in maximum pile bending moments. The latter feature can also be important under even relatively low-level cycling, as illustrated in Figure 4.10b with measurements from a second lateral loading set of cyclic centrifuge tests on piles installed in medium-dense fine Fontainebleau NE34 sand.

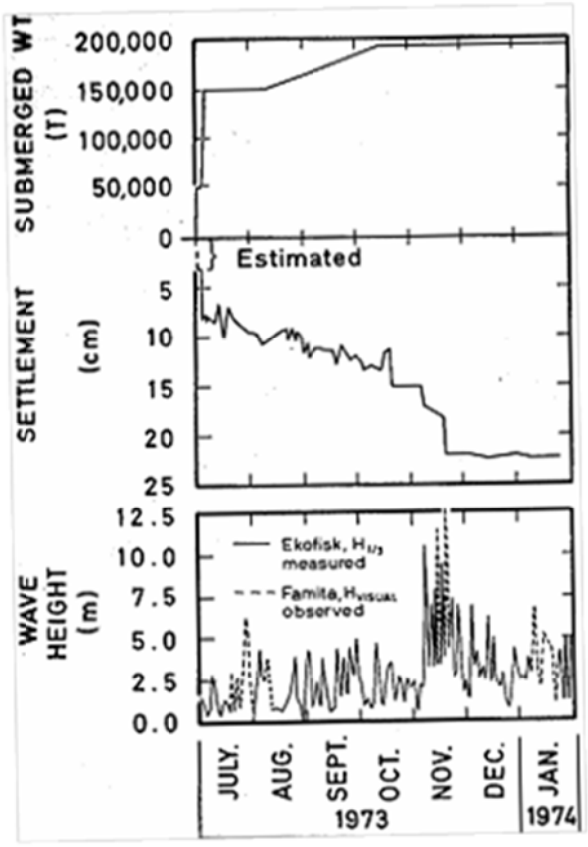

Figure 4.9: Measured settlements of the Ekofisk oil storage tank during installation, ballasting and storm loading (Clausen et al., 1975)

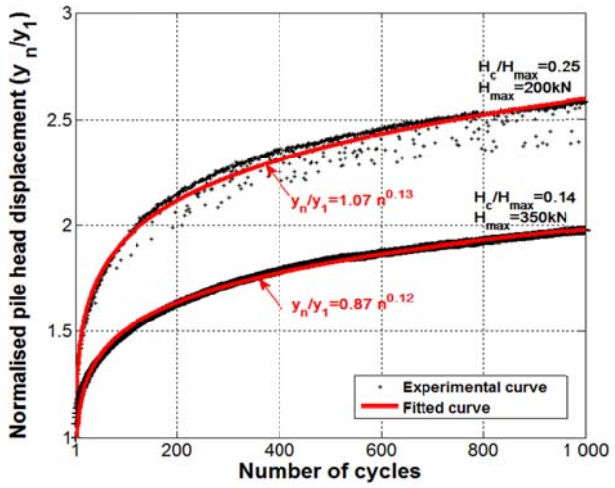

a) Horizontal displacements (y_N) normalised by y_1 displacement for first cycle against N (Khemakhem, 2012) from high-level centrifuge lateral loading tests on Kaolin at OCR = 1

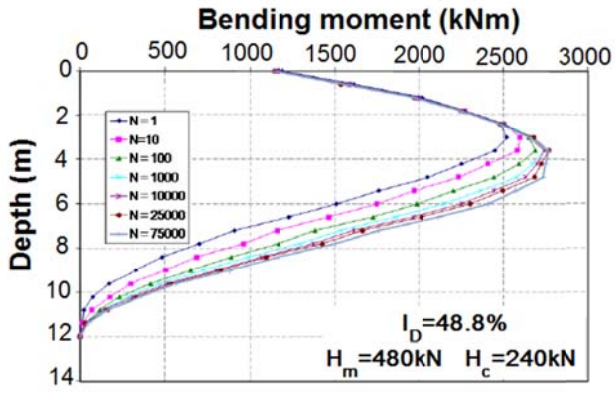

b) Bending moment in piles varying with number of cycles N from low level centrifuge lateral loading tests on medium dense sand (Rakotonindriana, 2009)

Figure 4.10: Results of centrifuge model tests on piles subject to cyclic horizontal loading

4.5 *Soil reaction stresses*

The above lateral pile loading cases provide examples of stiffness degradation under cyclic loading changing the lateral soil-structure contact pressure distributions and raising bending stresses within the (pile) structure. Analogous changes may develop through load cycling on the pressure distributions developed across the bases and sides of GBS foundations or suction caisson due to creep, consolidation and cyclic loading. Such changes have to be addressed to ensure that the structural design is sufficiently robust to cope with long-term soil pressure distributions and stiffness characteristics.

5 CALCULATION PROCEDURES FOR OFFSHORE SHALLOW FOUNDATIONS AND SUCTION ANCHORS

5.1 *Capacity*

Capacity is assessed by applying limit equilibrium, plastic limit or finite element procedures. Limit equilibrium and plastic limit methods involve assuming a failure mechanism and optimising the solution, searching for the most critical case. Examples of trial limit equilibrium failure surfaces are shown in Figure 5.1 for shallow foundation and anchor examples. Such analyses normally use simplified 2D models and account for 3D-effects by adding additional 'side shear' forces that are calibrated against 3D finite element analyses (e.g. Schjetne and Lauritzsen, 1976; Andersen and Jostad, 1999). However, the critical failure mechanism emerges in elastic-plastic finite element analyses without the user having to making any prior assumption; both 2D and 3D finite element analyses are practically feasible.

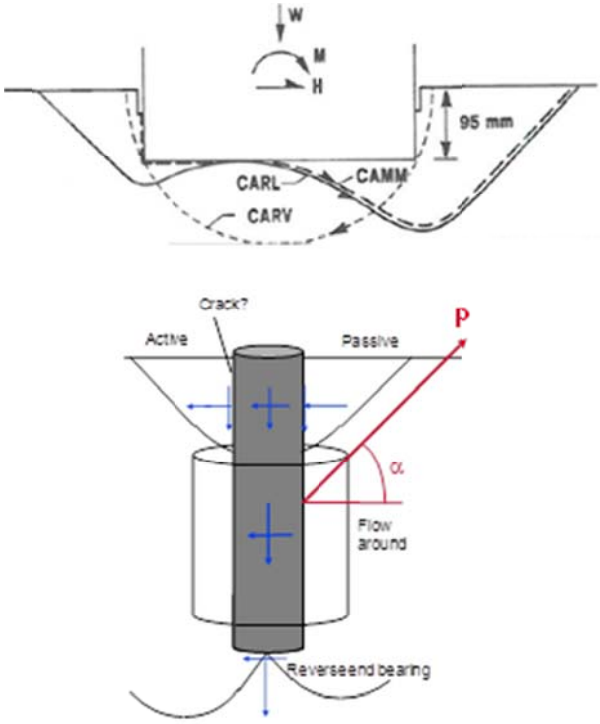

Figure 5.1: Examples of potential limit equilibrium failure surfaces

Finite element analyses also reveal details of the stress paths imposed on the underlying soil and around any potential failure mechanism. Six stress components have to be specified to describe the stress state fully at any given point, which reduces to four in 2-D plane stress/strain or axially symmetric cases. The familiar stress path parameters $q = (\sigma_1 - \sigma_3)$, $p' = (\sigma'_1 + \sigma'_2 + \sigma'_3)/3$ (or $t = q/2$ and $s' = (\sigma'_1 + \sigma'_3)/2$) describe the stress conditions of Triaxial Compression (TC) or Triaxial Extension (TE) tests fully, where α (the orientation of σ_1 relative to the vertical) and $b = (\sigma_2 - \sigma_3)/(\sigma_1 - \sigma_3)$ are fixed as $\alpha = 0$, $b = 0$ for TC and as $\alpha = 90^o$, $b = 1$ for TE respectively. But α and b can vary freely under more general 2-D stress conditions and it is necessary to track these variations. Direct Simple Shear (DSS) involve α and b changes. However, it is not possible with most apparatus to define the full (q, p′, α, b) DSS stress paths.

Figure 5.2 shows an example of an analysis reported by Jardine et al. (1997) that presents the contours of α that apply beneath a trapezoidally loaded shallow foundation on low OCR clay. The σ_1 axis is vertical under the centre line but rotates under the edges to eventually become horizontal outside the loaded area. Such stress axis rotation implies an associated rotation of potential slip failure plane orientations. The same analysis showed the 'b' parameter changing from an initial value of 0 to ≈ 0.4 as loading progresses.

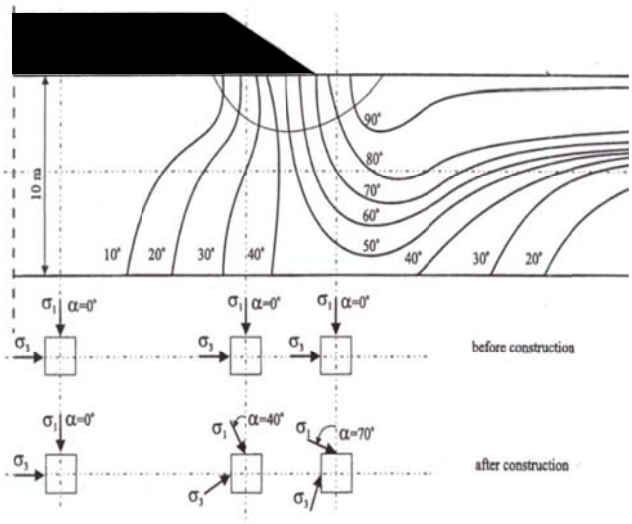

Figure 5.2: Contours of α (the orientation of σ_1 relative to the vertical underneath a trapezoidally loaded shallow foundation on low OCR clay; after Jardine et al., 1997. Note that σ_2 parameter b also changes to ≈ 0.4.

Advanced laboratory tests show that soil response, and in particular undrained shear strength, depends critically on the imposed combinations of q/p′, α (effects of direction, or anisotropy) (e.g. Bjerrum 1973) and b (effects of σ_2). Jardine et al 1997 report undrained shear strengths measured with Hollow Cylinder Apparatus (HCA) that can vary b and α over a wide range. Figure 5.3 illustrates multiple tests conducted by Menkiti 1995 on K_0 consolidated samples of HK, a clay-sand, tested at OCR = 1 in which 'b' was kept at a nominally plane strain value (b = 0.5) in tests that imposed a range of α values (between 0 and 90°). The s_u values obtained, expressed as ratios to the vertical effective consolidation stresses, show strong anisotropy with s_u/σ'_v falling continuously with α. The same figure shows data from DSS tests conducted in the HCA and TC and TE tests on K_0 consolidated samples that were conducted in both the HCA and in standard triaxial cells. The triaxial shear strengths fall below the plane strain HCA values, while the HCA simple shear failure develops with α ≈ 25°, rather than at α > 45° as assumed conventionally.

The s_u/σ_v' pattern shown in Figure 5.3 is typical of low OCR soils as is illustrated in Figure 5.4 by similar sets of data from 'plane strain' HCA tests conducted at OCR = 1 on clay, clay-sand and loose sand; similar results are found with HPF4 rock-flour silt (Zdravkovic and Jardine 2000). Nishimura et al. 2007 and Brosse 2013 show that highly overconsolidated natural stiff clays and mudrocks also have markedly anisotropic plane strain shear strengths, although they tend to develop their s_u minima around α ≈ 45°: see Figure 5.5. Other HCA tests conducted with constant α values but with variable b ratios show that the relative magnitude of σ_2 also affects the shear strengths. Zdravkovic et al. (2001) reported advanced finite element analyses with anisotropic soil models that demonstrated how the observed behaviour impacts significantly on the 3-D bearing capacity of offshore suction caisson anchors.

Simple shear tests can be undertaken in the HCA (see Nishimura et al., 2007 or Anh-Minh et al., 2011) under fully defined stress conditions. Such tests show that the peak horizontal shear stresses τ_{vh} usually falls below the true t_{max} and that the α values at which τ_{vh} reaches its maximum vary with K_0, shifting from around 25° at OCR = 1 (see Figure 5.3) to around 65° in very high OCR specimens; the b values typically fall between 0.35 and 0.65, depending also on K_o and OCR.

HCA and stress path triaxial experiments that include multi-axis bender element arrangements also show that soils' non-linear stiffness characteristics are often markedly anisotropic from small strains to large: see Zdravkovic and Jardine (1997), Kuwano and Jardine (2002), Gasparre et al. (2007), or Jardine (2013).

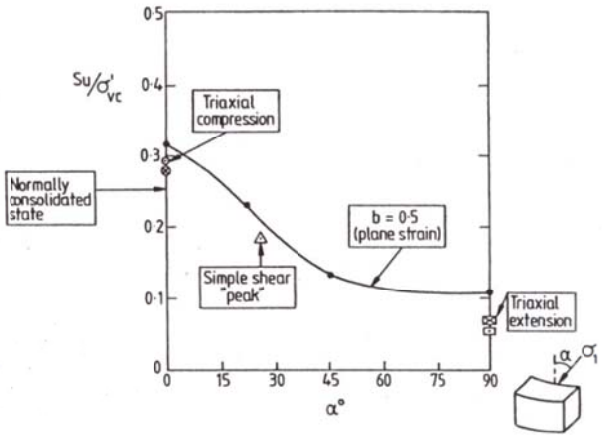

Figure 5.3: Variation with α of s_u/σ_v' in plane strain (b = 0.5) HCA tests on normally (K_0) consolidated HK clay-sand, CAU TC, TE and HCA SS shear strengths also shown; Jardine and Menkiti, 1999

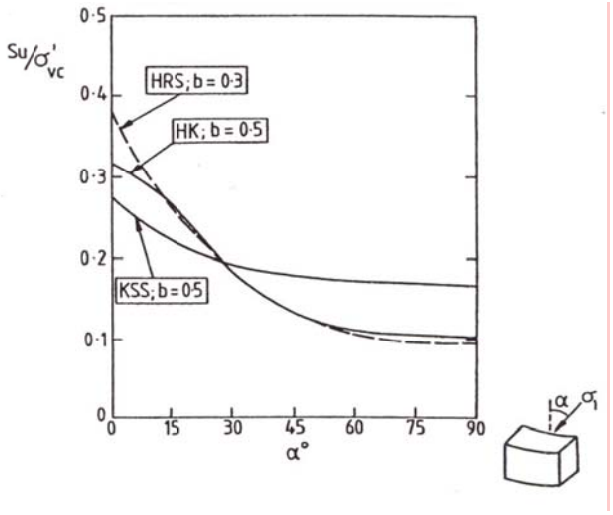

Figure 5.4: Variation with α of s_u/σ_v' developed in HCA tests (with b = 0.5) for normally (K_0) consolidated clay sand (HK), kaolin-silt-sand (KSS) and Ham River Sand (HRS); Jardine and Menkiti, 1999

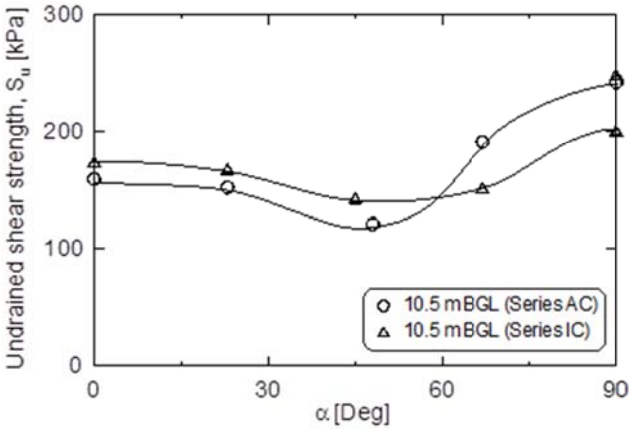

Figure 5.5: Variation with α of su developed in HCA tests (with b = 0.5) for high OCR stiff natural London clay; Nishimura et al., 2007

The stiffness and shear strength anisotropy of soils can be modified by consolidation to differently oriented effective stress regimes. While this may be achieved readily with sands, larger consolidation strains are required with clays. Figure 5.6 illustrates how this may be achieved in HCA tests, where b and α may be changed during consolidation to new values that may be maintained or modified during subsequent shear tests. Figure 5.7 illustrates the considerable impact on the s_u/σ_v' - α relationships seen in HCA tests on normally consolidated loose sands and dense silts in tests that rotated α to the full series of possible orientations prior to shearing under similar α values. Pre-shearing towards the final ultimate σ'_1 orientation clearly increases the subsequent undrained shear strength. Zdravkovic and Jardine (2001) provide further details of these experiments.

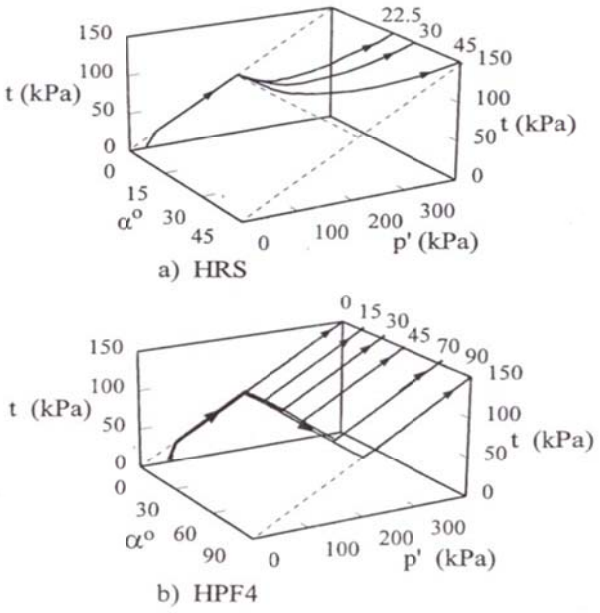

Figure 5.6: Effective stress paths applied in HCA tests on Ham River Sand (HSR) or HPF4 silt involving σ1 axis rotation during consolidation to a range of αc orientations, prior to shearing with b = 0.5 and σ1 axis orientation αs = αc; Jardine et al., 1997

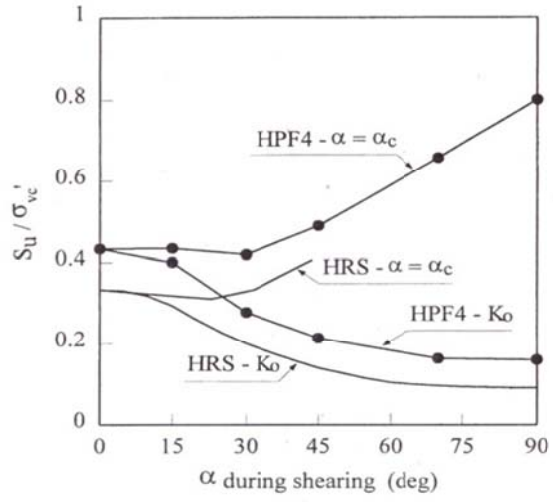

Figure 5.7: Variation of su/σv′ with αs from HCA tests on Ham River Sand (HSR) and HPF4 silt involving either (i) K0 (αc = 0) consolidation, or (ii) consolidation involving the σ1 axis rotated to = αc prior to shearing with b = 0.5 at range of αs orientations; Jardine et al., 1997

HCA testing is not employed widely in practical site characterisation. Anisotropy usually has to be gauged by performing simpler tests TC, TE or CAU tests on K_0 consolidated samples. The shear strengths established from CAU TC, TE and DSS tests cover a range of σ_1 orientations (representing a spread of α angles) and therefore reflect anisotropy. They may also provide conservative estimates for plane strain shear strengths. But because the tests each impose different b values at failure they inevitably mix the effects of anisotropy with those of relative σ_2 magnitude.

The NGI has developed and applied a simplified 'contour diagram' framework to (i) characterize and define potentially anisotropic soil behaviour under cyclic loading and (ii) undertake design with calculation procedures based on this framework; Andersen et al. (1988); Andersen (2009). Figure 5.8 illustrates the modes of shearing engaged around a potential shallow foundation failure mechanism, indicating which regions compare best with the conditions applying in the simplified DSS, TC CAU and TE CAU laboratory tests discussed above. The contour diagram framework defines the cyclic shear strength and the average, permanent and cyclic shear strains as functions of average and cyclic shear stresses and number of cycles. The shear stress and shear strain components are defined in Figure 5.9, and examples of contour diagrams for cyclic shear strength are presented in Figures 5.10 and 5.11. $\tau_{f,cy}/s_u$ is the normalised cyclic shear strength and γ_a/γ_{cy} represents the failure mode, i.e. the average and cyclic shear strains at failure. Examples showing contours of average and cyclic shear strains as function of average and cyclic shear stresses are presented later in Figures 5.14 and 5.15. Reference is made to Andersen et al. (1988) and Andersen (2009) for further explanation.

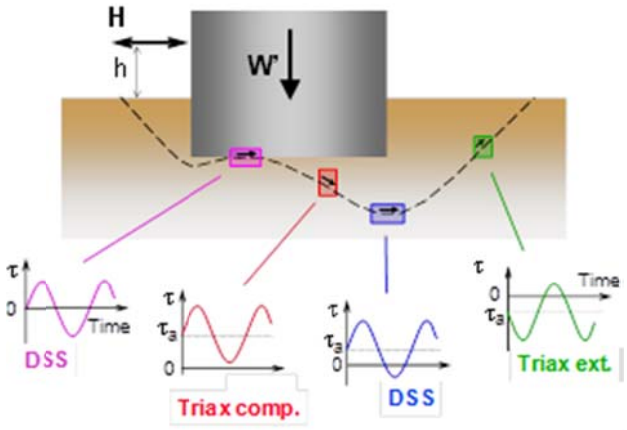

Figure 5.8: Stress conditions beneath a shallow foundation under cyclic loading (Andersen, 2009)

The calculation procedures based on the contour diagram framework have been used extensively in practical design of GBS foundations, suction anchors and monopiles for offshore wind power structures. Among these procedures is a limit equilibrium method to calculate the bearing capacity of foundations or pull-out capacity of anchors subjected to a combination of average and cyclic loading (Andersen and Lauritzsen, 1988). The procedure is based on (1) the condition that the average shear stress along the critical slip surface is in equilibrium with the average loads, and that the cyclic shear strength along the critical slip surface is in equilibrium with the maximum loads (sum of average and cyclic), and (2) the assumption of shear strain compatibility along the critical slip surface of both the average and cyclic shear strain components.

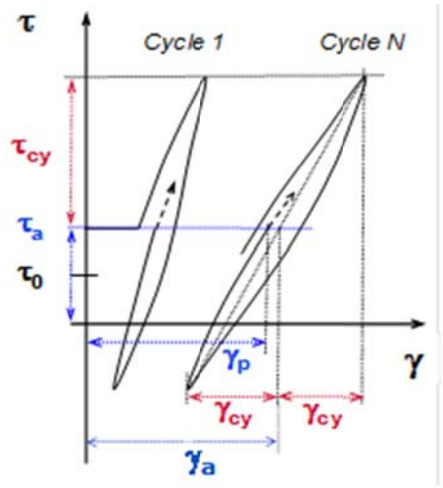

Figure 5.9: Definition of shear stresses and shear strains under cyclic loading (Andersen, 2009)

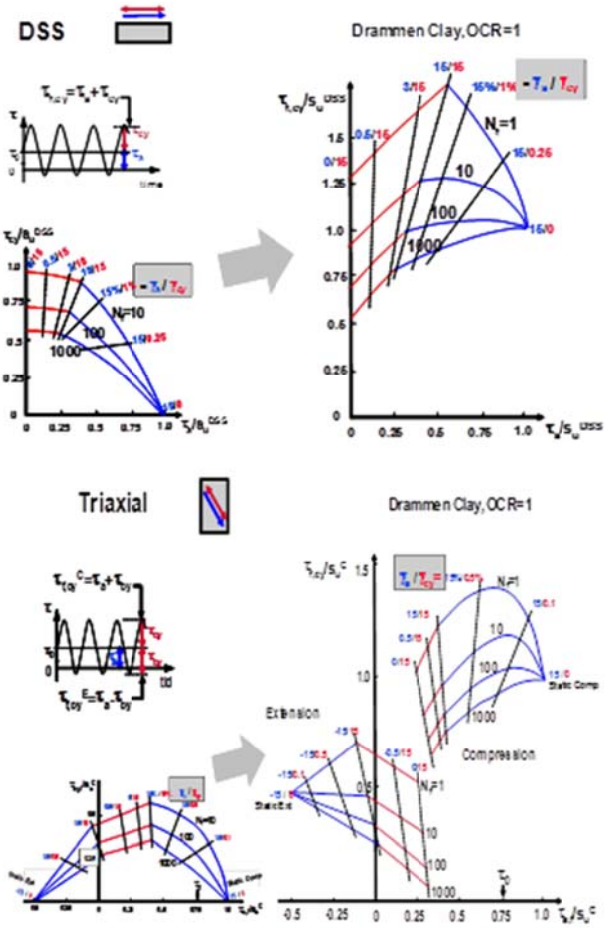

Figure 5.10: Examples of cyclic shear strength contour diagrams for DSS and triaxial stress paths (Andersen, 2009). Red indicates cyclic shear strain and range where failure mode is cyclic shear strain. Blue indicates average shear strain and range where failure mode is average shear strain (compression or extension)

In addition to the capacity, the strain contour analysis gives information on whether the failure mode involves large cyclic or permanent displacements. An approximation that simplifies the calculation is to assume that the ratio between the local cyclic and average shear stresses matches that ratio between the applied cyclic and average environmental loads. However, this simplification does not account for strain compatibility and the associated potential redistribution of the stress regime and inevitably sacrifices solution accuracy.

The wave trains that build up in offshore storms, and hence the cyclic shear stresses developed in soil foundation elements, usually vary from one wave, or cycle, to the next. The test results from regular, uniformly cycling, laboratory tests cannot be applied to model such storm sequences directly. It is usual to transform the storms spectrum of waves into equivalent batches of regular uniform waves, assuming that the damage can be represented by an equivalent number, N_{eq}, of uniform waves. This is achieved by considering the maximum cyclic shear stress that will give the same cyclic shear strain (Andersen, 1976) or the same cyclically induced pore pressure (Andersen et al., 1992) as the true loading composition. The transformation is based on the assumption that the normalized cyclic shear stress composition, $\tau_{cy}/\tau_{cy,max}$, is the same as the normalized resultant of the cyclic load composition, $|\mathbf{F}_{cy}|/|\mathbf{F}_{cy,max}|$ in all the governing soil elements. $\tau_{cy,max}$ can then vary from one element to another, but N_{eq} will be the same in all soil elements.

Pore pressure is used by NGI as the key 'memory parameter' for cyclic degradation in cases where drainage occurs during the storm. One can then calculate the net pore pressure generated by the cyclic loading and the simultaneous pore pressure dissipation. Contour diagrams of the type presented in Figure 5.11 provide the basis for the NGI accumulation procedures and Figure 5.12 presents an example.

Most cases involving clays do not experience significant pore pressure dissipation during the design storm, and it can be more convenient to use the cyclic shear strain as the cyclic degradation 'memory parameter'. One difficulty with the pore pressure approach in clays is that accurate pore pressure measurements are hard to make in laboratory during rapid cyclic testing due to the system compliance and time-lag problems inherent in conventional testing (see Gibson, 1963). Local pore pressure measurement techniques may overcome such problems: see Hight (1982).

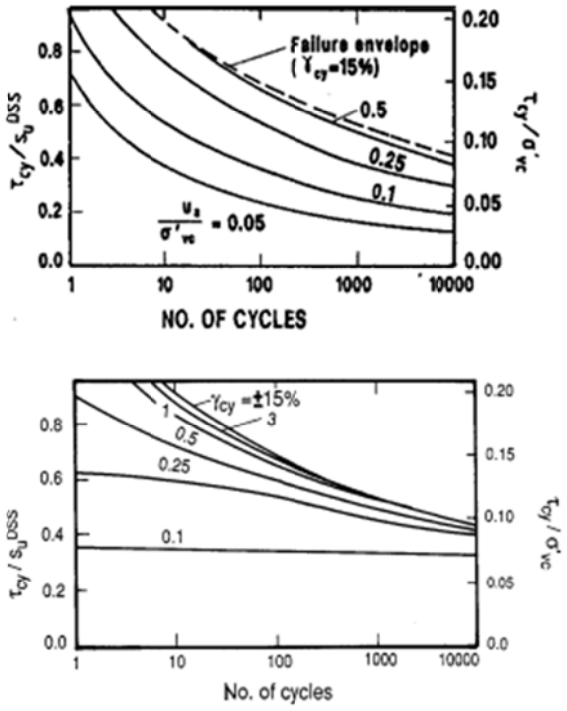

Figure 5.11: Examples of diagrams with permanent pore pressure (upper) and cyclic shear strain (lower) as function of cyclic shear stress and number of cycles. DSS tests with τa = 0 on Drammen Clay (Andersen, 2004)

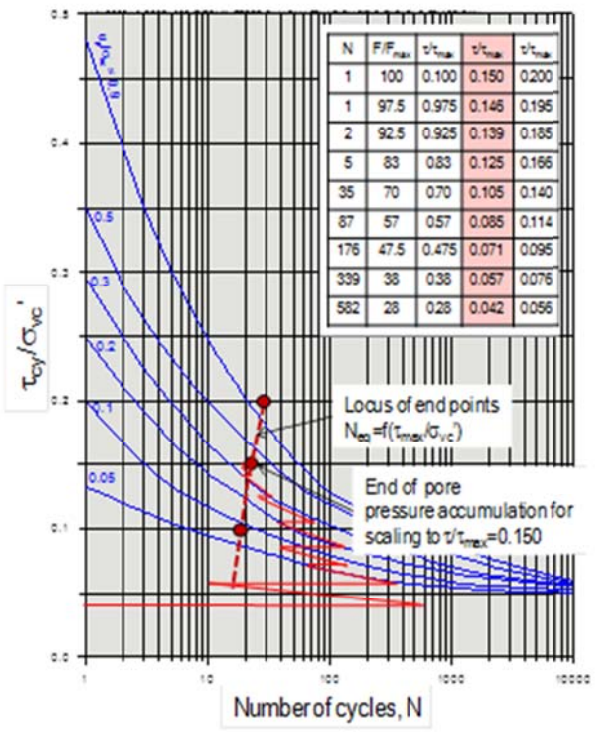

Figure 5.12: Example of pore pressure accumulation for a case with no drainage

It has become more common during the last decade to use the finite element method to determine not only displacements but also the bearing capacity of offshore structures; see for example Andresen et al. (2010). Displacements and capacities have been calculated with the NGI approach by assuming a constant N_{eq} for all the elements in the soil volume (see Andersen and Hoeg, 1991) with N_{eq} determined as described above.

Both the limit equilibrium and the finite element approaches described above have shown favourable agreement with results from model tests (e.g. Andersen et al., 1989; Jostad and Andresen, 2009). However, the assumption of a constant N_{eq} within the soil volume may underestimate (with some geometries) the effects of stress redistribution and progressive failure. A new finite element code, UDCAM, has been developed by NGI where the accumulation of pore pressure or cyclic shear strain is determined and continuously updated in each integration point based on the calculated cyclic shear stress in that point (Grimstad et al., 2013). UDCAM has a 3D formulation to aid analysis of monopile foundations for offshore wind-turbine structures. An extension of UDCAM to include pore pressure dissipation and redistribution during cyclic loading (PDCAM) is being developed. Grimstad et al. (2013) present examples where UDCAM is used to successfully back-calculate a GBS model test with cyclic loading and a 3D analysis of an offshore wind turbine monopile under cyclic environmental loads. Redistribution of pore pressure can be important at sites involving inter-layered clays and sands. Pore pressures generated by cyclic loading in cyclically susceptible sand and silt layers can flow into clay layers, leading to loss of shear strength. This redistribution process can be modelled in the finite element analyses.

Both limit equilibrium and finite element analyses need shear strength input data. As shown in Figure 5.10, the cyclic shear strength depends on the ratio between cyclic and average shear stresses, the simplified stress path (TC, TE, DSS), and number of cycles. Cyclic pore pressure generation and consolidation analyses involving reloading modulus and coefficient of consolidation are also required when the pore pressure procedure is applied and when drainage may be significant.

Andersen and Jostad (1999, 2002 and 2004) argue from model and field tests that the vertical resistance of skirted foundations and anchors is controlled during installation in low OCR, sensitive, clays by a large shear strain disturbance process that takes clay in the interface shear zone to a 'remoulded' state. It is necessary in design to model the set-up that takes places after installation at the interface and in the disturbed zone close to the skirt wall. DSS tests on reconsolidated remoulded samples are performed to indicate the shear strength that develops within such zones. The importance of modelling the set-up increases with increasing foundation L/D ratio. While set-up is most important in relation to vertical capacity, the degree of shaft adherence also affects the lateral capacity. This may be appreciated by noting that (in spatially uniform soil) the lateral capacity bearing capacity factor $N_c = q_f/s_u$ of a cylinder increases approximately from 9 to 12 between the 'smooth' case (where no shear stress can develop at the interface) and the 'fully rough' case when the full s_u is available in shear at the interface to help resist lateral motion.

The set-up of skirts penetrated into clay depends on the ratio between remoulded shear strength, the virgin loading consolidation characteristics of remoulded clay, the unload/reload loading consolidation characteristics of intact clay, and any thixotropic strength gain characteristics of the remoulded clay. A procedure to determine the set-up for skirts penetrated into clay is given in Andersen and Jostad (2002), who also recommend set-up factors for cases where site specific calculations are not performed. Clukey et al. (2013) summarize comparisons between calculated set-up factors and those measured in prototype and model tests, finding a reasonable match with current experience, which relates mainly to soft clays. As explained later in relation to driven piles, such procedure may be less applicable for low sensitivity, overconsolidated clays and soils that develop low residual shear strength shear surfaces with low φ' and δ values in their interface shear zone. The latter characteristics are best captured by interface ring shear tests rather than DSS or other low displacement undrained tests on remoulded samples.

Suction anchors installed by under-pressure, are relatively light and the 'still-water average' vertical shaft shear stress that has to be carried to support their weight is normally small compared to their shaft shear capacity. More significant 'average' still-water shaft stresses may have to be carried by skirted foundations, such as subsea templates, if they are not penetrated to depths that bring their base plates into full contact with the soil. Such maintained shear stresses pre-shear the interface shear zone soil close to the skirt wall, effectively rotating the σ'_1 orientation α during consolidation. As shown earlier, consolidation involving α rotation modifies the anisotropy of low OCR soils and can enhance undrained shear strength of low OCR soils, leading to additional long term shear strength gains in a spread of applications, including shallow foundation problems; e.g. Zdravkovic and Jardine (2001). Such effects can be modelled to some extent in pre-sheared DSS tests designed to match field conditions.

Pore pressure can be adopted as a memory parameter to define N_{eq} in cyclic analyses of large offshore foundations, provided that conditions remain undrained in the surrounding ground over any given single cycle. However, partial (or even full) drainage can apply with high permeability soils (such as clean sand) and short drainage paths. The operational field shear strength of dense sand may then be limited by the soil's inability to sustain any negative pore pressures set up by constrained dilatancy. This limitation is illustrated for triaxial and DSS stress paths in Figure 5.13. The limiting shear

strengths may be defined by the slopes of the respective failure lines and the assumed drained stress loading path directions.

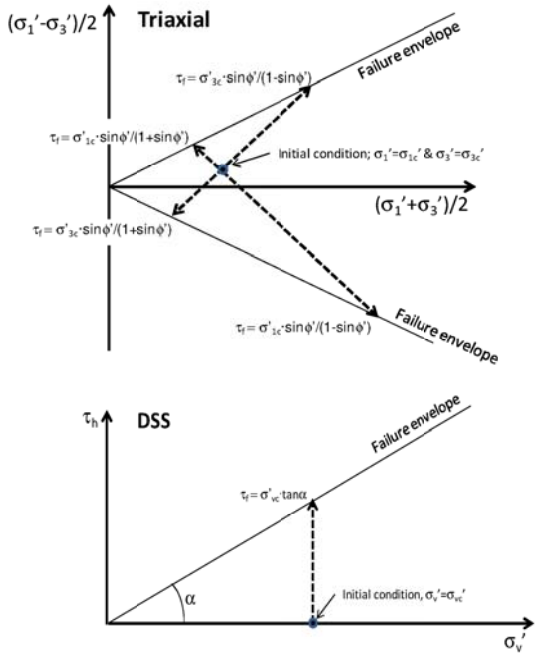

Figure 5.13: Shear strength for different stress paths when dilatancy in dense sand is not relied upon

5.2 *Cyclic displacements*

Structural assessments often require predictions for the horizontal, vertical and rotational cyclic displacements developed under the maximum wave or working load conditions. It is normally assumed that the maximum wave develops at the end of the design storm peak, at a stage when the prior cyclic degradation is most severe. Cyclic displacement assessments are generally not required for anchors because the movements are small compared to those developed in their flexible mooring chains.

Cyclic displacements are normally calculated by finite element methods. The effect of cyclic loading can be accounted for by an equivalent number of cycles approach, as set out Section 5.1. It has usually been assumed in the NGI approach that N_{eq} is constant within the whole soil volume. N_{eq} is then determined before starting the finite element analysis and is used to establish the cyclic stress-strain-strength data that is needed as input to the numerical analysis. As with capacity, the calculation accuracy can be improved by considering the effects of pore pressure or cyclic shear strain accumulation at each integration point in the finite element code. It is also important to model the set-up along any skirt walls.

The NGI finite element approach relies on functions being pre-specified from tests that relate average and cyclic shear strains to the applied average and cyclic shear stresses and number of cycles. As with the bearing capacity cases, different relationships are specified from multiple cyclic TC, TE and DSS tests run with suitable combinations of average and cyclic shear stresses. The finite element programme interpolates for stress conditions in between those specified based on the inclination of the major principal stress. The calculations thus account to some degree for the four-dimensional (q, p′, α and b) stress regime imposed in the field.

The laboratory results are visualised as shown in the examples in Figures 5.14 and 5.15. Pore pressure generation due to cyclic loading and consolidation characteristics are combined in cases where drainage needs to be considered. Simplifications can sometimes be made. For example, the cyclic stress-strain relationship may not always depend unduly on average shear stress. When this is evident from tests, it may be possible to calculate cyclic displacements by considering only the cyclic loading components.

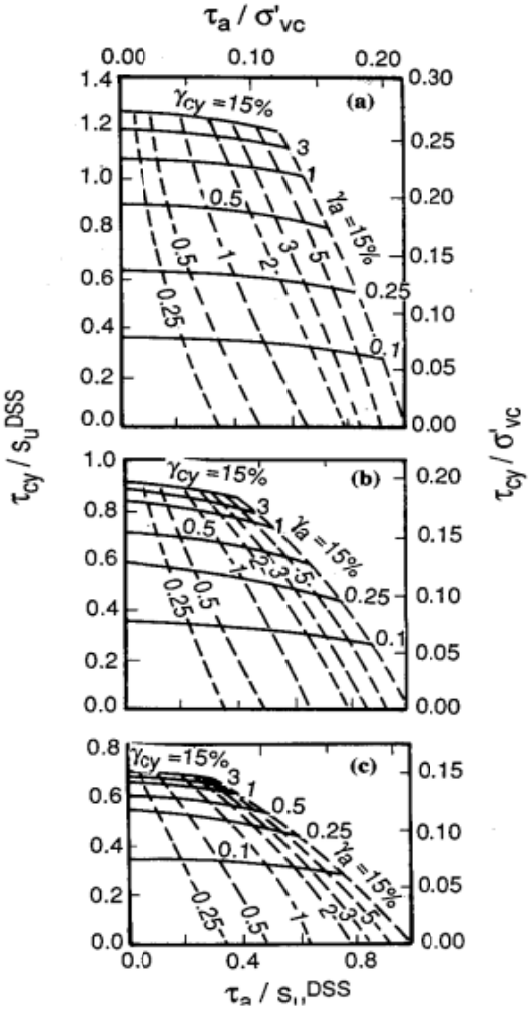

Figure 5.14: Examples of cyclic shear strain contour diagrams for DSS type stress paths on normally consolidated Drammen Clay.
a) N=1, b) N=10, c) N=100 cycles (Andersen, 2004)

The structural displacements result from the integration of strains over the entire soil volume. It is essential to define the highly non-linear shear stress-strain curve over the full strain range from the initial (very limited) linear G_{max} range up to large strain failure. Even if the strains become small at some distance from the structure, they may affect a large volume and make a significant contribution to the overall displacements. In cases where pore pressures dissipate significantly during cycling the soil's non-linear bulk stiffness and consolidation characteristics have also to be considered.

5.3 *Permanent displacements due to cyclic loading*

The permanent displacements developed due to cyclic loading result from: (1) straining (principally in shear) during the cycling, (2) subsequent volume changes due to dissipation of cyclically induced pore pressure and (3) drained and undrained creep. In the NGI approach, the permanent displacements developed during cycling are normally output from the finite element analyses used to calculate cyclic displacements, as described in Section 5.2 above.

Assessment of permanent displacement caused by pore pressure dissipation requires a semi-coupled finite element

consolidation formulation, as in the code PDCAM mentioned in Section 5.1. Approximate calculations can also be made assuming 1D-conditions beneath the foundation in cases where assessing the central settlements is the main aim. Simplified creep assessments can also be made for such cases.

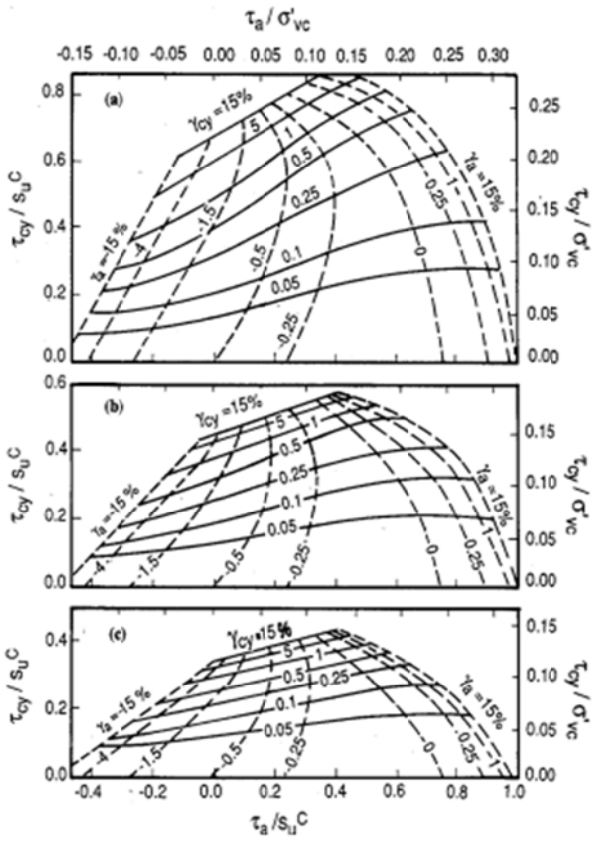

Figure 5.15: Examples of cyclic shear strain contour diagrams for triaxial type stress path on normally consolidated Drammen Clay.
a) N=1, b) N=10, c) N=100 cycles (Andersen, 2004)

The soil behaviour characteristics input into the analyses are the same as visualised and described for cyclic displacements assessment in Section 5.2, except that additional information is required about (1) the pore pressure generated by the cyclic loading and (2) the soils' reconsolidation characteristics. Examples of pore pressure diagrams are given in Figures 5.16 and 5.17, which follow the contoured format adopted earlier for shear strains in Figures 5.14 and 5.15.

Alternative displacement and stiffness calculation methods:

Still more advanced treatments are becoming feasible that may eventually provide the means to model together non-linear, hysteretic and anisotropic cyclic pore pressure generation and straining responses of soils with time dependent drainage. Such treatments must incorporate fully coupled treatments along with high-fidelity cyclic constitutive models that can be calibrated or checked directly against advanced laboratory tests.

At present such models are not applied in routine offshore practice. However, Wichtman (2005) reviews alternative explicit methods (including Boukovalas et al., 1984; Gotschol, 2002; Kaggwa et al., 1991 and Diyaljee and Raymond, 1982) and notes "a need for an explicit model exists which delivers the accumulation rates of the volumetric and the deviatoric strains".

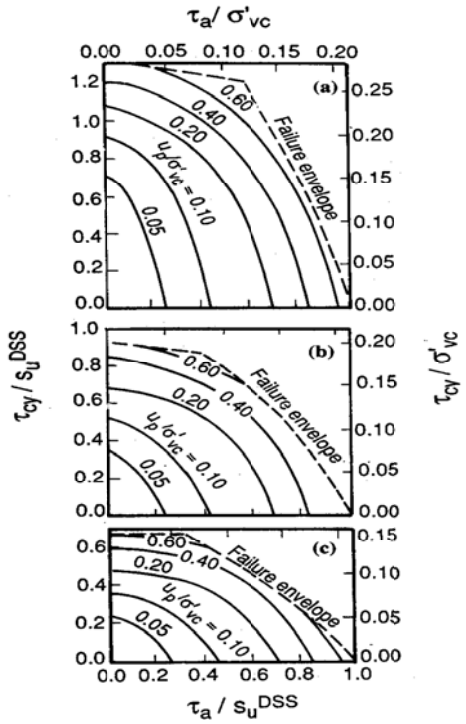

Figure 5.16: Examples of pore pressure contour diagrams for DSS type stress paths on normally consolidated Drammen Clay.
a) N=1, b) N=10, c) N=100 cycles (Andersen, 2004)

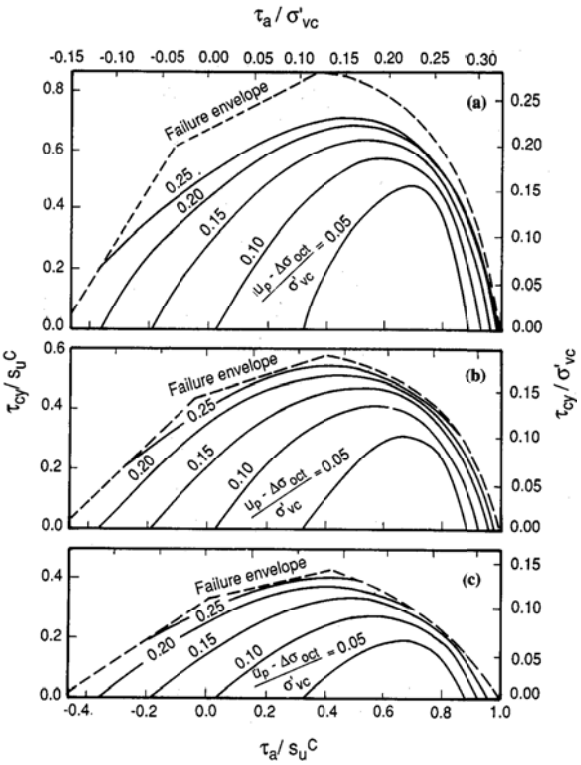

Figure 5.17: Examples of pore pressure contour diagrams for triaxial type stress path on normally consolidated Drammen Clay.
a) N=1, b) N=10, c) N=100 cycles (Andersen, 2004)

More challenging, implicit "time domain" procedures, (where each cycle is calculated with an appropriate constitutive model and iterated over many small strain increments) have also been implemented in finite element programs intended, in particular, for earthquake geotechnical engineering applications. Each cycle is calculated with an appropriate constitutive model and iterated over many small strain increments. Examples of elasto-plastic models (such as Prevost, 1977; Mroz et al., 1978; Chaboche, 1994), endochronic models (Valanis and Lee, 1984) or hypoplastic models (e.g. Gudehus, 1996 or Niemunis and Herle, 1997) have been proposed. This procedure becomes difficult after a significant number of cycles (say 50) because (i) computational resource costs become high and (ii) and errors can accumulate with the constitutive models and integration algorithms that may be employed. When considering large numbers of cycles, the explicit procedure appears more robust and appropriate. Wichtman, Niemunis and Triantafyllidis (2004) have recently developed a procedure that combines implicit and explicit elements. Careful validation will naturally be required to assess the new methods' reliability and predictive capabilities before they are adopted for routine use.

5.4 *Equivalent cyclic soil spring stiffnesses*

Equivalent overall soil spring stiffnesses, which are defined as the overall (secant) ratios between the amplitudes of particular components of cyclic foundation and the resulting displacement amplitudes, can be assessed from the output of the finite element analyses described in Section 5.2 and exported for use in soil-structure interaction analyses. However, as emphasised earlier, the soil response is likely to be highly non-linear and no single stiffness can match behaviour fully from small loads up to the maximum. Secant stiffnesses defined from the extreme maximum load case will be too soft to match the response seen at lower, more frequently encountered, cyclic loading levels. Interaction is necessary with structural engineers to ensure compatibility between the geotechnical and the dynamic analysis cases and parameter sets.

One simplified approach that has been applied in dynamic analyses of large diameter GBSs on clay is to calculate an 'operational' stiffness by inputting (over the peak period of the storm) into the cyclic finite element analyses an 'operational' cyclic load calculated as the Root Mean Square (RMS - equivalent to a standard deviation, as applied in alternating current electrical engineering) cyclic deviation from the mean load. The stress strain input is similarly defined in terms of RMS for the cyclic load composition in the peak period of the storm. The finite element output gives equivalent RMS displacements and stiffnesses, working from the soil cyclic data described in Section 5.2. Further details can be found in Andersen (1991).

Foundation damping behaviour, which can also be important, may be calculated from the finite element analyses by integrating the damping expected in each element over the soil volume. Such calculations have been implemented in the finite element program INFIDEL (Hansteen, 1991), which also performs stiffness calculations according to the method described above. INFIDEL can consider circular and elliptic geometries with axisymmetric or non-axisymmetric loads and with elastic far field elements that can extend to infinity horizontally. Such analyses require soil damping functions related to stresses or strains and the number of applied cycles.

The analyses described above give secant stiffnesses. The load-displacement relationships applying to individual cycles may also be established by applying Masing's rule and calculating the relative area retained within the load-displacement loop as the ratio.

6 CALCULATION PROCEDURES FOR PILES

The Commentary section of the industry standard recommendations (API RP2GEO 2011) for offshore design recognises several methods to calculate static axial pile capacity and lateral loading response. The API axial approach for clay relies on UU triaxial shear strength measurements. Alternative approaches that are used in some North Sea and other applications are the ICP-05 effective stress approach (Jardine et al., 2005), which combines an holistic approach to YSR assessment with sensitivity and interface shear measurements (and CPT measurements for base resistance), and the NGI-05 total stress procedure (Karlsrud et al., 2005) which relies on UU shear strength and plasticity index although Karlsrud (2012) proposed that the NGI-05 clay method for clays should be based on DSS undrained shear strength tests. API RP2GEO (2011) indicates a preference in sands for the Commentary 'CPT methods' which all require high quality CPT data, while the ICP-05 sand method also requires interface shear tests.

Methods for addressing cyclic loading, however, are not equally well developed. Review of (i) cyclic load tests on piles and (ii) cyclic loading on piled structures led Jardine et al. (2012) to conclude that cyclic loading effects can be more important for pile capacity than has been appreciated conventionally, particularly for structures with high ratios of cyclic to average loads. They argue that current design practice needs to be reconsidered and start by relating potential effects of axial load cycling to the static axial capacity considerations.

Jardine et al. (2012) argue that cyclic pile capacity depends on effective stresses, which can change due to stress redistribution and/or pore pressure generation. Storm loading conditions will usually lead to a principally undrained response and potential excess pore pressure generation in clays. When the permeability of sand is high enough to give drained conditions during storms, volume changes can develop that provide scope for possible radial straining close to the pile shaft. If the response is dilative, as it may be at high shear stresses in dense sand, the expanding interface shear zone reacts against the surrounding soil mass and generates radial stress increases. The reverse applies when the sand close to the shaft contracts under cyclic loading. However, as reviewed by Sim et al. (2013), the soil near to the pile shaft is subject to tight kinematic controls. Effective stress changes can develop in both sands and clays through constrained dilation without the necessity for any excess pore pressure changes.

6.1 *Effects of axial cycling on axial capacity*

Jardine et al. (2012) recommend that a graduated cyclic assessment process should be applied to evaluate cyclic effects of axially loaded piles (Figure 6.1), starting with simple summary interaction diagrams that relate the cyclic capacity to the static capacity and progress, if required, to full analyses of site specific soil-structure analyses considering local storm loading.

Examples of interaction diagrams for driven and jacked displacement piles are given in Figures 6.2, 6.3 and 6.4, which show results of in situ load tests on piles driven in clay, and Figures 6.5, 6.6 and 6.7 which show results of model or in-situ tests on displacement piles in sand. The Haga clay has medium plasticity, moderate sensitivity and is lightly over consolidated. Onsøy is a plastic, normally consolidated clay, while Lierstranda clay has low plasticity and low OCR. The Tilbrook Grange profile consists of low plasticity, very stiff, glacial till overlying highly plastic, high OCR, Jurassic Oxford clay; both strata have high OCR. Fontainebleau NE34 sand is a fine grained industrial silica sand that is widely used for centrifuge and other model studies in France and elsewhere, which was air-pluviated in a dense to medium-dense state for the model

experiments reported. As mentioned earlier, Dunkirk sand is a fine principally silica shallow marine deposit from Northern France that is considered typical of Southern North Sea sands and has a predominantly medium-dense to dense site profile: see Jardine et al. (2006). Labenne sand is a loose to very loose dune sand from SW France.

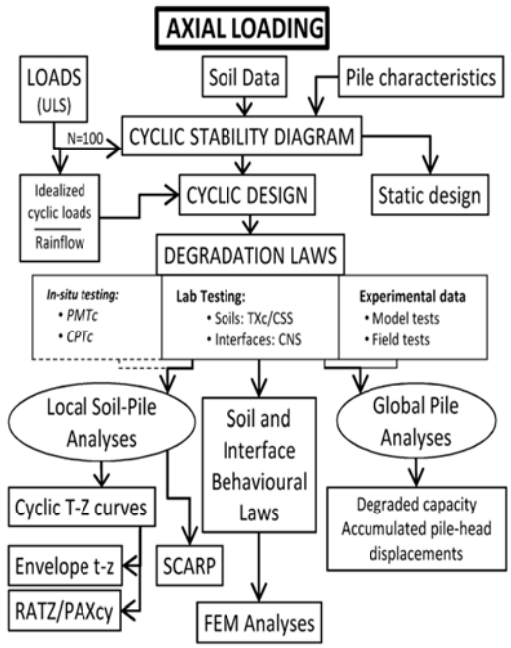

Figure 6.1: SOLCYP graduated design approach for piles under axial cyclic loading (Jardine et al., 2012)

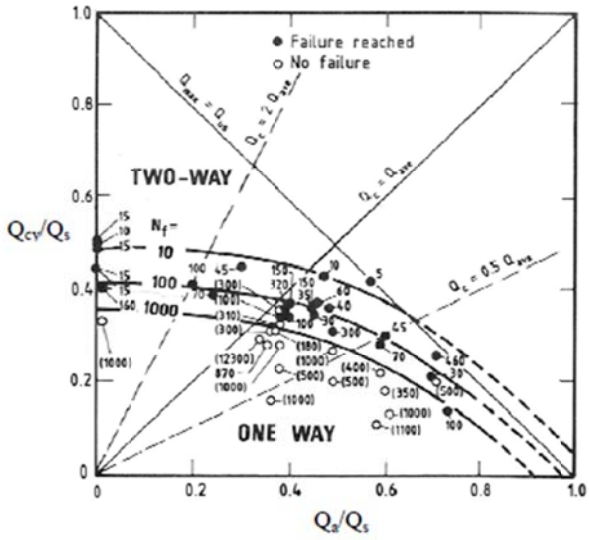

Figure 6.2: Interaction diagram with number of cycles to failure N_f at Haga as function of Q_a and Q_{cy} normalized by static tension capacity Qs (Karlsrud and Haugen, 1985b)

Equivalent interaction diagrams for bored piles are presented later in Section 11.

The interaction diagrams show the combination of average (Q_a) and cyclic (Q_{cy}) loads, normalised by the static shaft capacity (often defined in tension) that cause failure after a given number of cycles. For historical reasons the diagrams apply alternative forms. Figures 6.3, 6.4 and 6.8 plot cyclic failure load, Q_{max} rather than Q_{cy} on the vertical axis as in the other pile and soil element tests. However, as $Q_{max}=Q_a+Q_{cy}$ the two plot types contain the same information. The Haga clay set displayed in Figure 6.2 represent the most comprehensive set of available cyclic field test data.

Practical considerations lead to most axial cyclic pile load tests involving just one-way loading with $Q_{cy} < Q_a$. Such conditions plot in the lower right quadrant of interaction diagrams where cyclic degradation is at its least severe. While such data often plot close to the first diagonal 'no-damage' line potentially significant shaft capacity degradation (up to 25%) is seen under such conditions in some soils. High level cycling with low values of Q_a/Q_a leads to more severe effects in the two-way sector where failure can develop within 100 cycles under maximum loads less than one-half of the static capacity. Lehane et al. (2003) report field tests on pile groups installed in soft Kinnegar clay-silt, interpreting the results to show that both static shaft capacity and cyclic performance are affected negatively by group interaction.

In general, axial cycling affects sands and sensitive low OCR clays that have high drained peak friction angles, φ′, and interface shear δ values more severely than most other deposits. Carbonate sands are especially sensitive to cycling. Problematic low plasticity clays also exist that show high φ′ and δ values but develop low axial static capacities and are highly susceptible to cyclic loading. Normalized cyclic loading levels exist below which large numbers of cycles can be applied without impacting significantly on load-displacement behaviour. These 'zero damage' curves are most favourable in high OCR clays that develop low δ values resulting from residual shear surfaces during installation and under loading. Low level cycling can enhance pile capacity (Jardine and Standing, 2012).

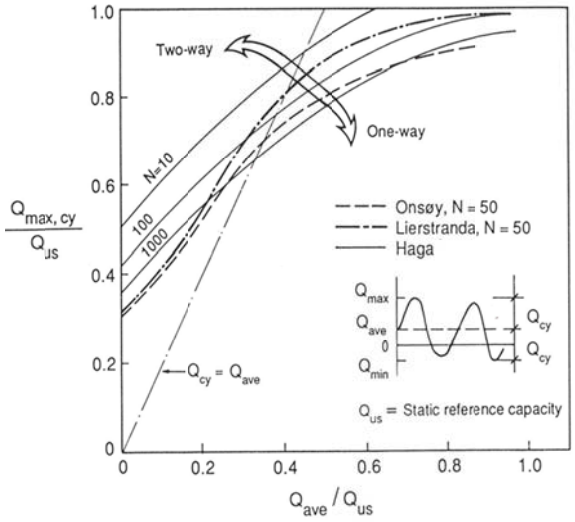

Figure 6.3: Interaction diagram with comparison of Onsøy and Lierstranda cyclic axial pile test capacities with Haga (Karlsrud et al., 1992b)

The interaction diagrams illustrate the crucial importance of knowing, even for screening assessments, the likely static axial shaft capacities, cyclic loading components and numbers of cycles. Interaction diagrams provide simple and helpful guidance when these parameters are known and good matches exist with the soil conditions at each site under review. But care must be taken to allow for a range of soil responses. For example, piles driven in high OCR plastic London or Flandrian clays (at Canons Park or Merville) provide contours that plot above those for Haga in Figure 6.2, while the contours for the more susceptible Lierstranda or Onsøy sites pass well below the Haga trends. A comparison of the positions of these sites N_f =

50 failure curves is given in Figure 6.8. It is interesting to observe in Figure 6.6 that the normalised cyclic behaviour of the piles in the loose to very loose Labenne dune sand does not seem to be significantly lower than in the medium dense to dense Dunkirk marine sand.

Cyclic interaction diagrams can be predicted by a range of procedures when suitable cyclic pile test data is unavailable. Karlsrud and Haugen (1985) matched their Haga clay cyclic pile tests results with site-specific monotonic and cyclic DSS laboratory tests. Their 'DSS' and 'pile test' cyclic failure interaction diagrams developed the same normalised patterns, provided the axes were normalized by the appropriate monotonic DSS strength or the pile shaft tension capacity respectively. This held true whether the DSS tests were conducted on intact or remoulded clay.

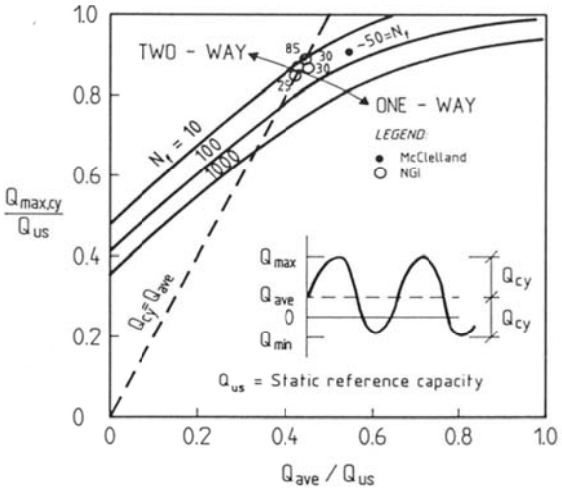

Figure 6.4: Interaction diagram with comparison of Tilbrook Grange and Haga cyclic axial pile test capacities (Nowacki et al., 1992).

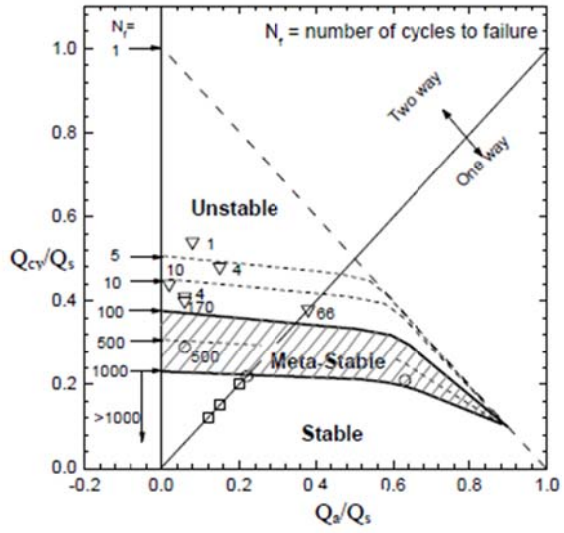

Figure 6.5: Shaft interaction diagram with number of cycles to failure Nf from Mini-ICP piles installed in medium dense Fontainebleau NE 34 sand under a vertical confining pressure of 150 kPa in the large INPG calibration chamber; after Rimoy et al., 2012.

Cyclic capacity clearly depends on the number of cycles N applied. In a design storm the cyclic load will vary from one cycle to the next, and the design storm composition needs to be transformed into a regular cyclic loading history by an equivalent number of cycles approach. This can be achieved with an accumulation procedure, using contour diagrams with either pore pressure, cyclic shear strain or shaft capacity damage as the memory parameter, as explained previously for shallow foundations.

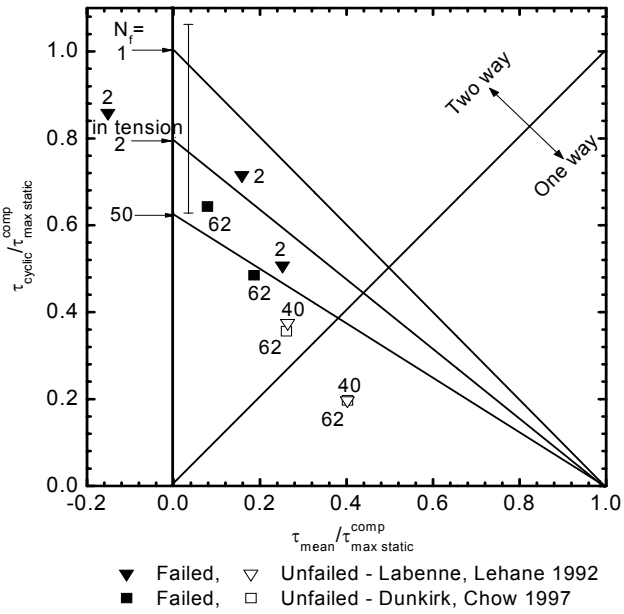

Figure 6.6: Interaction diagram with local cyclic shaft failure from ICP tests in sand at Labenne (loose to very loose dune sand) and Dunkirk (medium dense to dense marine sand). Open symbols = unfailed, interpreted from tests by Lehane 1992 and Chow 1997. (ICP = Imperial College Pile).

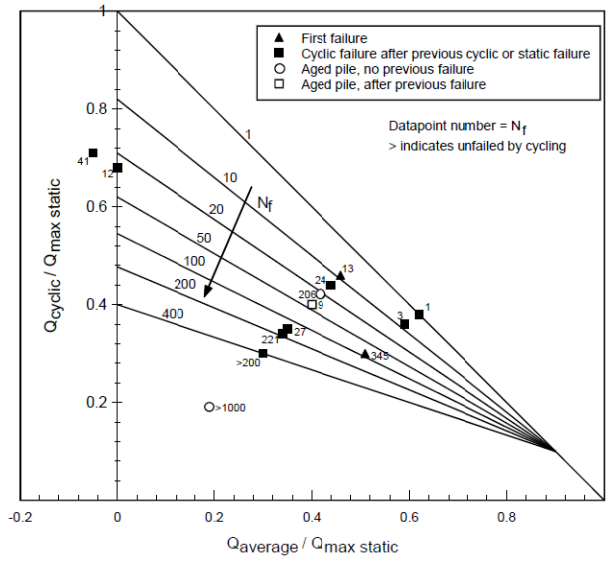

Figure 6.7: Summary interaction diagram from cyclic tests on steel tubular piles driven in dense sand at Dunkirk; after Jardine and Standing 2013. Piles loaded in tension

Field cyclic tests with highly instrumented piles (by Bond, 1989; Lehane, 1992 and Chow, 1997, supported in model tests by Tsuha et al., 2012) led Jardine et al. (2005a) to set out a simple method for predicting the potential reduction of local shaft resistance for piles subject to groups of uniform load cycles. Noting that shaft capacity reduces in both sands and clays in step with local radial effective stress changes that develop over the shaft they apply either Equation (3) for local

analyses of cyclic shaft degradation or an equivalent global 'A, B, C' form to develop overall interaction diagrams (see Jardine and Standing, 2012). Highly instrumented pile tests and undrained DSS tests have shown that in cases where $\tau_{vh} / \sigma'_v <$ tan δ, the relative loss in normal effective stress ($\Delta\sigma'_v / \sigma'_{vc}$) may be nearly independent of the average shear stresses applied and can be expressed with reasonable accuracy by either the simple function given below of normalised cyclic shear stress amplitude ($\tau_{cyc} / \tau_{max,stat}$) and number of cycles (N) such as the power law given below, or by an equivalent log (N) expression:

$$\frac{\Delta\sigma'_r}{\sigma'_{r0}} = A\left(B + \frac{\tau_{cy}}{\tau_{\max\, stat}}\right)N^C \qquad 3)$$

It may not always be appropriate to neglect the average shaft load component, as noted for example in the Drammen clay tests reported by Andersen (2004). More complex forms than Equation 3 can be developed and applied when this is proven by appropriate laboratory tests. Cyclic DSS, triaxial or HCA experiments may be undertaken to determine the material coefficients (such as the A, B and C terms in the equation given above) and define rates of radial effective stress reduction under cycling for both clays and sands; see for example the tests on Clair West of Shetland glacial tills described by Jardine et al. (2011). The approach requires laboratory test samples to be consolidated to the radial effective stresses predicted by the ICP methodology. It is very important to specify sufficiently long creep pause intervals in such tests. Pre-cycling should also be considered. As with shallow foundations, an accumulation procedure can be applied to consider irregular storm loading: see Jardine et al. (2011) and Merritt et al. (2012). The same principles can be applied in local beam column (T-Z) analyses of progressive cyclic failure (see Atkins, 2000).

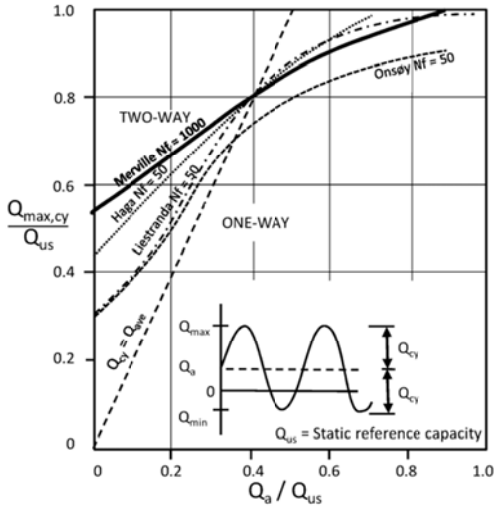

Figure 6.8: Comparison of Nf = 50 cyclic failure line for piles driven in several different clays

Some alternative procedures use 'global' purely empirical degradation laws calibrated to fit appropriate (good quality) experiments on model or field pile tests. Degradation laws have been proposed by, for example, Diyaljee and Raymond (1982) Poulos (1982) or Briaud and Felio (1986), the simplest of which are:

$$P(N)/P(1) = k \bullet N^{-m} \qquad (4)$$

or

$$P(N)/P(1) = 1 - t \bullet \mathrm{Ln}(N) \qquad (5)$$

where P(N) is the value at cycle N of the property P being considered. P(1) is the reference value which can be the value for monotonic loading. The parameters m and t depend on the type of soil, the pile-soil system (rigidity) and the installation method. They are also expected to depend on the load characteristics although they have been found independent in some experiments. As illustrated by the interaction diagrams, it is imperative that the degradation laws are based on the relevant ratio between average and cyclic loads. The degradation laws can be applied (essentially to extrapolate and/or interpolate) any credible experimental observations regarding both capacity and stiffness trends.

6.2 *Lateral and moment capacity*

No screening tool equivalent to the axial cyclic loading interaction diagrams discussed above has been proposed to date for lateral or moment loading. Analogy with axial loading suggests that critical situations may perhaps be identified by developing equivalent iso-contours of relative pile head displacements y/B as functions of normalised average and cyclic load components based on experiments or analyses. Another approach is to develop purely empirical stiffness degradation laws, as outlined above for axial loading. Khemakhem et al. (2012) and Rosquoët et al. (2013) set out such treatments from their centrifuge lateral loading pile experiments on soft clays and sands respectively.

6.3 *Numerical analyses of pile response*

The simplified 'global' cyclic axial pile capacity approaches described above do not consider the effect of pile axial flexibility, which leads to progressive degradation along the shaft from the pile head downwards. For long and flexible piles this can give a greater cyclic effect than that estimated based on interaction diagrams if the diagrams are based on less flexible piles. The lateral loading response depends more critically on the relative slenderness and flexibility of the piles. Relatively slender jacket piles respond quite differently to low length-to-diameter (L/D) monopiles or anchors.

If 'global' approaches such as those outlined above for axial capacity indicate that pile capacity may be degraded significantly by cycling, more detailed site specific analysis may be considered. More detailed analyses may also be needed to check for any critical impacts of un-modelled features such as variable soil layering or pile flexibility. Such analyses are also necessary if it is important to determine cyclic and permanent displacements, as well as equivalent cyclic soil spring stiffnesses.

Numerical beam-column analyses and more advanced finite element analyses can be undertaken to meet these aims. Jardine et al. (2012) discuss the potential use of completely implicit numerical analyses involving cycle-by-cycle analysis and realistic constitutive laws to model the soil and the interface behaviour. They note, however, that such treatments do not appear to have been applied yet in mainstream offshore practice. Explicit finite element procedures, which rely on empirical or experimental accumulation laws, offer feasible practical application options: see Andersen and Høeg (1991), Saue et al. (2010) or Grimstad et al. (2013).

As mentioned above a key aim is to capture in axial analyses the progression of cyclic degradation from the pile head downwards. When lateral loading is applied one must also consider whether gapping may develop along the upper part of the pile and lead to subsequent erosion from water circulating in any soil-pile crack. Lateral cyclic loading is likely to degrade the shaft resistance available between the lowest depth where shaft friction is completely eliminated by gapping, down to the level where lateral straining is sufficiently low to cause no significant damage; Merritt et al. (2012). Approximate p-y

analyses and small strain laboratory testing can provide guidance regarding the lower depth limit of this transitional range.

Any realistic numerical approach has to consider the effects of pile installation, which presents a considerable challenge. One key effect with displacement piles is the modification of soil properties around the pile. Extensive testing with highly instrumented piles (see Bond and Jardine, 1991 and 1995, Lehane et al., 1993, Lehane and Jardine, 1994a,b and Chow, 1997) demonstrated that local shaft shear resistance depends fundamentally on the effective radial stresses σ'_r applying at the interface. Soils, such as brittle plastic clays, that develop thin residual shear strength bands during displacement pile installation present low interface friction δ values that limit the τ_{rz} / σ'_r ratios and degree of cyclic damage that can be developed; Jardine (1991 and 1994). Piles driven in soils that develop high δ angles close to their $\varphi'_{critical\ state}$ angles experience large strain shearing which is considered within the NGI methodology as equivalent to remoulding. Examples of such soils include the Haga clay referred to earlier. Interface shear zones also develop around displacement piles driven in sands. Grain crushing takes place beneath the pile tip and a thin zone of finer and denser sand builds up over the pile shaft whose properties are distinctly different from those of the parent sand; see Yang et al. (2010).

The stress fields applying around pile shafts are modified considerably by pile installation. Total stresses increase sharply as the pile tip passes any given layer during installation and change with time after installation due to pore pressure redistribution and dissipation, creep and pre-shearing. All of these processes can change shaft capacity, although the trends vary with soil types. Jardine et al. (2006) showed that piles driven in sands can develop very significant gains in shaft capacity due to long term ageing processes. The latter are far clearer and more marked with piles that are not taken to failure during their ageing periods. These conclusions have been reinforced by Rimoy (2013). Monotonic and cyclic pre-shearing to failure can also add substantially to the capacity in high δ, low OCR, clays as illustrated in Figure 6.9. Thixotropy can cause similar increases in some cases. Andersen and Jostad (2002) consider that thixotropy can be as significant a factor as the radial effective stress development in some cases. They offer a procedure to allow for set-up effects in suction anchors design that might also be applied to driven piles. However, consideration must be given to potential brittleness when considering highly overconsolidated clays and dense sands. Full failure leads to sharp capacity losses through dilation and other processes in such soils: see Bond and Jardine (1995) and Jardine et al. (2006). In design the critical condition for capacity is normally that the design storm comes soon after installation, and one may then not be able to fully account for long term beneficial effects that are expected in clays with low OCR, particularly clays with low plasticity and sands. In overconsolidated clays and very dense sands, however, preshearing effects could be negative, and one should consider whether the long term situation can be critical. For fatigue, however, modelling of long term effects can be important.

The ICP effective stress methodology can be extended very naturally to consider cyclic capacity sands and clays. Shaft capacity reduces in step with the local radial effective stresses. Predictions of field behaviour rely on developing relationships between normal effective stress and cyclic loading parameters through field data or cyclic DSS, triaxial or hollow cylinder apparatus (HCA) laboratory tests. The approach is similar to that of Karlsrud and Nadim (1990), although the ICP approach requires laboratory test samples to be consolidated to the radial effective stresses predicted by the ICP methodology, which typically anticipates higher radial effective stresses than experiments by NGI (see Figure 6.10). The samples may be remoulded before testing when dealing with sensitive clays. It is important to allow suitable periods for creep and other ageing effects in such tests.

Karlsrud and Nadim (1990) proposed that monotonic (and cyclic) interface strength of should be calculated for clays on the basis of DSS tests on remoulded clay reconsolidated to normal (vertical) effective stresses matching the radial effective stress values σ'_{rc} interpreted as acting on the pile shaft after full pore pressure dissipation. The measured DSS shear strengths are corrected for the interpreted differences in the octahedral effective stresses developed in the DSS test and the pile 'disturbed' clay zone.

Karlsrud (2012) argues that the uncertainty in the effective stresses in the disturbed zone around the pile is a weakness in approaches that rely on effective stresses, and he preferred to retain empirical total stress approaches for defining monotonic and cyclic capacity in clays.

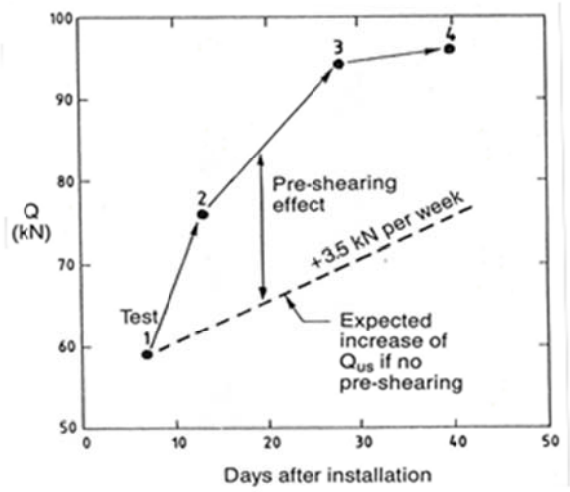

Figure 6.9: Influence of time and monotonic pre-shearing on monotonic axial pile capacity at Haga (Karlsrud and Haugen, 1985a

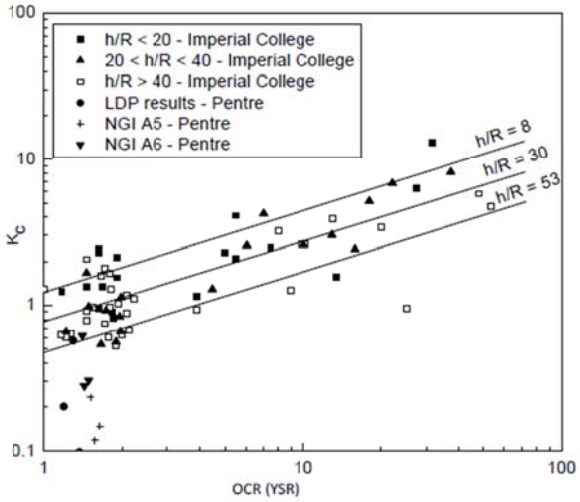

Figure 6.10: K_c trends with apparent OCR (YSR) and pile tip position (h/R) from Lehane (1992), adding measurements at Pentre by Imperial College by Chow (1997), Karlsrud et al. (1992) and McClelland Engineers (LDP)

The procedures based on laboratory tests are more uncertain for sands than for clays. Storm loading conditions will usually lead to a principally undrained response in clays. For sands, however, drainage may occur during a storm and volume changes can develop that provide scope for possible radial straining close to the pile shaft. If the response is dilative, as in the final stages of static loading to failure, the expanding interface shear zone reacts against the surrounding soil mass

and generates radial effective stress increases. The reverse applies when the sand close to the shaft contracts under cyclic loading.

The effective stress changes observed in field and model pile tests (Lehane et al., 1993, Tsuha et al., 2012) are not modelled in standard laboratory tests but may be addressed in more sophisticated explicit finite element analyses as described later. Constant Normal Stiffness (CNS) tests reproduce the kinematic conditions that apply in any linearly elastic soil mass and indicate how radial effective stresses may fall under cycling along a pile shaft. A challenging aspect is to set fully appropriate CNS values during practical applications as they depend on (i) the sand's anisotropic, non-linear and pressure dependent stiffness and (ii) the inverse of the pile's outside diameters (see Jardine et al., 2005; Pra-ai, 2013). Tsuha et al. (2012) report local effective stress measurements made during pile cyclic loading and argue that constant volume (undrained) tests provide upper bound, infinite CNS, conditions and deliver safe design parameters for both sands and clays.

The soil parameters required to inform any numerical analyses depend on the approach that will be chosen. The ICP approach relies, for clays and sands, on constant volume DSS or HCA tests to predict rates of effective stress decay, combined with interface shear effective stress testing. The NGI's total stress clay approach relies on monotonic and cyclic shear tests on both intact and reconsolidated remoulded soil. The cyclic shear strength depends on ratio between cyclic and average shear stresses, applied stress path (TC, TE or DSS), and the number of cycles. Pore pressure generation due to cyclic loading and consolidation characteristics has to be tracked if a pore pressure accumulation procedure is to be applied, and in cases where partial drainage needs to be considered. The undrained shear strengths, thixotropy strength gain and virgin loading consolidation characteristics of the remoulded clay are required, along with the undrained shear strength of reconsolidated remoulded clay and unload-reload consolidation characteristics of both intact and remoulded clay samples, if site-specific set-up calculations are to be undertaken with the NGI approach.

Beam column analyses

There are several computer programs to calculate axial and lateral cyclic capacities based on beam column analyses. The soil can be represented by:

- Envelopes, such as the "cyclic" API p-y curves, (equivalent "cyclic" t-z curves have yet to be recommended by API or ISO), based on routine site investigation testing with UU laboratory tests.
- Cyclic p-y or t-z curves obtained by degrading static capacity using simple degradation laws
- Cyclic t-z curves generated by a more sophisticated algorithm, such as those described below.

The offshore Industry has developed codes for soil-structure interaction analysis such as SPLICE developed by Clausen (NGI 2006) that consider a (usually) linear superstructure supported by a simplified non-linear pile foundation system. The piles are represented by beam-column p-y, t-z and q-z curves that can be specified from several built-in procedures (as specified by API, ISO or DNV for example) or by direct manual input. The user may then take into account aspects that may not be covered by existing rules or recommendations. Pile group interaction is treated by a linear elastic procedure and a range of options exists for soil spring representation.

Current oil, gas and wind industry standards (G.L., 1999 or DNV, 2010) specify API/ISO p-y procedures for horizontal load-deformation analysis. As discussed by Jardine et al. (2012) these standard p-y procedures have limitations and imperfections that merit attention. Measurements on instrumented piled structures demonstrate that the standard beam-column curves and elastic interaction analyses can over-predict movements of single piles and groups (Jardine and Potts, 1988 and 1992) and hence structural natural frequencies; see for example Kühn and Watson (2000). Centrifuge tests performed by Aderlieste et al. (2011) in sands indicate that pile diameter increases have a greater effect on spring stiffness and static/cyclic lateral capacity than predicted by the API formulation. Advanced numerical analysis also questions the basis of the p-y methods to large diameter piles. Finite Element studies by Achmus et al. (2005, 2008 and 2010) and Augustesen et al. (2009), inter alia, also show that the API procedures may not be appropriate for large monopiles in sands under monotonic loading. Other cyclic finite element analyses by Saue et al. (2010) and Grimstad et al. (2012) of monopiles made with the previously described NGI clay accumulation model indicate lower displacements, rotations, bending moments and shear forces than standard p-y calculations.

Computer programs are available commercially that apply beam-column methods to assess axial pile response under cycling. The earlier cyclic t-z codes include RATZ (Randolph, 1994), PAXCY (Karlsrud et al., 1986) and PAX2 (Nadim and Dahlberg, 1996).

RATZ utilizes the load-transfer scheme illustrated in Figure 6.11. Under monotonic loading, the t-z curve consists of:

- A linear stage $\tau_o = k \cdot w/r_o$ that extends up to a fraction $\xi\tau_p$ of the peak shear stress (ξ is a parameter between 0 et 1)
- A parabolic stage with initial gradient k and final gradient of zero when $\tau = \tau_p$
- A softening stage, where the current value of shaft friction is related to the absolute pile displacement by :

$$\tau_o = \tau_p - 1.1\left(\tau_p - \tau_f\right)1 - \exp\left(-2.4(\Delta w/\Delta w_{res})^{\eta}\right) \qquad (8)$$

where τ_f is the residual value of shaft friction, reached after an additional displacement of Δw_{res}, with Δw being the post-peak displacement. The parameter η controls the shape of the strain softening curve.

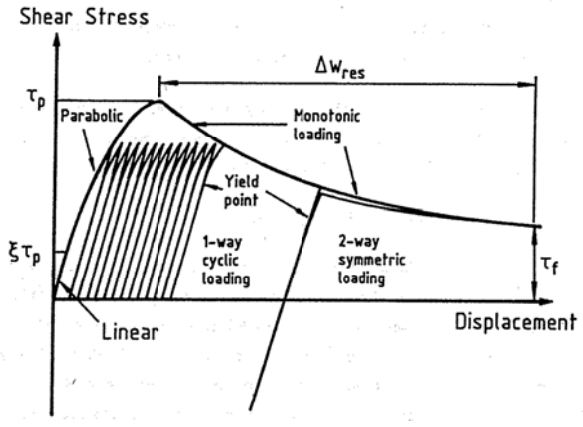

Figure 6.11: Load-transfer t-z curve used in RATZ

The accumulation of permanent displacement under cyclic loading is controlled by the parameter ξ which defines a yield point that is engaged on reloading. The post-yield plastic displacements are considered as equivalent to post-peak monotonic displacement. This leads to a gradual degradation of the shaft friction from peak to residual. An implicit assumption is that the load-transfer exhibits post-peak softening. The safe cyclic range can be varied in a way similar to that proposed by Goodman for metals. As noted above, many soil types that are susceptible to axial cyclic loading also show ductile static

behaviour. Key input parameters in RATZ are the nominal linear shear modulus, G, the yield threshold, ξ , the peak shaft friction, τ_p, the residual shaft friction ratio, τ_r/τ_p, and the displacement to reach residual shear stress, Δw_{res}. For non-linear strain-softening, the shape factor, η, determines the exponential shape. For cyclic loading, the cyclic residual shaft friction ratio, τ_{cr}/τ_p and the absolute value of the yield ratio, ξ must be specified. Static parameters can be obtained from standard engineering practice. Cyclic parameters require calibration on series of fatigue curves from DSS, TX or CNS tests using the internal RATZ algorithm.

Erbrich et al. (2010) present methods for calculating cyclic behavior of axially loaded drilled and grouted piles in compressible cemented carbonate soils and laterally loaded drilled and grouted or driven piles in uncemented carbonate soils, implemented in software called CYCLOPS and pCyCOS, respectively. The programs are beam column approaches with t-z and p-y models. The t-z formulation in CYCLOPS is developed from RATZ, with the RATZ model enhanced by including a variable bias parameter and an initial softening parameter, and the shape of the t-z curve is modified within and immediately outside of a gap zone formed during cyclic loading. A significant number of CNS test is needed for the model to be used in practical design. The p-y curve in pCyCOS is established from finite element analyses of a horizontal disk around the pile with input in the form of a cyclic stress strain curve from monotonic and cyclic simple shear tests. The present version focuses on two-way cyclic loading. The procedures in both programs have a theoretical basis, but include a number of factors determined from empirical calibration. Both programs require a competent user with considerable skill and care. The programs were developed for carbonate soils, but have potential for more general applicability.

Alternative t-z procedures include the code PAXCY/PAX2 (Karlsrud et al., 1986; Nadim and Dahlberg, 1996) which incorporates key features of the NGI's laboratory based approach for clays. Here the t-z springs are established by integrating with respect to radius the shear strains γ_{rz} developed in the disk of soil surrounding the pile segment. The soil around the pile is divided into the three zones reflecting different degrees of disturbance during installation with a thin remoulded zone closest to the pile wall. The cyclic soil response is based on shear strain contour diagrams of the type presented in Figure 5.14, which show the average and cyclic shear strains as functions of average and cyclic shear stresses after a given number of cycles. Ideally, contour diagrams should be established for all the three zones around the pile. However, the inner reconsolidated "remoulded" zone is assumed to govern capacity and displacements. The DSS test results are corrected for octahedral effective normal stress conditions as proposed by Karlsrud and Nadim (1990) and mentioned previously.

It is assumed that the pile's cyclic loading history can be expressed by load parcels that each contains a fixed number of cycles with constant average and cyclic loads. The pile response is calculated at the beginning and end of each load parcel. Diagrams of the type shown in Figure 5.14 are used to establish relationships between average shear stress, τ_a, and average shear strain, γ_a, and between cyclic shear stress, τ_{cy}, and cyclic shear strain, γ_{cy}. The two relationships are not independent, however, and iterations are performed until acceptable convergence is obtained between the calculated τ_a and τ_{cy} distributions along the pile.

The effects of cyclic loading on capacity and displacements are taken into account by using strain contour diagrams of the type shown in Figure 5.11. The strain accumulation procedure described previously is followed over the cyclic load history, and the equivalent number of load cycles at the beginning and end of the specified load parcels is determined.

PAX2 is a simplified version of PAXCY that allows the NGI approach to be applied more easily and rapidly. PAX2 assumes that the cyclic shear strain is independent of τ_a, eliminating need to iterate the τ_a and τ_{cy}-γ_{cy} relationships. The programme contains a database of normalized stress-strain functions, and the equivalent number of cycles can either be specified or estimated automatically based on storm duration, soil type, platform type, and ratio between average and cyclic loads. Worked calculation examples in Karlsrud and Nadim (1990) demonstrated that PAXCY predicts pile displacements and stress redistribution well along the shafts of piles tested at Haga under various combinations of average and cyclic loads. Parallel analyses made with PAX2 and RATZ show at least reasonable agreement for the static and cyclic load cases.

Atkins (2000) report an alternative t-z formulation based on the simple 'A, B, C' effective stress ICP procedure (Jardine et al., 2005) that can be used in clays or sands, provided suitable cyclic laboratory (DSS, triaxial or HCA) tests are undertaken. In this approach pile slip was the sole source of permanent pile head deflection under cycling, although cyclic stiffness also fell proportionally with shaft capacity degradation. As with the NGI approach, a cyclic accumulation method was used to address storm loading with relative local radial effective stress (and hence shaft capacity) loss being carried forward as the memory parameter. Atkins (2000) were able to reproduce the load displacement behaviour of cyclic tests performed in dense sands at Dunkirk with reasonable accuracy and went on to apply the approach in full soil-structure interaction analyses of offshore jackets experiencing extreme storm events.

The t-z beam-column programmes provide predictions for cyclic axial displacements and allow, in principle, permanent axial displacements to be tracked under-cyclic loading. The same degree of development has not been achieved in lateral p-y beam-column analyses. The 'cyclic p-y' variants do not address the gradual evolution of displacements under specified cyclic loading conditions, but simply give softer envelope curves that take some account of the degradation that might be expected under 'typical Gulf of Mexico' storms.

Simplified boundary element formulation

Poulos (1989) took a different approach to axial cyclic analysis in developing the SCARP code. Here a simplified boundary element formulation is used in place of the t-z beam-column formulation. The soil mass is represented by an elastic continuum, but allowance is made for end-bearing failure and pile-soil slip along the interface by specifying limiting values of the pile-soil stress at each pile element. Strain-softening of the interface can also be considered (Figure 6.12). The program allows for three major effects of cyclic loading: (1) degradation of shaft and end-bearing resistances and soil modulus, (2) loading rate effects and (3) accumulation of permanent displacements under non-zero average loads. The "reverse plastic stress" model, proposed by Matlock and Foo (1979) is assumed in which degradation D develops progressively during cycling with:

$$D = (1 - \lambda)\,(D' - D_{min}) + D_{min} \qquad (9)$$

where:
D = Current value of degradation factor
D' = Degradation factor for previous cycle
D_{min} = Minimum possible degradation factor
λ = Degradation rate parameter

SCARP tracks three degradation factors: D_τ for shaft resistance, D_b for base resistance and D_E for soil modulus. Each

expresses the ratio between the particular parameter and its corresponding value under static loading.

A loading factor D_R is applied in SCARP to the values of ultimate skin and base resistance and the soil modulus:

$$D_R = 1 = F_\rho \log_{10} (\zeta/\zeta_r) \quad (10)$$

where:
Fρ = Rate coefficient (typically 0.1 to 0.25)
ζ = Loading rate
ζr = Reference loading rate (from static loading test)

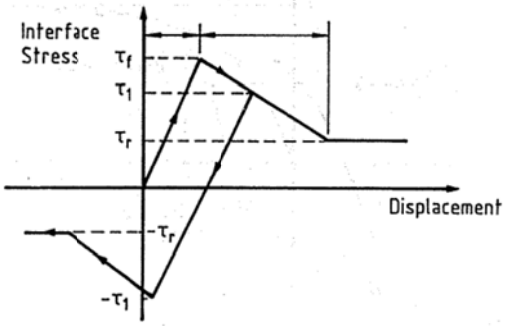

Figure 6.12: Strain-softening model curve used in SCARP

The incremental permanent soil displacements at the end of each cyclic parcel are computed from Diyaljee and Raymond's (1982) empirical expression:

$$\delta S_p = S_{pN}[n\delta X + (m\delta N/N)] \quad (11)$$

where:
δS_p =Increment in permanent soil displacement between cycle N and N+δN
δX = Change in stress level between cycle N and N+δN
S_{pN} = Permanent soil displacement at cycle N
m, n= Experimentally determined parameters, which are different for the shaft and base
$X = (P_o + 0.5P_c) /Q_c$
P_o = Mean load of loading parcel
P_c = Cyclic load amplitude of loading parcel
Q_c = Ultimate static capacity of the pile

Guidance is limited regarding input parameter selection for SCARP. Large ranges of values are proposed, based on laboratory and model tests with principally carbonate materials. One of the aims of the SOLCYP project (Puech et al, 2012) is to provide additional experimental data linking cyclic laboratory element and in-situ tests on clays and silica sands to trends from experiments on models of various scales and full scale piles.

Comparative studies by Chin and Poulos (1992) and others have shown that RATZ and SCARP lead to broadly comparable static load-displacement predictions, despite their fundamentally different approaches. However, the two codes' cyclic loading predictions can diverge considerably. Their use is most highly documented in relation to carbonate sediments. Further investigation and calibration over a wider range of geomaterial types is needed to increase confidence in quantitative predictions.

Explicit finite element procedures

Axial, lateral and rotational pile displacements are better considered by more advanced finite element analysis. Simplified, explicit, cyclic finite element procedures include those described for shallow foundations and suction anchors in Section 5.1 which are most suitable for monopiles with L/D ratios < 10. The calculations can also be used to establish p-y curves for monopiles (Saue et al., 2010 and Grimstad et al., 2013) to use in place of API guidance which may not be representative, as discussed above. Figure 6.13 shows the incremental displacements at failure of a 4.7m diameter, 16m long monopile for an offshore wind power structure in very dense sand. It was assumed here that conditions would be nearly undrained during storm loading due the pile's scale, so allowing the 'clay' procedures to be applied, although without the scope for high shear strengths to develop due to strong dilatancy.

The monopile is subjected to cyclic horizontal and moment loading at seabed level. The ratio between cyclic and average loads is high (2 to 10) and two-way loading was assumed. The ratio between overturning moment and horizontal load at seabed was 30m. The analysis involves 3D finite element analyses using cyclic laboratory data of the type described in Section 5.1, in this case assuming a fixed equivalent number of cycles of N_{eq}=10. The displacement pattern indicates a failure mode with active and passive zones in the upper part and a rotational failure in the lower part. The finite element analysis indicates a higher moment capacity than beam-column analysis using standard API p-y curves.

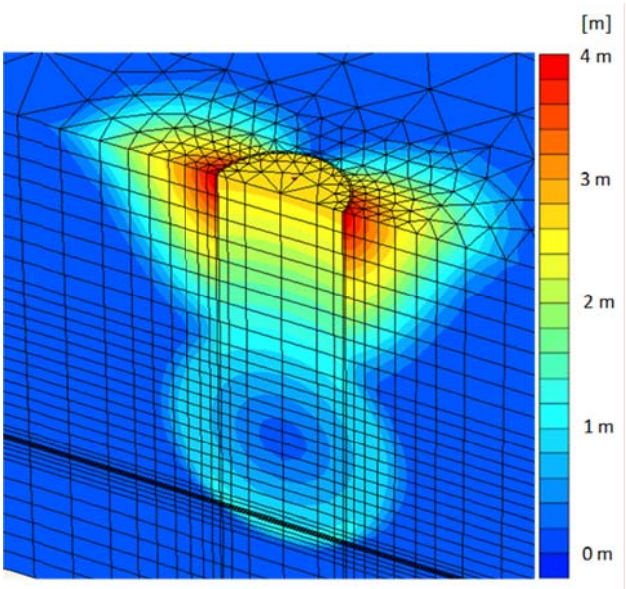

Figure 6.13: Incremental displacements at failure in a cross section of a PLAXIS 3D finite element analysis of a 4.7m diameter, 16 m long monopile in very dense sand (Saue et al., 2010)

6.4 *Equivalent cyclic soil spring stiffnesses*

Equivalent cyclic soil spring (axial, lateral or rotational) stiffnesses can be exported for dynamic soil-structure analyses that assess potential load amplification and fatigue trends by considering the cyclic loads and displacements given by the beam-column or finite element calculations. It is particularly important with wind-turbine structures to undertake fatigue calculations that address wind and wave loading throughout their working lifetimes. Very large numbers of small waves can be important in these assessments, and their impact depends on whether larger storms occur early or not in service and affect the stiffness under subsequent smaller cyclic loads.

The equivalent cyclic stiffnesses can be expressed as load-displacement curves defined at seabed level that are of course modified by the structure extending up from the sea bed.

7 CYCLIC SOIL PARAMETERS

Earlier sections have outlined the soil characteristics that need to be established to allow cyclic design assessments for shallow foundations, suction anchors, monopiles and piles. The necessary input parameters are re-summarized in Table 7.1 and in brief comments given below. The Table includes the parameters required to assess monotonic axial pile capacity because this step defines the key reference point for the cyclic axial interaction diagrams and degradation laws discussed in several parts of Section 6.

Shallow foundation assessment involves assessing drained frictional failure characteristics in cases involving sands when undrained conditions cannot be assumed to apply. Interface friction angles may also be needed to consider base sliding stability with low φ′ and δ soils, especially those with low sensitivity and potentially high OCRs.

Monotonic undrained shear strengths are crucial to the 'NGI' approach to cyclic characterisation in clays and undrained sands. The spread of tests required depends on the potential failure modes. If horizontal sliding is critical, for instance, compression and extension tests are less important than DSS experiments. Initial shear moduli are important to displacement and soil spring stiffness calculations, and may dominate the far-field response.

Cyclic testing is clearly crucial to cyclic shallow foundation assessments. Contour diagram reporting offers a convenient test data presentation format, independent of the calculation method eventually employed, as was illustrated in Section 5. Fatigue assessments require trends that may have been extended, potentially to hundreds of millions of cycles. Damping parameters are not always required, but may be called for with tall and slender structures.

Consolidation characteristics are needed to calculate dissipation and settlement rates stemming from cyclically induced pore pressures generated during storms. These processes are treated as being analogous to re-loading and are analysed with reloading moduli. The apparent pre-consolidation pressure is needed to determine the overconsolidation ratio, OCR (or Yield Stress Ratio – YSR), which is an important parameter in several respects, including cyclic behaviour.

Testing is undertaken on remoulded samples when site specific set-up analyses are performed in sensitive clays. The consolidation characteristics (modulus and permeability) contribute to analyses of set up times, while shear strength, sensitivity and thixotropy measurements are fed into analyses of the associated shear strength gains. Set-up factors may also be estimated as functions of plasticity and OCR following Andersen and Jostad (2002). Cyclic tests are not normally performed on remoulded clay as the skirt wall soils are assumed to have a similar cyclic response to the intact clay. But such tests can be considered in cases where the interface shear strength is likely to be crucial and/or significantly different to that of the intact soil.

The cyclic assessment of ***anchors*** requires a broadly similar range of input parameters to shallow foundations. However, noting that design is often dominated by overall holding capacity, deformation properties (e.g. shear modulus and damping) may not always be required. The emphasis on establishing shear strain and pore pressure trends can also generally be reduced, although knowing their relationships with cyclic shear stresses and numbers of cycles remains necessary to track the numbers of equivalent cycles and the cyclic strengths that determine cyclic holding capacity.

Monopiles may be designed following either the approaches set out for shallow foundations (requiring the parameter list discussed above) or those developed for longer (L/D > 10), which are reviewed below.

Deep, high L/D piles may be assessed by a range of alternative procedures, each of which involves a specific parameter assessment approach. Monotonic capacity prediction is the first step towards axial cyclic loading assessment. Depending on the methodology chosen, this may require CPT resistance, relative density, YSR, plasticity index, sensitivity, effective interface shear angles or monotonic UU/DSS undrained shear strengths. The interface friction angles required for effective stress methods should be determined through ring-shear tests, as described by Jardine et al. (2005a). Cyclic constant volume DSS or HCA experiments are needed to apply the simplified A,B,C ICP cyclic analysis method, while some cyclic procedures for sands call for drained cyclic CNS tests. In contrast, the NGI approach for clays requires intact DSS shear strength, sensitivity and thixotropy measurements. Tests on reconsolidated remoulded clay are also needed and cyclic DSS tests are called for if the PAXCY cyclic t-z approach is to be applied.

Explicit finite element cyclic analyses require similar parameter derivation approaches to shallow foundations or suction anchors, depending on the relative importance to design of predicting the foundations' load-displacement characteristics.

More advanced, fully implicit, finite element analyses involve a range of other procedures in which the constitutive modelling parameters are calibrated to fit specific static and cyclic tests. The scope for improving modelling through advanced testing is developing continuously. For example, Jardine (2013) sets out recent developments that can be applied to improve predictions for the monotonic and cyclic modelling of large displacement piles driven in sands by accounting for cyclic laboratory test behaviour as well as phenomena such as stiffness non-linearity and anisotropy, creep and time dependency, large displacement interface-shear characteristics, the stress regime imposed by installation, particle crushing beneath the pile tip and the development of an interface shear zone containing particle crushing products.

Table 7.1 Cyclic soil data for foundation design of shallow foundations, suction anchors, monopiles and piles

Soil parameter	Shallow foundations		Suction anchors		Monopiles		Piles	
	Clay	Sand	Clay	Sand	Clay	Sand	Clay	Sand
Frictional characteristics								
Peak drained friction angle, ϕ'		x		x		x		$x^{4,8}$
Undrained friction angle, ϕ_u'		x		x		x		x^{8}
Dilatancy angle, ψ		(x)		(x)		(x)		x^{8}
Slope of DSS drained failure line, α'		x		x		x		x^{8}
Slope of DSS undrained failure line, α_u		x		x		x		x^{8}
Interface friction angle, δ_{peak} and $\delta_{residual}$	$(x)^{1}$	$(x)^{1}$	$(x)^{1}$	$(x)^{1}$	$(x)^{1}$	$(x)^{1}$	$x^{4,8,(1)}$	$x^{4,8,(1)}$
Monotonic data								
Monotonic undrained shear strength, s_u^{C}, s_u^{DSS}, s_u^{E}	x	x	x	x	x	x	$x^{2,7,8}$	x^{8}
Initial shear modulus, G_{max}	x	x			x	x	x^{8}	x^{9}
Cyclic data								
Cyclic undrained shear strength, $\tau_{f,cy} = f(\tau_a, \tau_{cy}, N)$, triaxial and DSS	x	x	x	x	x	x	$x^{2,8}$	x^{8}
Cyclically induced pore pressure, $u_p = f(\tau_a, \tau_{cy}, N)$, triaxial and DSS	x	x		x	x	x	x^{9}	x^{9}
$u_p = f(\tau_{cy}, \log N)$ for $\tau_a=\tau_0$, triaxial and DSS	x	x		x	x	x	x^{9}	x^{9}
Cyclic stress strain data, γ_a, γ_p & $\gamma_{cy} = f(\tau_a, \tau_{cy}, N)$, triaxial and DSS	x	x		x	x	x	$x^{2,9}$	x^{9}
$\gamma_{cy} = f(\tau_{cy}, \log N)$ for $\tau_a=\tau_0$, triaxial and DSS	x	x	x	x	x	x	$x^{2,8}$	x^{9}
Drop in radial effective stress along shaft $\sigma'_r = f(\tau_{cy}, N)$, DSS			x^{10}		x^{10}		x^{10}	
Drop in radial effective stress along shaft $\sigma'_n = f(\tau_a, \tau_{cy}, N)$, CNS				x^{11}		x^{11}		x^{11}
Damping	(x)	(x)			(x)	(x)	(x^{9})	(x^{9})
Consolidation characteristics, intact soil								
Preconsolidation stress (and OCR)	x	x	x	x	x	x	x	x^{8}
Virgin, unloading and reloading constrained moduli	x	x	x^{6}	x	x	x	$x^{6,9}$	x^{8}
Permeability	x	x	x^{6}	x	x	x	$x^{6,9}$	x^{8}
Remoulded soil data								
Sensitivity, S_t	x^{6}		x^{6}		x^{6}		$x^{6,7,8}$	
Undrained shear strength of reconsolidated remoulded soil, DSS	x^{6}		x^{6}		x^{6}		$x^{5,6,7,8}$	
Cyclic undrained shear strength, $\tau_{f,cy} = f(\tau_a, \tau_{cy}, N)$, reconsol. DSS	$(x)^{6}$		$(x)^{6}$		$(x)^{6}$		$x^{5,6,7,8}$	
Virgin constrained modulus	x^{6}		x^{6}		x^{6}		$x^{6,8}$	
Permeability	x^{6}		x^{6}		x^{6}		$x^{6,8}$	
Thixotropy	x^{6}		x^{6}		x^{6}		$x^{6,(7),8}$	
Additional parameters for reference monotonic pile capacity								
Relative density, D_r								x^{3}
CPT resistance							x^{3}	x^{3}
Plasticity index, I_p							x^{3}	
Monotonic UU shear strength, s_u^{UU}							x^{3}	
ε_{50}							x^{3}	

(x): Generally not required

1) *May be required for low sensitive clay, high OCR clay and for low φ′ and δ soils*
2) *Input to PAXCY/PAX2 in clay. DSS only*
3) *To calculate reference monotonic capacity if using interaction diagrams or degradation laws*
4) *For design based on effective stress principles*
5) *If constructing interaction diagrams for piles based on DSS tests*
6) *In case of site specific set-up analyses*
7) *To calculate axial pile capacity in clay based on reconsolidated remoulded shear strength. DSS only.*
8) *In case of explicit finite element analyses*
9) *In case of explicit finite element analyses and where displacements are important*
10) *Simplified A,B,C method*
11) *In case of explicit finite element analyses where interface is modelled based on CNS tests*

8 LABORATORY TESTING

The cyclic soil parameters identified in the previous section can be determined by triaxial, DSS, oedometer, UU, bender element, resonant column, HCA, CNS and ring shear laboratory tests as indicated in Table 8.1. The last column in the table indicates papers that comprise database references for some key tests given in Table 10.1. A higher level guidance on planning and execution of geophysical and geotechnical ground investigations for offshore renewable energy projects is given in BSH (2008) and OSIG (2013).

Frictional characteristics. Drained effective-stress shear failure and dilatancy parameters can be determined from monotonic triaxial and DSS tests. As described in Section 4, HCA tests provide the best descriptions of the stress states developed in tests involving principal stress axis inclination (α) rotation, although sample preparation, apparatus control and data reduction are more complex and time consuming. Interface friction angles are best determined from ring-shear tests where the soil annulus is rotated against the required interface material. DSS or shear box tests where the sample is sheared back and forth have been used as alternatives, although the results are less satisfactory.

Monotonic shear tests. Undrained shear strength can be determined from monotonic triaxial compression, triaxial extension and DSS tests. The initial drained and undrained vertical Young's moduli and Poisson's ratios (E'_v, $E_{Uv,}$ υ'_{hv} and υ_{Uhv}) can be determined by means of local strain transducers in triaxial testing. The vertical shear stiffness G_{vh} may also be assessed through bender element shear wave velocity measurements made in triaxial, DSS or even oedometer tests. Care is needed to address potentially marked small strain stiffness anisotropy. The full set of cross anisotropic elastic parameters can be measured statically in instrumented HCA tests, or by assuming rate independence and combining multi-axis bender tests with instrumented triaxial probing tests: see Kuwano and Jardine (2002 and 2007), Gasparre et al. (2006) or Jardine (2013). Bender element signals measured in DSS tests may experience less disturbance due to side boundary reflections, but the transducers are positioned close together and may give uncertainty to the effective wave travel path length. Initial values of shear modulus G_{hv} may also be measured in resonant column tests, although this may be less cost-effective in cases where information is not required regarding small strain damping. Bender element and locally instrumented triaxial tests have the advantage of measuring initial shear moduli and shear strengths on the same sample.

The strain ranges over which most soils show linearly elastic behaviour are very small and most practical field problems are dominated by non-linear behaviour; Andersen and Aas (1980), Jardine et al. (1986), Andersen (1991), Andersen and Høeg (1991), Jardine (1994). Locally instrumented triaxial tests allow high quality information to be recorded continuously from very small strains up to failure. Resonant column tests also allow the non-linear range to be explored to some extent, although under dynamic conditions that involve cycling at relatively high strain rates. Soil moduli are known to vary with the imposed stress regimes and be affected by the time allowed for ageing. Stiffness is therefore best measured in apparatus that allows the in-situ (often K_0) effective stresses to be applied and in tests that include suitable pause periods for samples to reach low creep rates before assessing stiffness; Jardine (2013).

Cyclic parameters. Undrained or drained cyclic triaxial and DSS testing is performed to aid offshore foundation design. Stress-controlled cyclic loading systems are usually adopted because the critical perturbations are predominantly imposed by wave and wind loads that are estimated from interactive fluid-structure analyses. Mixed-boundary cyclic CNS and HCA testing may also be considered. Damping parameters can be found from the stress-strain loops of cyclic triaxial and DSS tests. Small strain damping is best determined in resonant column tests or from locally instrumented triaxial experiments.

Consolidation characteristics of intact soil. The vertical yield stresses σ'_{vy} (or pre-consolidation stresses) and overconsolidation ratios (or YSRs) of lightly over consolidated deposits can often be determined directly from oedometer tests on clay samples. Such yield points cannot be seen in tests on sands and are usually harder to interpret in heavily overconsolidated clay samples. OCR (or YSR) may also be inferred from knowledge of the site's geological history, from shear strength profiles or from in-situ test profiles. A cross-checked, holistic, approach is recommended in cases where the OCR (or YSR) has an important bearing in design as with, for example, the ICP pile design method for clays.

The constrained (usually non-linear) moduli that apply over moderate strain ranges may be estimated from oedometer tests on intact clay and on sand specimens prepared to the most representative in situ condition. The oedometer tests should be performed with two unload/reload sequences. The first unloading should generally be performed from a vertical effective stress appreciably greater than the estimated preconsolidation stress, which also helps to clarify the latter's determination. The second unload/reload stage should be applied at the end of the tests. These two unload/reload loops help to establish the slopes of the 'swelling' curves and inform the interpolation/extrapolation of unload/reload moduli at different effective stress levels to those applied in the test.

Oedometer tests involve relatively thin samples that experience considerable bedding strain at their ends and friction over their side walls. These potential imperfections can be eliminated by undertaking drained stress path triaxial tests equipped with local strain transducers; see Jardine et al. (1984) or Tatusoka et al. (1997). Such triaxial tests are more demanding and require closer control than standard tests, especially if zero lateral strain or other mixed boundary conditions are required.

Permeability can be measured in the oedometer tests, but for clean sand it is necessary to check that the flow resistance of filters and other equipment is sufficiently small or correctable to have no significant influence on the measurements. Low-resistance triaxial permeability tests should be performed when necessary.

Remoulded soil testing. Clay sensitivity can be measured by fall cone, laboratory vane or UU tests on tests on intact and remoulded clay (e.g. De Groot et al., 2012). Undrained monotonic or cyclic DSS or triaxial tests may be performed on samples remoulded by hand before being set-up and consolidated to the desired testing stresses. Remoulded testing may also follow earlier testing of samples in an intact state where large strain undrained cyclic tests may be followed by final undrained shear stages. Oedometer tests on remoulded samples may provide constrained moduli and the permeability information.

Thixotropy may be investigated through tests on remoulded clay samples by fall cone or shear vane tests on specimens that are stored under constant water content conditions over a time series such as 1, 8 hours and 1, 2, 4, 8, 15, 30 and 60 days. It is important that the samples are well sealed and the remoulded strength and the water content of the multiple samples tested should also be measured to check that their basic properties are unchanged by storage or drying.

Sampling and specimen preparation. The load carrying capacity of foundations in sand is dominated by the sand's in-

situ state, or relative density, which is usually assessed through CPT testing. The in-situ densities and water contents of high permeability samples are usually disturbed by standard tube sampling techniques which tend to loosen dense samples and densify loose deposits. Ground freezing techniques offer the only sure way of retaining the in-situ states of sands. While clays may usually be sampled without drainage affecting their water contents and unit weights, they suffer degrees of disturbance to their shear strengths, stiffnesses and YSRs that depend on the sampling technique adopted.

The difficulties of representative sampling pose questions regarding sand and silt test specimen preparation. It has been shown (e.g. Silver et al., 1976, Mulilis et al., 1977 and Hoeg et al., 2000) that sands' static and cyclic behaviour depends on the preparation method. In several cases, however, samples prepared by wet tamping (Andersen, 2009) or water pluviation (Vaid et al, 1999) have given similar cyclic shear strength as high quality frozen samples and NGI recommend adopting either technique, unless the sand has been deposited under dry conditions. Experience at Imperial College has also led to air or water pluviation being preferred; Kuwano and Jardine (2002). However, when fines are present even a few per cent of silt or clay makes reconstitution difficult, especially with clays. The properties of clay-sands (or 'dirty' sands) are highly dependent on their fines contents (Georgiannou and Hight, 1990). Use of "intact" clay-sand samples that are reconsolidated to in-situ stress conditions may then be preferable, even if such specimens have been disturbed. Whether the sampling disturbance leads to strengths and stiffnesses that are too high or too low depends on the in-situ state of the soil before sampling.

Laboratory test reconsolidation paths. The general recommendation is that reconstituted sand and silt samples should be taken through stress paths that re-trace their in-situ stress history, including any prior overconsolidation. For soft to very hard clays tests conducted after direct re-consolidation to in-situ stresses provide the best estimates of the in-situ response to loading: see Smith et al. (1992), Hight and Jardine (1993) or Lunne et al. (2006). High quality sampling techniques exist that can deliver good quality samples of most clay types.

While triaxial (and HCA) equipment offers full control over the consolidation effective stress paths, radial effective stresses cannot be controlled directly in DSS apparatus. NGI practice is to pre-load DSS samples to about 85% of the effective yield or pre-consolidation stress measured in 24 hour oedometer tests in order to generate an appropriate radial stress. However, this procedure may not be appropriate for DSS tests on stiff to hard clays which may have yield or pre-consolidation stress values of several MPa that are hard to establish in DSS tests.

Lean, low plasticity, low OCR clays suffer from tube sampling more than other types. Lunne et al. (2006) report difficulties encountered in testing disturbed samples of such deposits. Void ratio reductions sustained during reconsolidation can lead to a representatively dilative response on final shearing and shear strengths that over-predict those available in-situ. Lunne et al. (2006) recommend limiting the shear strengths to the shear stress values developed at 3% shear strain in such cases. Research at Imperial College has underlined the importance to stiffness measurements of partially re-tracing the recent stress history, choosing reconsolidation paths that lead to minimal shear and volume strains (see Jardine et al., 1991; Smith et al., 1992; Gasparre et al., 2007). The latter procedure history has less effect on the shear strength of most clays.

An awareness of sampling disturbance effects led Ladd and Foot (1964) to propose the SHANSEP re-consolidation procedure for samples with lower quality in which samples are K_0 consolidated to stresses 1.5 to 2 times yield or pre-consolidation stress and swelled back to a range of OCRs before being sheared. The normalised behaviour revealed by these tests is then assumed to apply in-situ. Research on natural clays led to this procedure being considered inappropriate for markedly 'structured' soils (see for example Leroueil and Vaughan, 1990; Le et al., 2008). However, SHANSEP approaches may be applicable to predicting properties that will be available in-situ after experiencing effective stresses far greater than those applying initially in-situ.

Monotonic consolidation and shear loading rates. Tests need to be consolidated and sheared at appropriate rates. Even clean sand can gain shear strength and stiffness significantly over time. Extended duration tests may be impractical in most projects and judgement has to be exercised: Andersen (2009). However, consolidation stresses should be held until pore pressures dissipate fully in all cases. The hold periods should extend for at least one overnight period, even with sands.

Most monotonic tests conducted at NGI and Imperial College on clays and sands are typically run with shear strain rates of about 2 to 4.5%/hr. These rates allow good rates of data collection and undrained pore pressure equalisation in most soils. Additional tests may be run at different rates to check time and rate dependency; care needs to be taken with pore pressure data in faster tests and mid-height pore pressure measurements are recommended when testing clays: see Hight (1982). Strain rates may also be varied during testing, which offers efficiency but may complicate shear strength determination. An example of such a test is presented in Figure 8.1 where the shear rate was varied by multiples of 10 in the pre-and post-peak domains. An approximately isotach response is seen in which the properties vary as functions of axial strain rate. Other patterns of behaviour are possible. Tatsuoka (2011) gives a comprehensive account of such time dependent behaviour in a wide range of geomaterials.

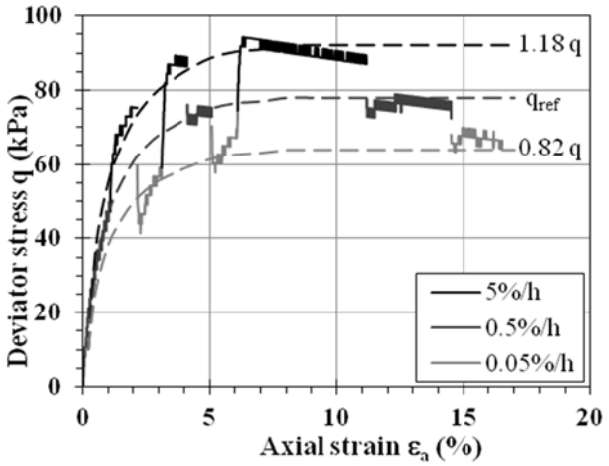

Figure 8.1: Example of rate effect measured on Gulf of Guinea clay (after Colliat et al., 2012)

Specimen pre-conditioning by cyclic pre-shearing. The cyclic response of soils, particularly sands, depends critically on whether they have experienced prior cycling. Samples may be pre-sheared in the laboratory to match the history of loading expected in-situ prior to the main design event. In this context, pre-shearing signifies conditioning the sample by cyclic loading with drainage applied either during or after the pre-shearing. The practice established by NGI for pre-shearing dense sand strata beneath large GBS platforms has been to apply ≈400 cycles at τ_{cy}/σ'_{vc} = 0.04 to model the build-up period of the design storm or the impact of earlier, less severe, storms.

A similar logic can be applied to driven piles foundations that experience extreme stress cycling during their installation (Jardine et al., 2013) and in earthquake engineering, where many sites will have experienced prior ground shaking. Pre-shearing generally increases cyclic shear strength in normally consolidated (even very dense) sand, provided it does not

generate large shear strains that can break down the soil structure. It may also reduce the effects of sampling disturbance, preparation and re-consolidation methods (Andersen, 2009) although this requires more systematically study.

The lower permeability of clays and their lower cyclic susceptibility lead to pre-shearing being less appropriate in most GBS design cases. Consideration has to be given to the extended times available for dissipation of any pore pressures set up by earlier storms or storm build-ups. Pre-shearing usually leads to property improvements in low OCR clays, but the effects may be less positive or negative in high OCR deposits: Andersen (1988). In the latter case, the critical design situation could apply at a time well after installation when the clays may have been degraded by prior cyclic loading, swelling and drainage.

Cyclic loading tests. Suites of tests are needed for each critical soil unit that will affect the GBS, pile, anchor or other foundation under consideration. Tests may be eliminated from some units by considering the foundation's zones of loading influence and the potential importance of key layers in cyclic response. Noting that cyclic properties depend on degree of apparent overconsolidation, more than one suite of tests may be required within single units where OCR (or YSR) varies significantly with depth or when the soil beneath the foundation is consolidated under the weight of the structure to a higher consolidation stress than outside. Tests need to be run on samples taken as close to each other as possible to avoid variability affecting the patterns of behaviour.

Cyclic testing suites designed to provide input for the NGI's 'cyclic contour' methodology to construct cyclic contour diagrams such as those shown in Figures 5.10 to 5.11 and 5.14 to 5.17 are usually conducted undrained and stress controlled to match offshore storm loading. Each cyclic test applies one combination of average and cyclic shear stresses. Parallel monotonic 'control' tests are conducted under similar conditions (TC, DSS or TE) and on similar samples to the cyclic program and follow the same reconsolidation and pre-shearing paths. The monotonic tests define the zero cyclic load case and are used to normalize the shear stresses in tests conducted on clays.

The precise number of cyclic tests undertaken depends on whether full contour suites are needed. The degree of ambition in cyclic testing may reflect the project's stage of development (feasibility vs. detailed design) and the engineering consequences of significant uncertainty remaining in the cyclic response data. The testing strategy also depends on whether established sets of contour diagrams exist for soils comparable to those present at the site in question. One set that is often referred to is the complete suite undertaken for Drammen clay at OCRs of 1, 4 and 40; Andersen (2004).

The first step at a new site is to perform a limited programme involving perhaps three pairs of cyclic TC and DSS tests accompanied by monotonic TC, DSS and TE tests that may be compared with the library of existing cyclic data sets. If no reasonable contour diagram match is obtained, further suites of cyclic tests can be added until a reliable overall contour set is achieved. If a comprehensive definition of the contour diagrams is chosen, tests with high and low level cyclic shear stresses should be applied. The cyclic tests shall also be run with different combinations of average and cyclic shear stresses to fully define the contour diagrams. Referring to Figure 5.9, the average shear stress applied in cyclic triaxial tests, τ_a, is the sum of the initial shear stress prior to cyclic loading, τ_0, and the average shear stress, $\Delta\tau_a$, due to average environmental loads (from for instance waves, wind and current) and $\tau_a = \tau_0 + \Delta\tau_a$. The soil is consolidated under τ_0, but $\Delta\tau_a$ can be applied undrained or drained, depending on the design conditions. The impact of this choice can be significant, as shown for very dense Baskarp sand by Andersen and Berre (1999). Consolidation analyses are required to decide whether $\Delta\tau_a$ should be applied drained or undrained in sands and mixed strata. Dissipation times are usually long when considering storm loading on clays, leading to undrained conditions being adopted. When $\Delta\tau_a$ is applied under drained conditions the triaxial contour diagrams depend on whether $\Delta\tau_a$ is imposed by (i) increasing the vertical stress, or (ii) reducing the radial stress.

The higher level tests are usually run to failure, but tests involving low cyclic shear stresses may have to be stopped after perhaps 5000 cycles without any failure developing. Cyclic failure is usually defined at NGI as a point where either the average or the cyclic shear strain reaches 15%. Specimens that do not fail cyclically can be subjected to final monotonic shear to failure stages, or be consolidated back to their original consolidation stresses while recording the resulting volume changes.

The cyclic periods developed under storm wave loading generally vary between 10s and 20s. Test results are not expected to be affected significantly by cyclic periods varying between these limits and a 10s period has been adopted at NGI to reduce testing times and extend the numbers of cycles that can be applied in given periods. Shorter periods apply in earthquakes (1s or less) and under wind loading (where 3 to 4s may be typical), while periods can extend to 30s to 60s in the long duration swell conditions that can occur in some offshore areas. Cyclic testing rates should be varied to more appropriate values when considering such cases.

Alternative testing strategies may be adopted when considering other cyclic design procedures. For example, the simplified A, B, C effective stress cyclic axial pile design approach (Jardine et al., 2005a) calls for sufficient constant volume DSS or HCA testing to establish how normal effective stresses will reduce due to shaft shear stress cycling. Samples should be consolidated to the radial effective stresses acting on the pile wall at end of equalization as predicted by the ICP methodology. The main testing focus is on varying the ratio of τ_{cy} / σ'_{n0}; only limited testing is usually required with non-zero average initial shear stresses τ_a / σ'_{n0} (applied prior to cycling) to check whether this parameter is influential and needs to be considered. The testing suites are also designed considering that the ratio of τ_{rz} / σ'_r cannot exceed tan δ at the pile-soil interface. Cyclic stiffness may be assessed through a fully non-linear 'small strain' approach based on high quality, locally instrumented triaxial or HCA tests, as outlined by Jardine et al. (2005b) or Jardine (2013).

Emerging explicit finite element approaches for assessing cyclic pile response may well call for different mixes and types of triaxial, DSS or HCA tests, even if the contour diagrams network is likely to define the required data for most soil models. Drained CNS testing may be called for to calibrate model interface conditions. The difficulties of choosing single CNS values were reviewed earlier; further guidance on this point is given by Pra-ai (2013).

Table 8.1 Laboratory tests to determine required cyclic soil parameters

Parameter	Test Type														
	Triaxial			DSS											
	Drained mono	Undrained mono	Cyclic	Drained mono	Undrained mono	Cyclic	Drained cyclic CNS	Oedometer	Unconfined compr.	Bender element	Resonant column	Hollow cylinder	Ring shear interface	Comment	Ref. to data base (see Table 10.1)
Frictional characteristics															
Peak drained friction angle, ϕ'	x														a/b/c
Undrained friction angle, ϕ_u'		x													a/b/c
Dilatancy angle, ψ	x														a/b/c
Slope of DSS drained failure line, α'				x								x[1]			
Slope of DSS undrained failure line, α_u					x							x[1]			
Interface friction angle, δ_{peak} and $\delta_{residual}$													x		d/e
Monotonic data															
Monotonic undrained shear strength, s_u^C, s_u^{DSS}, s_u^E		x			x							x			f/g/h
Initial shear modulus, G_{max}										x[2]	x[3]				h
Cyclic data															
Cyclic undrained shear strength, $\tau_{f,cy} = f(\tau_a, \tau_{cy}, N)$,			x			x									g/i/j/ k/l/m
Cyclically induced pore pressure, $u_p = f(\tau_a, \tau_{cy}, N)$,			x			x									
$u_p = f(\tau_{cy}, \log N)$ for $\tau_a = \tau_0$,			x			x									
Cyclic stress strain data, γ_a, γ_p & $\gamma_{cy} = f(\tau_a, \tau_{cy}, N)$,			x			x									
$\gamma_{cy} = f(\tau_{cy}, \log N)$ for $\tau_a = \tau_0$,			x			x									
Drop in radial effective stress along shaft $\sigma'_r = f(\tau_{cy}, N)$, clay						x[12]									
Drop in radial effective stress along shaft $\sigma'_r = f(\tau_a, \tau_{cy}, N)$, sand							x[13]								
Damping			x			x					x				h/j/k
Consolidation characteristics, intact soil															
Preconsolidation stress (and OCR)								x							
Virgin, unloading and reloading constrained moduli	x[11]							x[4]							a
Permeability	x[11]							x[5]							a
Remoulded soil data															
Sensitivity, S_t									x[6]						q
Undrained shear strength of reconsolidated remoulded soil					x										h
Cyclic undrained shear strength, $\tau_{f,cy} = f(\tau_a, \tau_{cy}, N)$, reconsolidated soil						x									j/k
Virgin constrained modulus								x							
Permeability								x							
Thixotropy														x[7]	h
Parameters for reference monotonic pile capacity															
Relative density, D_r														x[8]	n/o/p
CPT resistance														x[9]	n
Plasticity index, I_p														x[10]	
Monotonic UU shear strength, s_u^{UU}									x						
ε_{50}									x						

1) *Alternative to DSS, but with more difficult sample preparation*
2) *Can be included as part of monotonic and/or cyclic tests*
3) *Bender element tests an alternative unless damping at small shear strain is needed,*
4) *Oedometer tests should be run with 2 unload/reload sequences*
5) *Consider triaxial set-up for clean sands where perm. may be high*
6) *Determined in UU tests, fall cone or lab vane on intact and remoulded clay.*
7) *Test aged remoulded clay samples stored at constant water content*
8) *Normally interpreted from in situ CPTU. Can also be based on in situ water content/unit weight, but these can be uncertain*
9) *From in situ CPTU*
10) *From routine index testing*
11) *Alternative to oedometer tests to eliminate testing imperfections*
12) *For simplified A, B, C method*
13) *In case of some explicit finite element analyses where drained CNS tests are used to model interface*

9 INTERPRETATION/PRESENTATION OF RESULTS

Some of the more important factors that should be considered in the interpretation and presentation of data from cyclic laboratory tests performed for principally offshore engineering applications are discussed briefly below.

Monotonic behaviour

Noting that all such programs have to start with retrieved soil samples and involve monotonic shear tests it is also important to consider the following issues in test interpretation:

- Sample disturbance must be assessed. Lunne et al. (2006), Berre et al. (2007), Lunne and Andersen (2007) and Andersen et al. (2008) discuss this issue and suggest ways of correcting for sample disturbance.
- Care is needed with oedometer tests. Andersen and Schjetne (2012) proposed a mathematical formulation to express virgin loading, unloading and reloading moduli that accounts for differences in stiffness and non-linearity on each of these branches. The formulation allows moduli to be defined for stress levels and stress increments different to those applied in the test.
- Remoulded and reconsolidated remoulded shear strengths should be related to the original intact shear strength.
- Tests that investigate thixotropy in shear strength data should be plotted against logarithmic time, together with the corresponding water content and remoulded shear strength measurements. Original intact shear strength should also be reported.
- It is important when assessing angles of shearing resistance φ' from effective stress path plots to account for the differences between peak, critical and residual shear states. Peak monotonic shear strength corresponds to any peak in the stress strain curve or, if none is apparent, as the shear stress at a shear strain of 15%.
- DSS test interpretation should involve establishing the slopes of the horizontal shear stress against vertical effective normal stress plots, without making any a priori assumption regarding their possible relationship to φ'.
- Where interface shear tests are performed for driven pile analysis they should involve several metres of fast 'conditioning' pre-shear, which may be performed (when using the apparatus described by Bishop et al. 1971) with the gap between the interface and the upper confining ring closed. The principal output from the tests is the plot of τ/σ'_n against shear displacement obtained in slow 'open-gap' tests performed after fast shear and reconsolidation. These tests often show peak angles after small displacements and achieve their ultimate values within perhaps 30mm of travel; both angles should be recorded. Jardine et al. (2005) give full details of the test procedures.
- HCA experiments offer the capability of applying/measuring four dimensions of stress and strain and so following the foundation loading paths and soil responses more rigorously than conventional laboratory tests. Zdravkovic and Jardine (2000 and 2001) and Nishimura et al. (2007) provide examples of how the tests may be conducted and the results interpreted for a range of soil types.
- The initial Young's and shear moduli of soils are known to depend fundamentally on the applied effective stresses, and are often expressed as fractional power functions of these stresses that may include void ratio functions (see Jardine, 1994 or 2013). Initial stiffnesses can be presented in a range of normalised styles, including presentation as ratios of undrained shear strengths. But it must be made clear how normalisation has been undertaken and sufficient information provided for future users to express the data in the format required for their particular analytical approach.
- It is important to remain aware in test interpretation of the intense non-linearity and potential anisotropy of most soils, from small strains to large.

Cyclic data

- Earlier sections have emphasised the strong dependence of soils' cyclic response on: stress path (as seen in TC, TE and DSS tests); the ratio between average and cyclic shear stresses τ_a and τ_{cy}; the number of cycles N; and whether the average shear stress is applied under drained or undrained conditions. It is therefore convenient to provide separate diagrams for triaxial and DSS tests and group the cyclic results as set out in Section 5 where cyclic shear strength is related to τ_a and τ_{cy} and N; see Figure 5.10.
- Cyclic and average shear strains are related to τ_a and τ_{cy} and N; see Figures 5.14 and 5.15.
- Permanent 'excess pore pressure' are related to τ_a and τ_{cy} and N (Figures 5.16 and 5.17).
- In triaxial tests, the pore pressure increment related to the increase in mean normal stress $(p = \sigma_1 + \sigma_2 + \sigma_3)/3$, imposed when $\Delta\tau_a$ is applied, is subtracted to make the data more general (Figure 5.17).
- Cyclic shear strain and permanent pore pressures are expressed as functions of τ_{cy} and N for given values of τ_a (Figure 5.11).
- Damping parameters may also be plotted in contour diagrams, although this has not been general practice. .

As indicated in Section 8, full contour sets are not required for all design cases. Also, the testing strategy and interpretation can be optimised by making use of existing data sets obtained with potentially similar soils. References to such data libraries are given in the next section.

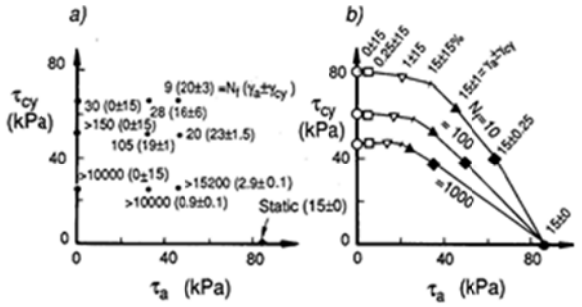

Figure 9.1: Example of data points and corresponding contours in τ_{cy} vs. τ_a type diagram showing number of cycles to failure and failure mode in DSS tests on normally consolidated Drammen Clay (Andersen, 2004)

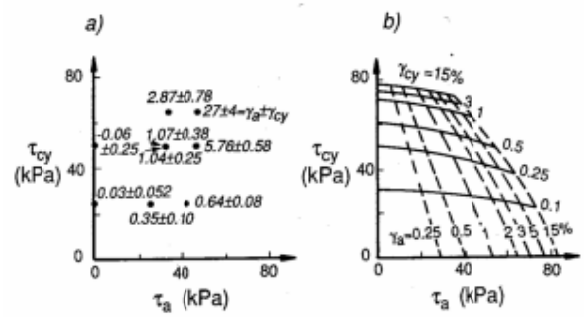

Figure 9.2: Example of data points and corresponding contours in τ_{cy} vs. log N type diagram showing average and cyclic shear strains after 10 cycles in DSS tests on normally consolidated Drammen Clay (Andersen, 2004)

The NGI contouring procedure starts with plotting the individual data outputs as illustrated by DSS test examples in Figures 9.1 and 9.2. The intersection with the horizontal axis in diagrams of the type in Figures 9.1 and 9.2 represents monotonic conditions and the companion static test data are plotted on this line. The contour diagrams can be used directly in the NGI's cyclic analysis toolset. They also form a basis that can be used as input to and to formulate or test other mathematical models.

10 CYCLIC AND STATIC ADVANCED GEOTECHNICAL TESTING DATA BASES

Advanced laboratory test data are often unavailable at the start of projects and it may indeed be unfeasible to conduct such tests at any stage in some settings. Lists of published high quality results can provide useful support in such circumstances. Table 10.1 offer a selection of references to such databases. The last column in Table 8.1 is linked to the further commentary and details given in Table 10.1. The main focus is on advanced static and cyclic laboratory testing.

This paper has concentrated on summarising contributions that are well known to the Authors and their colleagues and has not attempted to offer a full review of the large volume of relevant and significant work by others. This selectivity is maintained in the referencing made here and in the supporting data given in Table 10.1. Naturally, considerably more information, and many more references, are available in the broader literature.

Table 10.1 Literature with data on cyclic soil parameters in Tables 7.1 and 8.1

Reference	Description / Comment	Ref. param. in Table 8.1
Frictional characteristics		
Andersen & Schjetne 2013	Diagrams with frictional soil characteristics of sand as functions of relative density and effective normal stress from triaxial tests	a
Bolton 1986		b
Schmertman 1978		c
Jardine et al. 2005	Interface friction angles for clay	d
Ho et al 2011	Interface friction angles for sand	e
Monotonic data		
Lunne & Andersen 2007	Undrained shear strength of normally and lightly overconsolidated clays correlated to the preconsolidation stress. Shear strength anisotropy factors. Shows anisotropy is higher (smaller factors) the less disturbed the clay is. Reason; TC strength more affected by sample disturbance than TE and DSS	f
Andersen 2004	Normalised shear strength as function of OCR.	g
Jardine et al 1997, Zdravkovic & Jardine 2001, Nishimura et al 2007	HCA tests on range low OCR and high OCR soils showing anisotropic dependence of shear strength on parameters b and α	f/g
Andersen et al. 2008	Initial shear modulus of clay normalised both to vertical effective stress and to undrained shear strength as function of I_p and OCR.	h
Jardine et al 1984, Jardine 1994, Zdravkovic & Jardine 1997, Tatsuoka et al 1999, Kuwano & Jardine 2002, 2007, Gasparre et al 2007	Anisotropy and non-linearity of stiffness from very small strains to large, from dynamic and static tests in locally instrumented traixial and HCA apparatus	h
Cyclic data		
Andersen 2004	Complete set of cyclic contour diagrams for Drammen clay (I_p=27%). Triaxial and DSS tests with OCR= 1, 4 and 40. Most comprehensive contour set for clay. Also presents comparison of cyclic shear strength diagrams for 8 different clays with I_p ranging from 7% to 100%.	g
Jeanjean et al. 1998	Cyclic contour diagrams for triaxial and DSS tests on normally consolidated clays with I_p=30-70% from Marlin deepwater site in Gulf of Mexico.	i
Kleven & Andersen 1991 Andersen et al. 1991	Complete set of cyclic contour diagrams and damping ratio for the Great Belt Bridge clay till (I_p=7%-12%) for OCR=1 and 3. Triaxial and DSS tests. In addition, DSS contour diagrams for OCR=40 and for remoulded clay.	j k
Andersen & Berre 1999	Cyclic contour diagrams for very dense Baskarp sand with grain size similar to typical fine uniform North Sea sands (D_{50}=0.15mm and 3% fines. Because Baskarp sand is somewhat more angular than typical North Sea sands, one has been cautious to rely on the high strengths of Baskarp sand. However, more recent tests on actual North Sea sands seem to support Baskarp data.	l
Andersen 2009	Diagrams to establish cyclic shear strength of sand and silt as function of number of cycles, preshearing, OCR, D_r and water content. From published literature and NGI files. Refs. to other published papers on cyclic behaviour of sand. Some information on effect of load period for clay and sand.	m
Andersen et al. 2008	Damping from two-way stress controlled cyclic DSS tests on clay as function of cyclic shear strain and number of cycles.	h
Lunne & Andersen 2007	Effect of sample disturbance on cyclic parameters	f
Consolidation characteristics, intact soil		
Andersen & Schjetne 2013	c_v of clay as function of void ratio (or water content) and clay content. c_v of sand as function of void ratio (or water content) and D_{10}. Mathematical expressions and empirical constants for loading, unloading and reloading constrained moduli of sand and silt.	a
Remoulded soil data		
DeGroot et al. 2012	Discussion on ways to determine remoulded strength and S_t.	q
Andersen et al. 2008	Reconsolidated remoulded shear strength normalised by original intact shear strength as function of OCR for various clays. Diagram with thixotropy ratio as function of activity, time and sensitivity.	h
Parameters for reference monotonic pile capacity		
Lunne et al. 1997	Guidance on use and interpretation of CPT and CPTU. Determination of D_r.	n
Jamiolkowski et al. 2001	Updated determination of D_r from CPT (clean sand).	o
Jardine et al 2005	Lab and field procedures required to apply ICP-05 method in clays and sands	
Emerson et al 2008	Determination of D_r from CPT at shallow depth (clean sand).	p

11 APPLICATIONS TO OTHER TYPES OF STRUCTURES AND CYCLIC REGIMES

As outlined in the introduction, cyclic loading issues are considered carefully in some fields outside offshore engineering including: earthquake geotechnical design, pavement engineering, blast-resistant design, some harbour/marine works and machine foundation design. However, other types of mainstream civil engineering structures exist that are subjected to repeated loading patterns involving a degree of regularity in amplitude and period. These "cyclic" loads may be essentially environmental (seasonal, or induced by waves, wind, currents or tides) or operational in origin. Some examples of structures that may potentially be affected by cyclic loading that may not always be addressed in design include:

- Wind-turbines on land, which are submitted to wind and rotor/blade forces. The key geotechnical issue is to ensure that the foundation stiffness requirements match those required by the turbine manufacturer.
- Coastal structures including harbours, breakwaters and sea protection barriers.
- Energy transport pylons: winter storm events have demonstrated the inadequacy of some foundation concepts to resist extreme cyclic wind forces.
- High rise towers and chimneys are sensitive to wind cyclic loading.
- High speed train foundations and bridges, which transmit intense frequent and discontinuous traffic loads to the soil.
- Structures subject to variable industrial loading, such as static and travelling cranes and hydraulic turbines as well as vibrating machinery.
- Anchored rafts for coastal energy plants that are submitted to tidally varying ground water uplift pressures.
- Large storage tanks subject to regular loading and unloading cycles.

Load characterization

It is common in building works and civil engineering to consider applied loads as essentially static or quasi-static. In accordance with existing codes and standards, critical loads are defined by the maximum values expected under various load cases (operational - SLS, extreme - ULS, accidental- ALS). These approaches do not address fully the dependence emphasized throughout this paper of soils' cyclic response on mean stress and cyclic stress amplitude, loading frequency, number of cycles and cyclic stress path, which is well-established in offshore geotechnics. A greater awareness of these issues is urgently required in general civil engineering.

The cyclic loading conditions applied in the wider range of civil engineering needs to be characterised properly. Field measurement studies will provide critically needed new information. Figure 3.1 offers a provisional summary of some significant cyclic loading conditions by plotting representative periods against number of cycles.

Our present knowledge is concentrated in the zone defined by periods of typically less than 100s and N < 10,000 which corresponds to the current earthquake and offshore engineering demands. There is clearly a need to investigations to cover higher numbers of cycles to meet wind turbine and high-speed train challenges and also to consider longer loading period events. The latter deserves particular attention because of the strain rate dependence of shear strength in clay and the scope for partial or full drainage applying over large loading periods, even in low permeability soils.

In the same way, the accumulation of cyclic loading displacements and potential damage (or ageing benefits) need to be assessed over the whole lifetimes of facilities, rather than just one design storm. Low level cycling can be beneficial to capacity if accompanied by drainage and pre-shearing. However, negative effects are also possible in dilative low permeability soils, as discussed earlier.

Foundation types

The methodologies for cyclic design of offshore foundations set out in the preceding were divided into essentially two types: (i) monolithic rigid bodies with low depth to width L/D ratios and (ii) piles where L/D usually exceeds 10.

The first group, typically involving shallow foundations, were considered in the NGI framework by limit state or FEM analyses. Simplified approaches could be made in which cyclic shear strengths were applied around static critical failure surfaces. More advanced analyses considered the equilibrium of the average loads and average shear stresses along with strain compatibility along the potential failure surface (Andersen and Lauritzsen, 1988). Deep caissons such as offshore wind monopiles may be considered by similar approaches, or considered as piles (Jardine et al., 2012).

One critical aspect with deep caissons/monopiles is their sensitivity to lateral displacements and stiffness under a high number of cycles. This aspect has been addressed by deriving degradation laws from model pile tests (Peralta, 2010; Le Blanc et al., 2010), through simplified explicit FEM analyses (Andersen and Høeg, 1991; Saue et al., 2010 or Grimstad et al., 2013); the explicit procedure proposed by Wichtman (2005) can also be applied (see Abdel-Rahman and Achmus, 2005).

Well-designed deep piles tend to behave as flexible elastic bodies under cyclic loading. Their behaviour has been modelled traditionally by elastic continuum approaches or simplified t-z, p-y beam column approaches, although these conventional approaches suffer from a number of significant limitations, as emphasised by Jardine et al. (2012).

The range of foundation concepts used in building or civil engineering structures is much broader than that applied in offshore applications. Application of offshore shallow foundation procedures to strip footings and offshore pile techniques to deep onshore piles is relatively straightforward. However, new or modified approaches are needed for more complex piled raft, rigid inclusions, high pressure anchored, or reinforcement earth and other foundation techniques. The need to employ sophisticated physical modelling or FEM simulations can be envisaged for many such applications.

The SOLCYP project (Puech et al., 2012) is offering a significant contribution to making cyclic analysis feasible for conventional piled foundations. As shown in Figure 6.1, the SOLCYP cyclic assessment process starts with the use of cyclic axial stability diagrams. A key aim is to develop charts covering a wider variety of soil types and pile installation techniques, with an emphasis on better matching the range employed in mainstream building and civil engineering activities. Diagrams are being generated within SOLCYP from field tests involving:

- Closed-end (full-displacement) driven steel piles.
- Non-displacement augered, cast-in-place, bored reinforced concrete piles.
- Partial displacement screw piles formed by helical tool that penetrated by a combination of jacking and rotation with the concrete piles being cast in place and reinforced after concreting.

The diagrams were derived from tests on suites of similar piles installed at two French experimental sites. The first, at Merville, involved the stiff overconsolidated Flanders clay, which is from the same geological unit as the UK London clay. The second involved a dense to very dense sand at the Loon-Plage site which is located with about 1km of the Dunkirk test site utilised by Imperial College (Jardine et al., 2006; Rimoy et

al., 2013) and involved similar strata. The piles were submitted to reference monotonic tests and suites of extensive one-way and more limited two-way cyclic tests. The SOLCYP programme integrated these field tests with other streams of centrifuge (e.g. Guefresh et al., 2012) and large calibration chamber tests that complemented and cross-checked the field results.

Examples of axial cyclic stability diagrams obtained for bored piles in dense sand and in one-way mode are presented in Figures 11.1 and 11.2, drawing on data from both field bored piles and centrifuge model simulations. The consistency between the two data sets is encouraging and highlights the marked sensitivity to cyclic loading of piles bored in sand under even one-way loading. The arguments advanced in this paper show that still more intensive effects can be expected under two-way loading conditions.

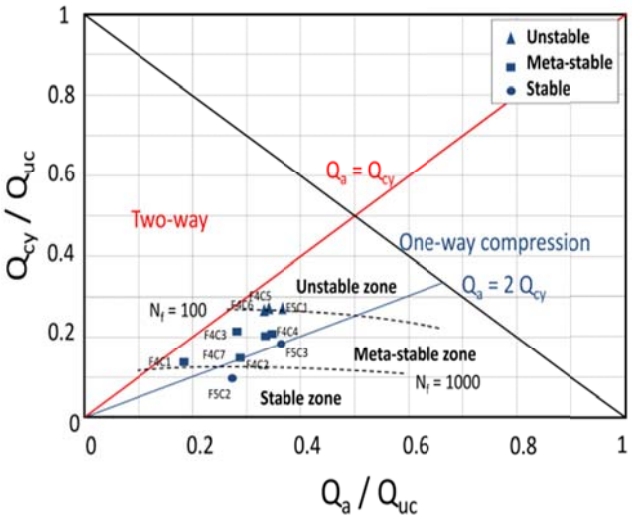

Figure 11.1 Cyclic stability diagrams for cast-in-place piles in dense sands: in situ tests, bored piles, Loon-Plage (Puech et al., 2013). Piles loaded in compression

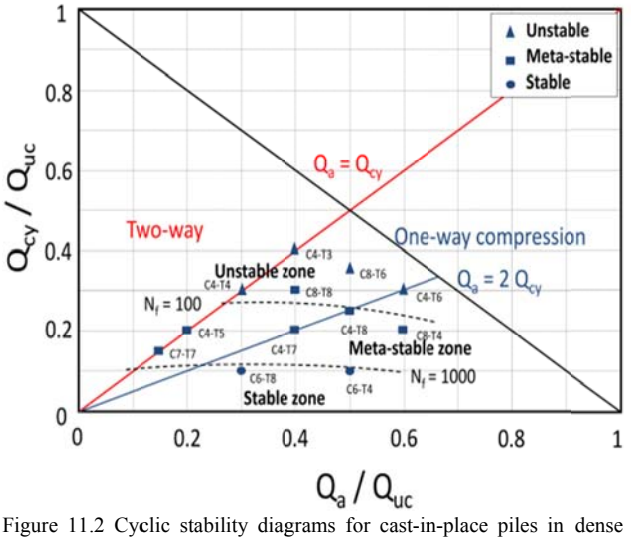

Figure 11.2 Cyclic stability diagrams for cast-in-place piles in dense sands: Centrifuge tests, Fontainebleau sand (Puech et al., 2013). Piles loaded in compression

12 CONCLUSIONS

- Cyclic loading generated by wind and wave loading is of crucial importance in offshore foundation engineering.
- Considering the cyclic loading induced by wind-turbine rotation is also a key concern in the offshore renewable energy sector.
- Offshore foundation designers often have to consider cyclic bearing capacity and stiffness, as well as permanent displacements due to cycling and potentially changing patterns of soil reaction stresses.
- These features have been illustrated first by examples drawn from offshore Gravity Base Structure (GBS) prototype observations as well as field and model test observations with piled foundations.
- The stress paths induced by foundations under static and cyclic loads and the corresponding responses seen in cyclic laboratory element tests have also been reviewed.
- Procedures have then been set out that can address the necessary design concerns for GBS, suction anchor, driven piles and other foundation types.
- A main objective of this paper has been to give guidance for obtaining the soil parameters for design of foundations under cyclic loading, and a review is offered of the ways in which the key soil parameters can be determined.
- While cyclic design is undertaken routinely for GBS foundations, it is often neglected in offshore pile design. The latter omission could have significant consequences in certain cases and closer attention is required especially in cases involving high ratios of cyclic to average axial pile-head loads.
- Offshore engineering cyclic design approaches may be applied across a wide range of applications where load cycling can be generated by seasonal changes, earthquakes, ice, traffic, machinery and other natural or anthropogenic processes.
- Important examples of other type of structures that must be designed to resist cyclic loading include sea protection barriers, wind turbines and road or rail pavements.
- Recent research into the response of traditional civil engineering foundation types, such as piles bored in sands has revealed a marked sensitivity to cyclic loading that clearly merits careful consideration in a wider range of design settings.

13 ACKNOWLEDGEMENTS

The Authors wish to acknowledge the many contributions made by their current and former colleagues at Norwegian Geotechnical Institute and Imperial College, in the SOLCYP project team and elsewhere for their extensive contributions made to the work described on the cyclic behaviour of soils and foundations. They also acknowledge gratefully the support provided over many years by multiple national and international governmental and industry sponsors.

14 REFERENCES

Abdel-Rahman K. and Achmus, M. 2005 Finite Element Modelling of horizontally loaded Monopile Foundations for Offshore Wind Energy Converters in Germany, *International Symposium, Frontiers in Offshore Geotechnics* (ISFOG), Perth, Australia, Sept. 2005.

Achmus M, Abdel-Rahman K and Peralta P. 2005. On the Design of Monopile Foundations with respect to Static and Quasi-Static Cyclic Loading. *Copenhagen Offshore Wind* 2005.

Achmus M, Abdel-Rahman K and Kuo YS. 2008. Design of monopile foundations for offshore wind energy plants. *11th Baltic Geotechnical Conference-Geotechnics in Maritime Engineering*, Gdansk, vol.1, 463–470.

Achmus M, Albiker J and Abdel-Rahman K. 2010. Investigations on the behaviour of large diameter piles under cyclic lateral loading, *Proc. International Symposium, Frontiers in Offshore Geotechnics*, ISFOG, Perth.

Aderlieste EA, Dijkstra J and van Tol AF. 2011. Experimental investigation into pile diameter effects of laterally loaded monopiles. *Proceedings of the 30th International Conference on Ocean, Offshore and Arctic Engineering,* OMAE 2011. Rotterdam, The Netherlands.

Andersen K.H. 1976. Behaviour of clay subjected to undrained cyclic loading. *Int. Conf. on Beh. of Offsh. Struct., BOSS'76*. Trondheim. Proc., Vol. 1, pp. 392 403. Also NGI Publ. 114, pp. 33 44.

Andersen K.H. and Aas P.M. 1980. Foundation performance. Shell Brent "B" Instrum. Project; Seminar. London. Proc., pp. 57 77. Org. by Soc. for Underwater Techn., London. Also NGI Publ. 137.

Andersen K.H. and Lauritzsen R. 1988. Bearing capacity for *foundations* with cyclic loads. *J. Geotech. Engrg.,* ASCE, 114 (5), 540 555.

Andersen K.H., Kleven A. and Heien D. 1988. Cyclic soil data for design of gravity structures. *J. Geotech. Engrg*., ASCE, 114 (5), 517 539.

Andersen, K.H. 1988. Properties of soft clay under static and cyclic loading. Invited lecture. *International Conf. on Eng. Problems of Regional Soils*, Proc., pp. 7 26, Beijing, China, 1988. Edited by Chinese Institution of Soil Mechanics and Foun¬da¬tion Engineering. Also in NGI Pub. 176.

Andersen K.H., Dyvik R., Lauritzsen R., Heien D., Hårvik L., Amundsen T. 1989. Model tests on gravity platforms. II: Interpretation. *J. Geotech. Engrg*., ASCE, 115, 1550-1568.

Andersen K.H. 1991. Foundation design of offshore gravity structures. Ch. 4 in *"Cyclic Loading of Soils. From Theory to Design"*. Ed. by M.P. O'Reilly and S.F. Brown. Publ. by Blackie and Son Ltd., Glasgow and London.

Andersen K.H. and Høeg K. 1991. Deformations of soils and displacements of structures subjected to combined static and cyclic loads. *X ECSMFE*, Firenze, Proc., Vol 4, pp. 1147-1158.

Andersen K.H., O.E. Hansteen and M. Gutierrez 1991. Bearing capacity, displacements, stiffness and hysteretic damping of Storebælt bridge piers under ice loading. *Seminar on Design of Exposed Bridge Piers*. Danish Society of Hydraulic Engineering. Copenhagen, Denmark, 22 January 1991. Also published in NGI Publ. 199.

Andersen K.H., Dyvik R., Kikuchi, Y. and Skomedal E. 1992. Clay behaviour under irregular cyclic loading. *Proc. Int. Conf. on Behaviour of Offsh. Structures*, London, Vol. 2, pp. 937-950.

Andersen K.H. and T. Berre 1999.Behaviour of a dense sand under monotonic and cyclic loading. Geotechnical Engineering for Transportation Infrastructure. *12th European Conference on Soil Mechanics and Geotechnical Engineering*. Amsterdam, The Netherlands. Proc. Vol.2, p. 667-676. Publ. by A.A. Balkema.

Andersen, K.H. and Jostad H.P. 1999. Foundation design of skirted foundations and anchors in clay. *Offsh. Techn. Conf*., Houston, Proc., Paper 10824.

Andersen K. H. and Jostad H. P. 2002. Shear strength along outside wall of suction anchors in clay after installation. *Proc. XII ISOPE Conf.*, Kyushu, Japan.

Andersen K.H. 2004. Cyclic clay data for foundation design of structures subjected to wave loading. Keynote Lecture; *Proc. Int. Conf. on Cyclic Behaviour of Soils and Liquefaction Phenomena*, CBS04, Bochum, Germany. Proc. p. 371-387, A.A. Balkema, Ed Th. Triantafyllidis.

Andersen, K.H., T. Lunne, T.J. Kvalstad and C.F. Forsberg 2008. Deep water geotechnical engineering. *XXIV Nat. Conf. of the Mexican Soc. of the Soil Mechanics*, Aguascalientes, 26-29. Nov. 2008. Proc. Vol IV. 57p. Also: Norwegian Geotechnical Institute, Oslo, Norway. Publ. No. 208.

Andersen K.H. 2009. Bearing capacity of structures under cyclic loading; offshore, along the coast and on land. *21st Bjerrum Lecture* presented in Oslo 23 Nov. 2007. Can. Geotech. J. 46: 513-535. Also: Norsk Geoteknisk Forening, Bjerrums Foredrag Nr. 21.

Andersen, K.H. and K. Schjetne 2012. Data base of friction angles of sand and consolidation characteristics of sand, silt and clay. ASCE *J. of Geotechnical and Environmental Engrg*. July 2013.

Andersen L.V., Hahdatirad M.J., Sichani M.T. and Sorensen J.D. 2012. Natural frequencies of wind turbines on monopole foundations in clayey soils – A probabilistic approach. *Computer and Geotechnics* 43 (2012) I-II.

Andresen L., Jostad H. P. and Andersen K. H. 2010. Finite Element Analyses Applied in Design of Foundations and Anchors for Offshore Structures. *Int. J. of Geomech*., ASCE.

Anh-Minh, N., Nishimura, S., Takahashi, A. and Jardine, R.J. 2011. On the control systems and instrumentation required to investigate the anisotropy of stiff clays and mudrocks through Hollow Cylinder Tests. *Deformation Characteristics of Geomaterials. Proc*. IS-Seoul, Pub. Hanrimwon, Seoul, Vol. 1, Eds. Chung et al, p 287-294.

Atkins Consultants Ltd 2000. Cyclic degradation of offshore piles. *HSE Offshore Technology Report OTO 2000 013*. Health and Safety Executive, London.

Augustesen AH, Brodbaeck KT, Moller M, Sorensen SPH, Ibsen LB, Pecersen TS and Andersen L. 2009. Numerical modelling of large-diameter steel piles at Horns Rev. *Proc. 12th Civil, Structural and Environmental Engineering Computing*, Topping-Costa Neves-Barros Edts, Civil-Comp Press, Stirlingshire, Scotland, Paper 239.

API 2000. Recommended practice for planning, designing and constructiong fixed offshore platforms – Working stress design. RP2A-WSD, American Petroleum Institute.

API RP2GEO. 2011. API Recommended Practice, Geotechnical and Foundation Design Considerations, First Edition, American Petroleum Institute, April 2011.

ASTM.1985. Standard practices for cycle counting in fatigue analysis. Designation E 1049-85, vol. 03. 01 of Metal Test Methods and Analytical Procedure. pp. 836-848.

Benzaria O. 2013. Contribution à l'étude du comportement des pieux isolés sous chargements cycliques axiaux. *Thèse*. Université de Paris-Est. A paraître.

Benzaria O., Puech A. and Le Kouby A. 2012. Cyclic axial load-tests on driven piles in overconsolidated clay, *7th Int. Conf. on Offshore Site Investigations and Geotechnics*, OSIG, London.

Benzaria A., Puech A. et Le Kouby A. 2013a. Essais cycliques axiaux sur des pieux forés dans l'argile surconsolidée des Flandres. *Proceedings 18th ICSMGE,* Paris.

Benzaria A., Puech A. et Le Kouby A. 2013b. Essais cycliques axiaux sur des pieux forés dans des sables denses. *Proceedings 18th ICSMGE*, Paris.

Berre, T., T. Lunne, K.H. Andersen, S. Strandvik, and M. Sjursen 2007. Potential improvements of design parameters by taking block samples of soft marine Norwegian clays. *Can. Geotech J.* 44: 698-716.

Bishop, A.W., Green, G.E., Garga,V.K., Andresen, A. and Brown, J.D. 1971. A new ring shear apparatus and its application to the measurement of residual strength. *Geotechnique*, 21, No 4, pp 273-328.

Bjerrum, L. 1973. Problems of soil mechanics and construction on soft clays. State-of-the-Art Report to Session IV, *8th International Conference on Soil Mechanics and Foundation Engineering*, Moscow. Proc., Vol. 3, p. 111-159.

Bolton, M.D. 1986. "The shear strength and dilatancy of sands". *Geotechnique,* Vol. 36, No. 1, pp. 65-78.

Bond, A. J. and Jardine, R. J. 1991. The effects of installing displacement piles in a high OCR clay. *Geotechnique*, Vol 41, No. 3, pp 341-363.

Bond, A J and Jardine R J 1995. Shaft capacity of displacement piles a high OCR clay. *Geotechnique*, 45, No 1, pp3-23.

Boukovalas G., Whitman R.V. and Marr W.A. 1984. Permanent displacement of sand with cyclic loading. *J. Geotech. Engrg*., ASCE 110: 1606–1623.

Briaud J.L. and Felio G.Y. 1986. Cyclic axial loads on piles: analysis of existing data. *Canadian Geotechnical Journal*, 23,362-371.

BSH - a) Standard: Design of Offshore Wind Turbines 2007, b) Guidance for use of the BSH standard „Design of Offshore Wind Turbines“ 2011, c) Ground investigations for offshore wind farms 2008, Federal Maritime and Hydrographic Agency (BSH), Hamburg and Rostock.

Chaboche J.L. 1994. Modeling of ratchetting: evaluation of various approaches. *Eur. J. Mech. A/Solids* 13: 501–518.

Chin JT and Poulos HG. 1992. Cyclic axial loading analyses: a comparative study. *Computers and Geotechnics* 13: 137–158.

Chow FC. 1997. Investigations into displacement pile behaviour for offshore foundations*. PhD thesis*, Univ. London (Imperial College)

Clausen C.J.F., DiBiagio E., Duncan J.M and Andersen K.H. 1975. Observed behaviour of the Ekofisk oil storage tank foundation*. 7th Offsh. Techn. Conf.*, Houston 1975. Proc., Vol. 3, pp. 399 413. Also NGI Publ. 108.

Clausen CJF, Aas PM and Karlsrud K. 2005. Bearing capacity of driven piles in sand: the NGI approach. *Proc. ISFOG'05*, Perth, WA, 677–681.

Clukey, E., Gilbert, R.B., Andersen K.H. and Dahlberg, R. 2013. Reliability of Suction Caissons for Deep Water Floating Facilities. *ASCE Geotechnical Special Publication* No. 229; Foundation Engineering in the Face of uncertainty.

Colliat, J.L., Dendani, H., Puech, A. and Nauroy, J.F. 2010. Gulf of Guinea deepwater sediments: geotechnical properties, design issues and installation experiences. *Proc. 2nd Int. Symposium on Frontiers in Offshore Geotechnics, ISFOG 2010*, Perth, Australia.

DeGroot, D.J., T. Lunne, K.H. Andersen and A.G. Boscardin 2012. Laboratory measurement of the remoulded shear strength of clays with application to design of offshore infrastructure. *7th Intern. Offshore Site Investigation and Geotechnics Conference*; Sept. 2012, London, UK, Proc. p. 355 366.

Diyaljee V.A. and Raymond G.P. 1982. Repetitive load deformation of cohesionless soil. *J. of Soil Mech. and Found. Engrg.* 10: 1215–1229.

DNV 1979. Rules for the design, construction and inspection of offshore structures. Det Norske Veritas, Høvik, Norway. 67p.

DNV. 1992. Classification Note 30-4, Foundations. Det Norske Veritas, Oslo.

DNV-OS-J101. 2010. Design of Offshore Wind Turbines Structures, DnV Offshore Standards, Det Norske Veritas, Oslo.

Dyvik R., Andersen K.H., Madshus C. and Amundsen T. 1989. Model tests of gravity platforms. I. Description. *J. Geotech. Engrg*., ASCE 115 (11) 1532-1549.

Emerson, M., Foray, P., Puech, A. and Palix, E. 2008. A global model for accurately interpreting CPT data in sands from shallow to greater depth.Proceedings of the *3rd International Conference on Site Characterization ISC'3*, Taipei, Taiwan. Pages 687-694.

Erbrich C.T., O'Neill M.P., Clancy P. and Randolph M.F. 2010. Axial and lateral pile design in carbonate soils. *Frontiers in Offshore Geotechnics II. Proc.,* Gourvenec & White (eds). 2011 Taylor & Francis Group, London, ISBN 978-0-415-58480-7, p. 125-154.

GL Rules and Guidelines. 2005. IV Industrial Services. Part 2-Guidelines for the Certification of Offshore Wind Turbines, Germanischer Lloyd, Reprint 2007.

Gasparre, A., Nishimura, S., Anh-Minh, N., Coop, M.R. & Jardine, R.J. 2007. The stiffness of natural London clay." Symposium in Print on Stiff Clays. Géotechnique, 57(1), pp 33-48.

Georgiannou V N , Burland, J B and Hight, D W 1990. The undrained behaviour of clayey sands in triaxial extension and compression. *Geotechnique,* Vol 40, No 3, pp 431-450.

Gibson R E 1963. An analysis of system flexibility and its effect on tire lag in pore water measurements. *Géotechnique,* Vol 13, No 1, pp 1-11.

Gotschol A. 2002. Veränderlich elastisches und plastisches Verhalten nichtbindiger Böden und Schotter unter zyklisch-dynamischer Beanspruchung, *Schriftenreihe Geotech.,* Univ. Gh Kassel, Heft 12.

Grimstad G., Andersen K.H., Saue M., Jostad H.P., Shin Y.S. and You D.Y. 2013. An undrained cyclic accumulation model used in monopile design. Submitted for publication.

Gudehus G. 1996. A comprehensive constitutive equation for granular materials. *Soils and Foundations* 36: 1–12.

Guefrech A., Rault G, Chenaf N., Thorel L., Garnier J., Puech A. 2012. Stability of cast in place piles in sand under axial cyclic loading . *Proc. 7th Int. Conf. Offshore Site investigation and Geotechnics*. OSIG, London. pp.329-334.

Hansteen O.E. 1980. Dynamic performance. Shell Brent "B" Instrum. Project; Seminar. London 1979. Proc., pp. 57 77. Org. by the Soc. for Underwater Techn., London. Also NGI Publ. 137.

Hansteen, O.E. 1991. Description of INFIDEL – a non-linear 3D finite element program. NGI Report 514090-3, rev. 1.

Hight, D W 1982. A simple piezometer probe for the routine measurement of pore pressures in triaxial tests on saturated soils. *Geotechnique,* Vol.32, No.4, pp 396-402.

Hight, D W and Jardine, R J 1993. Small strain stiffness and strength characteristics of hard London Tertiary clays. *Proc. Int. Symp. on Hard Soils - Soft Rocks,* Athens, Greece, Vol 1, Balkema, Rotterdam, pp 533-522.

Ho, Y.K., Jardine, R.J. and Anh-Minh, N. 2010. Large displacement interface shear between steel and granular media. *Geotechnique*, Vol. 61, No. 3, pp 221.234.

Høeg, K., Dyvik, R. and Sandbækken, G. 2000. Strength of undisturbed versus reconstituted silt and silty sand specimens. ASCE, *J. Geotech. and Geoenv. Engrg*. 126(7): 606-617.

ISO 19 902. 2007. International standard for the design of fixed steel offshore platforms, International Standards Office, British Standards Institute, London.

Jamiolkowski, M., Lo Presti, D.C.F and Manassero, M. 2001. Evaluation of Relative Density and Shear Strength of Sands from CPT and DMT. In *Proceedings of Conference on Soft Ground Construction*: pp. 201-238. ASCE.

Jardine, R J, Symes, M J and Burland, J B 1984. The measurement of soil stiffness in the triaxial apparatus. *Geotechnique* 34, No.3, pp 323-340.

Jardine R J, Potts D M, Fourie A B, and Burland J B 1986. Studies of the influence of non-linear stress-strain characteristics in soil-structure interaction. *Géotechnique*, 36, No 3, pp377-396.

Jardine, R. J. and Potts, D. M. 1988. Hutton Tension Leg Platform Foundations: an approach to the prediction of pile behaviour. *Geotechnique*, Vol.38, No.2, pp 231-252.

Jardine R. J., St John, H. D., Hight, D. W. and Potts, D. M. 1991. Some practical applications of a non-linear ground model. *Proc. Xth ECSMFE*, Florence, Vol. 1, pp 223-228.

Jardine, R.J. 1991. The cyclic behaviour of large piles. Chapter in *'The Cyclic Loading of Soils*', Eds. Brown & O'Reilly, Blackie & Son, Glasgow, pp 174-248.

Jardine R J and Potts D M 1993. Magnus foundations: Soil properties and predictions of field behaviour. *Proc. Conf. Large scale pile tests in clay*. Thomas Telford, London, pp 69-83.

Jardine, R.J. 1994. Review of offshore pile design for cyclic loading: North Sea clays. HSE Offshore Techn. Report, OTN 94 157.85.

Jardine, R J 1994b. One perspective on the pre-failure deformation characteristics of some geomaterials. Keynote lecture. *Proc. International Symposium on pre-failure deformation characteristics of geomaterials*. Hokkaido, Japan, Balkema, Vol. II, pp 855-886.

Jardine, R. J., Zdravkovic, L., and Porovic, E. 1997. Anisotropic consolidation including principal stress axis rotation: experiments, results and practical implications. Invited panel contribution, *Proc XIVth ICSMFE*, Hamburg, Balkema, Volume 4, pp2165-2168

Jardine, R. J. and Menkiti, C. O. M. 1999. The undrained anisotropy of K_0 consolidated sediments. *Proc. 12th ECSMGE*, Amsterdam. Balkema, Vol 2, pp1101-1108.

Jardine, R.J. and Standing, R.J. 2000.Pile load testing performed for HSE cyclic loading study at Dunkirk, France. Offshore Technology Report OTO 2000 007; Health and Safety Executive, London. Vol, 1, 160.p., Vol, 2, 200p.

Jardine, R.J., Chow, F.C., Overy, R. and Standing, J. 2005a. ICP design methods for driven piles in sands and clays. Thomas Telford Ltd, London, p 105.

Jardine, R.J., Standing, J.R.and Kovacevic, N. 2005b. Lessons learned from full-scale observations and the practical application of advanced testing and modelling. Keynote paper, *Proc International Symposium on Deformation Characteristics of Geomaterials*, Lyon, Vol 2, pub Balkema, Lisse, Vol. 2, pp 210-245.

Jardine, R.J, Standing, J.R and Chow, F.C. 2006. Some observations of the effects of time on the capacity of piles driven in sand. *Geotechnique* Vol 55, No. 4, pp 227-244.

Jardine, R.J., Aldridge, T. and Evans, T.G. 2011. Offshore foundation engineering in extremely dense glacial tills West of the Shetland Islands. *Proc. 15th ECSMGE*, Athens, Millpress, pp 879-884.

Jardine, R.J., Andersen, K. and Puech, A. 2012. Cyclic loading of offshore piles: potential effects and practical design. Keynote Paper. *Proc 7th Int. Conf. on Offshore Site Investigations and Geotechnics*, SUT London, pp 59-100.

Jardine R.J. and Standing, J.R. 2012. Field axial cyclic loading experiments on piles driven in sand. *Soils and Foundations*. Vol. 52, No 4, pp 723-737.

Jardine R.J, Zhu, B.T., Foray, P. and Yang, Z.X. 2013. Measurement of Stresses around Closed-Ended Displacement Piles in Sand. *Geotechnique* 63, No. 1, 1–17.

Jardine R. J. 2013. Advanced laboratory testing in research and practice: the Second Bishop Lecture. *Proc 18th ICSMGE*, Paris, 20p.

Jeanjean P., Andersen K.H. and Kalsnes B. 1998. Soil parameters for design of suction caissons for Gulf of Mexico deepwater clays. *Offshore Technology Conf.*, Houston, Proc., Paper 8830 (1998).

Jostad H.P and Andresen L. 2009. A FE procedure for calculation of displacements and Capacity of foundations subjected to cyclic loading. *Proc. COMGEO I*, Juan-les-Pins, France.

Kaggwa W.S., Booker J.R. and Carter J.P. 1991. Residual strains in calcareous sand due to irregular cyclic loading. *J. Geotech. Engrg*., ASCE 117: 201–218.

Karlsrud K and Haugen T. 1985a. Axial static capacity of steel models piles in overconsolidated clay, *Proc. 11th Int. Conf. on Soil Mech. and Found. Eng*., San Francisco.

Karlsrud K and Haugen T. 1985b. Behaviour of Piles in clay under cyclic axial loading-results of field model tests. *Proc. Behaviour of Offshore Structures*, BOSS'85, 589–600.

Karlsrud K. Nadim F and Haugen T. 1986. Piles in clay under cyclic loading: Field tests and computational modelling. Proc. 3rd Int. *Conf. on Numerical Methods in offshore Piling*. Nantes, France, May 1986, 165–190.

Karlsrud K. and Nadim F. 1990. Axial pile capacity of offshore piles in clay. *Proc. Offshore Technology Conference*. OTC 6245. Houston, USA.

Karlsrud K, Hansen S.B, Dyvik R and Kalsnes B. 1992a. NGI's pile tests at Tilbrook and Pentre – Review of testing procedures and results. *Proceedings of the Conference on Recent large-scale fully instrumented pile tests in clay*, London, 405–429.

Karlsrud K., Kalsnes B., and Nowacki F. 1992b. Response of piles in soft clay and silt deposits to static and cyclic axial loading based on recent instrumented pile load tests. *Proc. Offshore Site Investigation and Foundation Behaviour*. London, 549–583.

Karlsrud K, Clausen CJF and Aas PM. 2005. Bearing capacity of driven piles in clay: the NGI approach. *Proc. ISFOG'05*, Perth, WA, 775–782.

Karlsrud K. 2012. Prediction of load-displacement behaviour and capacity of axially loaded piles in clay based on analyses and interpretation of pile load test results. *PhD thesis*, NTNU, Trondheim, Norway.

Khemakhem M. 2012. Etude expérimentale de la réponse aux charges laterales monotones et cycliques d'un pieu foré dans l'argile, *Thèse*, Ecole Centrale de Nantes, 314pp.

Khemakhem M., Chenaf N., Garnier,J., Favraud C and Gaudicheau P. 2012. Development of degradation laws for describing the cyclic lateral response of piles in clays. *7th Int. Conf. Offshore Site Investigation and Geotechnics,* SUT, London.

Kleven A. and K.H. Andersen 1991. Cyclic laboratory tests on Storebælt clay till. Seminar on *Design of Exposed Bridge Piers*. Danish Society of Hydraulic Engineering. Copenhagen, Denmark, 22 January 1991. Also published in NGI Publ. 199.

Kraft, L.M., Ray R.P. and Kagawa.T. 1981. Theoretical t z curves. *J. Geotech. Engrg*., ASCE, 107, GT11: 1543 1561.

Kühn M. 2000. Dynamics of offshore wind energy converters on monopile foundations – experience from the Lely offshore wind farm. Oral contribution reported in EPSRC Offshore Wind Energy Network. *Workshop on Structure and Foundation Design of Offshore Wind Installations*. CLRC Rutherford Appleton Laboratory (1 March 2000).

Kuwano, R. and Jardine R.J. 2002. On the applicability of cross anisotropic elasticity to granular materials at very small strains. *Geotechnique*, Vol 52, No 10, pp 727-750.

Kuwano, R. and Jardine, R.J. 2007. A triaxial investigation of kinematic yielding in sand. *Géotechnique*, 57., No. 7, p. 563-580.

Ladd C.C. and Foott R. 1974. New design procedure for stability of soft clays. *J. Geotech. Engrg*., ASCE, 100, GT7: 763 786.

Lauritzsen R. and Schjetne K. 1976. Stability calculations for offshore gravity structures. *Proc., 8. Offsh. Tech. Conf.*, Houston, Tex., 75-82.

Le, M.H., Nauroy, J.F., De Gennaro, V., Delage, P., Thanh, N., Flavigny, E., Colliat, J.L., Puech, A. and Meunier, J. 2008. Characterization of soft deepwater West Africa clays: SHANSEP testing is not recommended for sensitive structured clays. *Proc. Offshore Technology Conference*, OTC paper 19193, Houston.

LeBlanc C., Houlsby G. T.and Byrne B. W. 2010. Response of stiff piles in sand to long-term cyclic lateral loading, *Geotechnique* 60, No. 2, 79–90

Lehane BM. 1992. Experimental investigations of pile behaviour using instrumented field piles. *PhD thesis*, University of London (Imperial College).

Lehane, B.M., Jardine, R.J., Bond, A.J. and Frank, R. 1993. Mechanisms of shaft friction in sand from instrumented pile tests. *ASCE Geot. Journal*. Vol 119, No 1, pp 19-35.

Lehane, B M and Jardine, R J 1994a. Displacement pile in glacial. *Canadian Geotechnical Journal*, Vol. 31, 1, pp 79-90.

Lehane, B M and Jardine, R J 1994b. Displacement pile in soft marine clay. *Canadian Geotechnical Journal*, Vol. 31, 2, pp 181-191.

Lehane, B.M., Jardine, R.J. and McCabe, B.A. 2003. Pile Group Tension Cyclic Loading: Field test programme at Kinnegar, N.Ireland. HSE Research Report 101; HSE Books, p42.

Leroueil, S and Vaughan, P R 1990. The general and congruent effects of structure in natural soils and weak rocks. *Geotechnique*, Vol 50, No 3, pp 467-488.

Lunne, T., Robertson, P.K., Powell, J. 1997. CPT and piezocone testing in geotechnical practice. Textbook: Spon Press, Taylor and Francis Company, London.

Lunne T., Berre T., Andersen K.H., Strandvik S. and Sjursen M. 2006. Effects of sample disturbance and consolidation procedures on measured shear strength of soft marine Norwegian clays. *Can. Geotech. J.* 43: 726-750.

Lunne, T. and K.H. Andersen 2007. Soft clay shear strength parameters for deepwater geotechnical design. Keynote Address; *Proc., 6th International Offshore Site Investigation and Geotechnics Conference*; Confronting New Challenges and Sharing Knowledge, p. 151-176, 11-13 September 2007, London, UK.

OSIG 2013. Guidance notes for the planning and execution of geophysical and geotechnical ground investigations for offshore renewable energy developments (Draft 02/05/13). Society for Underwater Technology, London.

Menkiti, C O 1995. Behaviour of clay and claey-sand, with particular reference to principal stress rotation. *PhD Thesis*, University of London.

Merritt, A., Schroeder, F., Jardine, R., Stuyts, B., Cathie, D., Cleverly, W. 2012. Development of pile design methodology for an offshore wind farm in the North Sea. Proc 7th Int. Conf. on Offshore Site Investigations and Geotechnics, SUT London, pp 439-448.

Mroz Z., Norris V.A. and Zienkiewicz. 1978. Simulation of soil behavior under cyclic loading by using a more general hardening rule. Univ. College Swansea, Dept. of Civil Engrg., Institute for Numerical Methods in Engineering.

Mulilis, J.P., Seed, H.B., Chan, C.K., Mitchell, J.K. and Arulanandan, K. 1977a. Effects of sample preparation on sand liquefaction. *ASCE, J. Geotech. Engrg*. 103(2): 91-108.

Mulilis, J.P., Mori, K., Seed, H.B. and Chan, C.K. 1977b. Resistance to liquefaction due to sustained pressure. *ASCE, J. Geotech. Engrg.*, 103(7): 793-797.

Nadim F and Dahlberg R. 1996. Numerical modeling of cyclic pile capacity in clay. *Proc. Offshore Technology Conference*, OTC paper 7994, Houston, USA.

Niemunis A. and Herle I. 1997. Hypoplastic model for cohesionless soils with elastic strain range. Mech. of Cohesive-Frictional Materials 2: 279–299.

Nishimura, S., Minh, N.A. and Jardine, R.J. 2007. Shear strength anisotropy of natural London clay. Symposium in Print on Stiff Clays. *Géotechnique*, 57(2), pp 49-62.

NGI 2006. SPLICE

Nowacki F, Karlsrud K and Sparrevik P. 1992. Comparison of recent tests on OC clay and implications for design. *Proceedings of the Conference on Recent large-scale fully instrumented pile tests in clay*. London, 511–537.

Peralta P. 2010. Investigations on the behaviour of large diameter piles under long-term lateral cyclic loading in cohesionless soil, *PhD Thesis*, Leibnitz University, Hannover, pp 201.

Poulos HG. 1982. Single pile response to cyclic lateral load. *Journal of the Geotechnical Engineering Division* 108: 355–375.

Poulos HG. 1989. SCARP USERS'S MANUAL. Centre for Geotechnical Research, The University of Sydney, Australia.

Pra-ai, S. 2013. Essais et modélisation du cisaillement cyclique sol-structure à grand nombre de cycles. Application aux pieux, *Thèse de Doctorat*, IMEP2, Université de Grenoble (to be published).

Prevost J.-H. 1977. Mathematical modeling of monotonic and cyclic undrained clay behaviour. *Int. J. for Num. Methods in Geomech.* 1: 195–216.

Puech A., Canou J., Bernardini C., Pecker A., Jardine R., and Holeyman A. 2012. SOLCYP: a four year JIP on the behavior of piles under cyclic loading. *Offshore Site Investigation and Geotechnics*, SUT, London.

Puech A., Benzaria O., Thorel L., Garnier J., Foray P. et Jardine R. 2013. Diagrammes de stabilité cyclique de pieux dans les sables. *Proceedings 18th ICSMGE, Paris.*

Rakotonindriana M.J. 2009. Comportement des pieux et des groupes de pieux sous chargement latéral cyclique, *Thèse de Doctorat* ENPC / LCPC.

Randolph MF. 1994. RATZ program manual: Load transfer analysis of axially loaded piles. Dept. of Civil and Resource Engineering, University of Western Australia.

Rimoy SP, Jardine RJ, Silva M, Foray PY, Tsuha CHC and Yang Z. 2012. Local and global behaviour of cyclically loaded instrumented model displacement piles in sand. *In: Proc. 7th Offshore Site Investigation and Geotechnics: Integrated Geotechnologies – Present and Future*. London: SUT.

Rimoy, S., Jardine, R.J and Standing, J.R. 2013. Displacement response to axial cycling of piles driven in sand. *Geotechnical Engineering*, 116 (2): 131-146.

Rimoy, S.P. 2013. Ageing and axial cyclic loading studies of displacement piles in sands. *PhD Thesis*, Imperial College London.

Rosquoët F., Thorel L., Garnier J. and Chenaf N. 2013. Pieu sous charge latérale dans les sables: développement de lois de dégradation pour prendre en compte l'effet des cycles. *Proceedings 18th ICSMGE, Paris*

Saue M., Langford T. and Mortensen N. 2010. Design of monopile Foundations in Sand for Offshore Windfarms. *Intern. Symp.on Frontiers in Offsh. Geotechnics (ISFOG)*. Nov. 2010, Perth, Australia.

Schmertmann, J. H. 1978. Guidelines for cone penetration tests, Performance and Design, Report 446 FHWA-TS-78-209, US Department of Transportation.

Silver, M.L., Chan, C.K., Ladd, R.S., Lee, K.L., Tiedemann, D.A., Townsend, F.C., Valera, J.E. and Wilson, J.H. 1976. Cyclic triaxial strength of standard test sand. *ASCE, J. Geotech. Eng.*, 102(5): 511-524.

Sim, W.W., Aghakouchak, A. and Jardine, R.J. 2013. Effects of duration and amplitude on cyclic behaviour of over-consolidated sands under constant volume conditions. *Geotechnical Engineering,* 116 (2): 111-121.

Smith P.R., Jardine R.J. and Hight, D.W. 1992. On the yielding of Bothkennar clay. *Geotechnique,* Vol 41, No 2, pp 257-274.

Tatsuoka, F., Jardine, R. J., Lo Presti, D., Di Benedetto, H. and Kodaka, T. 1997. Characterising the pre-failure deformation properties of geomaterials. Theme Lecture, *Proc XIVth ICSMFE*, Hamburg, Volume 4, Balkema, Rotterdam, 1999, pp 2129-2164

Tatsuoka, F. 2011. Laboratory stress-strain tests for developments in geotechnical engineering. 1st Bishop Lecture, *Deformation Characteristics of Geomaterials. Proc.* IS-Seoul, Hanrimwon, Vol. 1, p 3-53.

Tsuha, C.H.C, Foray, P.Y., Jardine, R.J., Yang, Z.X., Silva, M. and Rimoy, S.P. 2012. Behaviour of displacement piles in sand under cyclic axial loading. *Soils and Foundations*, Vol. 52, No 3, pp 393-410.

Vaid, Y.P., Sivathayalan, S. and Stedman, D. 1999. Influence of specimen reconstitution method on the undrained response of sand. *ASTM Geotech. Testing J.* 22(3): 187-195.

Valanis K.C. and Lee C.F. 1984. Endochronic theory of cyclic plasticity with applications. *J. of Applied Mechanics* 51: 367–374.

Wichtmann T. 2005. Explicit accumulation model for non-cohesive soils under cyclic loading. In: Triantafyllidis Th. (ed.). *Schriftenreihe des Institutes für Grundbau und Bodenmechanik der Ruhr-Universität* Bochum, Heft 38.

Wichtmann T., Niemunis A. and Triantafyllidis Th. 2004. Strain accumulation in sand due to drained uniaxial cyclic loading. In: Triantafyllidis Th. (ed.). *Cyclic Beh. of Soils and Liquefaction Phenomena*. London: Taylor & Francis Group.

Yang, Z.X., Jardine, R.J., Zhu B.T., Foray, P. and Tsuha, C.H.C.. 2010. Sand grain crushing and interface shearing during displacement pile installation in sand, *Géotechnique*, Vol 60, No 6, pp 469-482.

Zdravkovic L. and Jardine, R.J. 1997. Some anisotropic stiffness characteristics of a silt under general stress conditions. *Geotechnique*, 47, No 3, 407-438.

Zdravkovic, L. and Jardine, R.J. 2000. Undrained anisotropy of K_0 consolidated silt. *Canadian Geotechnical Journal*, Vol 37, No.1, pp 178-200.

Zdravkovic, L. and Jardine, R.J. 2001. The effect on anisotropy of rotating the principal stress axes during consolidation. *Geotechnique*, 51, 1, pp 69-83

Zdravkovic, L., Potts, D.M. and Jardine, R.J. 2001. A parametric study of the pull-out capacity of bucket foundations in soft clay. *Geotechnique*, 51, 1 pp 55 -67.